UNIVERSIDADE D
COIMBRA

Rita Mateus Lopes

Using a high-throughput genetic screen to identify *Plasmodium* molecules that interact with the host's innate immune system

Dissertação no âmbito do Mestrado em Investigação Biomédica, ramo de Infeção e Imunidade, orientada pelo Doutor António Manuel Barbeiro Mendes e pela Doutora Teresa Maria Fonseca de Oliveira Gonçalves, apresentada à Faculdade de Medicina da Universidade de Coimbra

Julho de 2023

Faculdade de Medicina da Universidade de Coimbra

Using a high-throughput genetic screen to identify *Plasmodium* molecules that interact with the host's innate immune system

Rita Mateus Lopes

Dissertação no âmbito do Mestrado em Investigação Biomédica, ramo de Infeção e Imunidade, orientada pelo Doutor António Manuel Barbeiro Mendes e pela Doutora Teresa Maria Fonseca de Oliveira Gonçalves, apresentada à Faculdade de Medicina da Universidade de Coimbra

Julho de 2023

UNIVERSIDADE D
COIMBRA

Dissertação apresentada à Faculdade de Medicina da Universidade de Coimbra para cumprimento dos requisitos necessários à obtenção do grau de Mestre em Investigação Biomédica com especialização em Infeção e Imunidade. O trabalho apresentado foi realizado no Instituto de Medicina Molecular - João Lobo Antunes (iMM-JLA, Lisboa) sob orientação científica do Doutor António Manuel Barbeiro Mendes e co-orientação da Doutora Teresa Maria Fonseca de Oliveira Gonçalves.

Agradecimentos

Em primeiro lugar, um obrigado a ti, Miguel, pela oportunidade que me deste de fazer parte do teu grupo de laboratório. Obrigada pelo apoio e disponibilidade nas situações mais stressantes, pela partilha de conhecimento, pelos momentos de lazer proporcionados à equipa e, acima de tudo, pelo grande exemplo de paixão pela ciência.

A ti, António, o maior e mais sincero agradecimento. Obrigada pela orientação, pela paciência, pelo apoio, pela disponibilidade, face às circunstâncias e à vida acelerada, que arranjaste para me ajudar e dar uma palavra de incentivo quando era necessário. Quando as coisas não correram tão bem, apelaste sempre à minha perseverança, acreditaste em mim e fizeste-me vê-las de outra perspetiva de maneira a sair sempre por cima. És um verdadeiro exemplo de empenho e de força.

Aos restantes membros do grupo por me acolherem e acompanharem ao longo do percurso. Carla, Fontinha, Helena, Raquel e Sofia, obrigada pela disponibilidade, ajuda e ensinamentos partilhados. Um especial agradecimento à Catarina e à Diana, as minhas mentoras diretas, por toda a partilha de conhecimento e esclarecimento de dúvidas, pelas horas no biotério e a contar parasitemias, pelo apoio e disponibilidade demonstrados. À Ana pela pessoa extraordinária que é e pela preocupação para comigo. À Andreia pela simpatia, amabilidade e palavras sábias.

Quero também agradecer aos Figueiredos pela companhia no laboratório, pelas conversas (científicas e existenciais) e pela ajuda prestada sempre que necessária. Um especial agradecimento à Marta pela simpatia, boa disposição e por testar a nossa audição diariamente.

Não posso deixar de agradecer ao Professor Henrique Girão por me ter aceite no mestrado e pelo apoio e disponibilidade ao longo do percurso. Também à Professora Teresa Gonçalves pela partilha de conhecimento e pelo voto de confiança enquanto orientadora interna.

Aos amigos que a Universidade de Coimbra me deu e que na vida levarei, especialmente à Ruivinho, à Diana e à Bea, por estarem sempre lá para ouvir os meus dramas e as minhas reclamações, por me ajudarem nas minhas indecisões e por acreditarem em mim, mesmo quando eu não acreditava. Por todas as horas em videochamada, pela partilha de lágrimas e sorrisos e pelas aventuras vividas e ainda por viver. Ao Vaquinha, por aturar os meus humores, pelas piadas sem piada, pelas chamadas de atenção e por, mesmo estando dias e dias sem falar, ser uma constante na minha vida.

Às minhas amigas de longa data, Martins, Cat, Patty e Inês, por tudo o que já vivemos e por terem sempre uma palavra amiga para dizer. Um especial obrigado a ti, Martins, por seres a

“sis” do coração, por libertares o meu lado extrovertido, por partilharmos momentos de euforia e também de acalmia. À amizade mais recente, Laura, pelas conversas diárias, pelos conselhos e por me fazeres simpatizar com o Sporting.

O meu obrigado mais especial vai para a minha família. Aos meus pais pelo apoio incondicional. Por me darem asas para voar rumo à capital, por acreditarem em mim desde sempre e para sempre, por me incentivarem a querer sempre mais, por me ampararem nos momentos menos bons e por estarem ao meu lado em todas as alturas. Ao meu irmão preferido (é o único) pelas discussões, pelos desabafos e pelos momentos de companhia sem dizer nada, pelas horas de guitarrada, panquecas de final de tarde ou gelados tardios. Aos meus avós, pelas chamadas dia sim dia não, por me darem mimos quando ia a casa e por me encherem a marmita ao domingo de coisas boas que aqueciam a alma quando estava longe.

Um obrigado também a todos os que não mencionei, mas que de uma maneira ou de outra me ajudaram a chegar onde estou hoje.

Abstract

Malaria is a mosquito-borne infectious disease caused by *Plasmodium* parasites that remains a major health concern as a significant cause of morbidity and mortality worldwide. Despite numerous efforts, the development of effective vaccines as well as therapeutic measures has been challenged by the scarcity of knowledge on the immune responses elicited on the vertebrate host by the parasite. Due to its asymptomatic nature, for many years it was assumed that the liver stage of infection does not contribute to the establishment of pathology. Nevertheless, *Plasmodium* triggers an innate type 1 IFN response in the liver to control parasite load. Malaria parasites have evolved a machinery to modulate the host's immune response. However, the specific functions of parasite genes during their liver stage development remain poorly characterized.

This thesis aims to identify *Plasmodium* molecules that interact with the host's innate immune system and contribute to the outcome of the liver stage of *Plasmodium* infection. To this end, we used a high-throughput genetic screening tool based on the infection of immunocompetent and immunodeficient mice by pools of *P. berghei* knockout (KO) mutants. We demonstrated, following the development of the parasites throughout its life cycle, that frozen blood infected with KO parasites can be maintained and shipped across Europe, and we validated the reproducibility of our proposed methodology by showing that the pool of parasites, as well as their frequency and abundance, at each stage of the life cycle, is similar between two replicates. Next, we screened 192 *Plasmodium* genes in C57BL/6J and *Ifnar1*$^{-/-}$ mice, in which type I IFN response is ablated, to identify possible proteins that are directly involved in parasite evasion and/or modulation of the type I IFN response in the liver. The data revealed that 21 of these genes were likely essential for parasite growth in the liver, regardless of the host's immune status. Further analysis revealed that 3 genes were required for growth in the presence of an intact immune system, which were not required for growth in immunodeficient mice. From the 79 KO parasites present in the blood of both mouse models we highlighted 7 for their different developmental profile between WT and *Ifnar1*$^{-/-}$ mice, based on their ability to survive and capacity to replicate in each group of mice. Despite these evidences, our literature review did not identify a link between the genes identified and the type 1 IFN response during the liver stage infection.

This thesis validates the use of the barcode-based NGS sequencing approach to study the effects of the host immune system on parasite development, enabling the identification of different KO parasites that respond differently to different immune pressures. Moreover, it reveals that certain parasite genes may be required to counter host immune responses in the liver.

Keywords: Malaria, *Plasmodium* genes, Liver stage infection, Type I-IFN response, *Plasmo*GEM vectors, *P. berghei* knockout mutants, High-throughput genetic screen.

Resumo

A malária é uma doença infeciosa transmitida por mosquitos e causada por parasitas do género *Plasmodium*, que continua a ser uma das principais preocupações em termos de saúde por ser uma causa significativa de morbilidade e mortalidade em todo o mundo. Apesar de inúmeros esforços, o desenvolvimento de vacinas e de intervenções terapêuticas eficazes tem sido dificultado pela falta de conhecimentos sobre as respostas imunitárias induzidas pelo parasita no hospedeiro vertebrado. Devido à sua natureza assintomática, durante muitos anos assumiu-se que a fase hepática da infeção por *Plasmodium* não contribui para o estabelecimento da patologia. No entanto, o parasita desencadeia uma resposta inata de interferão (IFN) tipo 1 no fígado para controlar a carga parasitária. Ao longo do tempo, os parasitas da malária desenvolveram uma maquinaria refinada para modular a resposta imunitária do hospedeiro, no entanto, as funções dos genes do parasita envolvidos no desenvolvimento da fase hepática permanecem mal caracterizadas.

Esta tese tem como objetivo identificar moléculas de *Plasmodium* que interagem com o sistema imunitário inato do hospedeiro e contribuem para o resultado da fase hepática da infeção. Para tal, utilizámos uma ferramenta de rastreio genético de alto rendimento baseada em pools de mutantes knockout (KO) de *P. berghei* em ratinhos imunocompetentes e imunodeficientes. Demonstrámos, através do acompanhamento do desenvolvimento dos parasitas ao longo do seu ciclo de vida, que o sangue congelado infetado com parasitas KO pode ser mantido e enviado para toda a Europa, e validámos a reprodutibilidade da nossa metodologia proposta, mostrando que o conjunto de parasitas, bem como a sua frequência e abundância, em cada fase do ciclo de vida, é semelhante entre dois replicados técnicos. Em seguida, analisámos 192 genes de *Plasmodium* em ratinhos C57BL/6J e *Ifnar1*$^{-/-}$, nos quais a resposta de IFN de tipo I é abolida, para revelar possíveis proteínas que estão diretamente envolvidas na evasão e/ou na modulação da resposta IFN de tipo I no fígado por parte do parasita. Os dados revelaram que 21 destes genes são provavelmente essenciais para o crescimento do parasita no fígado, independentemente do estado imunitário do hospedeiro. Uma análise mais aprofundada revelou que 3 genes foram necessários para o crescimento na presença de um sistema imunitário intacto, enquanto não foram necessários para o crescimento em ratinhos imunodeficientes. Dos 79 parasitas KO presentes no sangue de ambos os modelos de ratinho, destacámos 7 pelo seu perfil de desenvolvimento diferente entre ratinhos WT e *Ifnar1*$^{-/-}$, relativamente à sua capacidade de sobrevivência e capacidade de replicação em cada grupo de ratinhos. Apesar destas evidências, a nossa revisão literária não identificou uma ligação clara entre os genes identificados e a resposta de IFN tipo 1 durante a fase hepática da infeção.

Esta tese valida a utilização da abordagem de sequenciação NGS baseada em códigos de barras para estudar os efeitos do sistema imunitário do hospedeiro no desenvolvimento do parasita, permitindo a identificação de diferentes parasitas KO que respondem de forma diferente a diferentes pressões imunitárias. Além disso, revela que certos genes do parasita podem ser necessários para contrariar as respostas imunitárias do hospedeiro no fígado.

Palavras-chave: Malária, Genes do *Plasmodium*, Infeção na fase hepática, Resposta de interferão tipo 1, Vetores *Plasmo*GEM, Mutantes *knockout* de *P. berghei*, Rastreio genético de elevado rendimento.

Table of contents

Figures Index

Tables Index

Abbreviations

ABC	ATP Binding Cassette
ACK	Ammonium-Chloride-Potassium
ACT	Artemisinin combination treatment
Bcl-2	B-cell lymphoma 2
cAMP	Cyclic adenosyl mono-phosphate
CDF	Cation diffusion facilitator
CM	Cerebral malaria
CSP	Circumsporozoite protein
DC	Dendritic cell
DNA	Deoxyribonucleic acid
ECM	Experimental cerebral malaria
EDTA	Ethylenediamine tetraacetic acid
EEF	Exo-erythrocytic form
EPAC	Exchange protein directly activated by cAMP
FELASA	Federation of European Laboratory Animal Science Associations
gDNA	Genomic DNA
GO	Gene ontology
HO-1	Heme oxygenase-1
HSPGs	Highly sulfated heparan sulfate proteoglycans
ICAM-1	Intercellular adhesion molecule-1
IFN	Interferon
IFNAR	IFN-α/β receptor
IL	Interleukin
iMM JLA	Instituto de Medicina Molecular João Lobo Antunes
IPT	Intermittent preventive treatment
iRBC	Infected red blood cell
IRF	IFN-regulatory factor

IRS	Indoor residual spraying
ISG	IFN-stimulated genes
ISGF	IFN-stimulated gene factor
ISRE	IFN-stimulated responses element
ITN	Insecticide treated bed-net
JAK	Janus kinase
KO	Knockout
LRP	Low-density lipoprotein receptor-related protein
OAT	Ornithine amino transferase
MAVS	Mitochondrial antiviral-signaling protein
MCP	Monocyte chemoattractant protein
MDA5	Melanoma differentiation-associated protein 5
MDR	Multidrug resistance
MIMS	Laboratory for Molecular Infection Medicine Sweden
mTOR	Mammalian target of rapamycin
NF-κB	Nuclear factor-kappa B
NK	Natural killer cells
NKT	Natural killer T cells
ORBEA	Órgão Responsável pelo Bem-Estar Animal
PABA	Para-aminobenzoic acid
PAMP	Pathogen-associated molecular pattern
***Pb*A**	*P. berghei* ANKA
PBLP	*Plasmodium* BEM46-like protein
PBS	Phosphate-buffered saline
PCR	Polymerase chain reaction
PEXEL	*Plasmodium* export element
PRR	Pattern recognition receptor
PV	Parasitophorous vacuole

RBC	Red blood cell
RDT	Rapid diagnostic test
RIG	Retinoic acid-inducible gene
ROS	Reactive oxygen species
RPMI	Roswell Park Memorial Institute
RT	Room temperature
SEM	Standard error of the mean
SMC	Seasonal malaria chemoprevention
SPECT	Sporozoite microneme protein essential for cell traversal
SPF	Specific-pathogen-free
spz	Sporozoite
STAT	Signal transducer and activator of transcription
TNF	Tumour necrosis factor
TRAP	Thrombospondin-related anonymous protein
TYK	Tyrosine kinase
UIS	Upregulated in infective sporozoites
WHO	World Health Organization
WT	Wild-type

Introduction

1. Introduction

1.1. Malaria: epidemiology, etiology, and socio-economic burden

Malaria is a mosquito-borne parasitic disease that remains a major health concern worldwide, due to its high rate of morbidity and mortality[1]. This infectious disease is endemic in several regions of the world, particularly in the tropical and subtropical regions[2]. The 2021 World Health Organization (WHO)'s World Malaria Report estimated that in 2020 there were 241 million cases of malaria in 85 endemic countries, an additional 14 million cases compared with 2019, owing to disruptions to the provision of malaria services (prevention, diagnosis, and treatment) during the COVID-19 pandemic. The largest increase in the number of cases occurred in countries in the WHO African Region, which reported approximately 95% of the cases, followed by 2.4% in the WHO Eastern Mediterranean Region and 2% in the WHO South-East Asian Region (Fig.1.1). The report also reveals the devastating toll of malaria, with an estimated 627,000 deaths reported, a 12% increase compared to 2019. Approximately 47,000 of the additional 69,000 deaths by malaria were due to the disruptions during the pandemic[1]. Once again, the WHO African Region was the most affected one, registering 96% of all deaths. Although there are several population groups, particularly young children, pregnant women, and immunosuppressed people, at high risk of contracting malaria, children aged under 5 years old suffer the most, with maximum mortality, accounting for 77% of total malaria deaths[1,3].

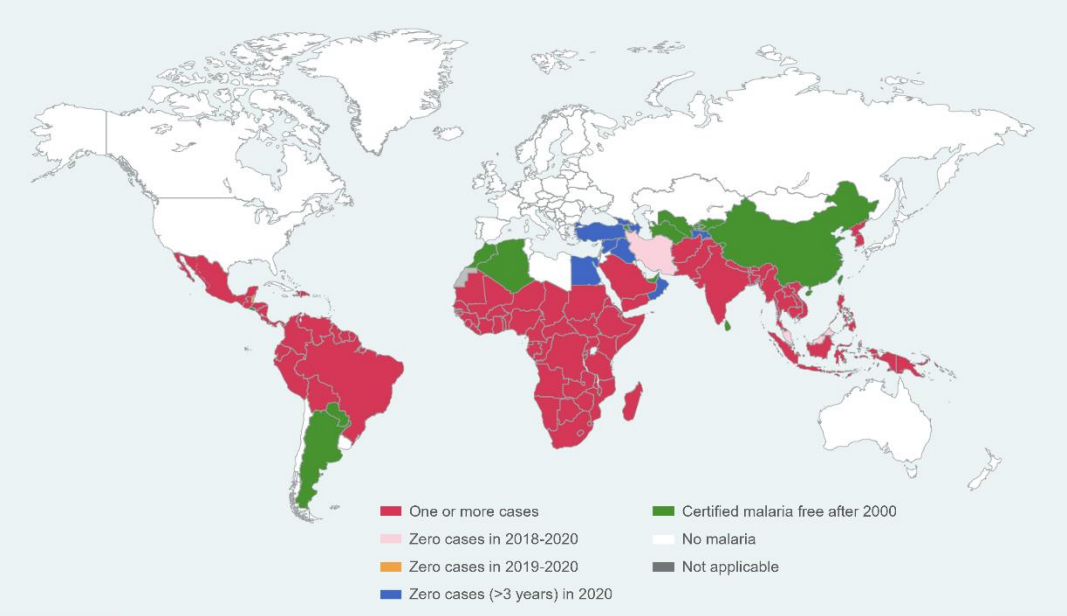

Figure 1.1. Global incidence cases of malaria in 2020. World map showing countries with malaria cases in 2000 and their status by 2020. Countries with zero cases for at least 3 consecutive years received the certification of malaria free status from the WHO. Adapted from World Malaria Report, 2021[1] (Source: WHO database).

The causative agents of malaria are obligate intracellular parasites of the *Plasmodium* (*P.*) genus[4], which belongs to the phylum Apicomplexa, and are transmitted to a large range of vertebrate hosts, including humans[5], through the bite of an infected female *Anopheles* mosquito. There are six species of *Plasmodium* parasites known to cause malaria infections in humans: *P. falciparum*, the predominant species in Africa, is responsible for the most severe form of infection, cerebral malaria, and for the majority of malaria deaths[2]; *P. vivax*, which has the widest distribution, throughout the tropics, subtropics and temperature zones, is responsible for relapses due to its dormant hepatic forms[5]; *P. malariae*, which is associated with nephrotic syndrome following chronic infection[6]; *P. ovale*, whose manifestations of the disease are usually not severe, despite also giving rise to dormant forms and, consequently, relapses[5]; *P. knowlesi*, once thought to only infect macaques, is now known to cause severe complicated malaria in humans, especially in the Southeast Asia[7]; and *P. simium*, the species most recently identified as capable of infecting humans[8]. Together, *P. falciparum* and *P. vivax* account for the majority of malaria infections[2,9].

Despite continuous efforts, malaria still remains one of the greatest health burdens in the world. Malaria has significant measurable direct and indirect costs, which affect the quality of life of individuals, the capability of healthcare infrastructures to respond to the disease and, consequently, the productivity and economic development of countries where the disease is endemic[10]. In Africa, malaria is perceived as a disease of poverty as well as a cause of poverty[11], with the global cost of its impact estimated at 12 billion US$ annually only in this continent[12]. The continued evolution of the parasites contributes to the development of resistance to antimalarial drugs and insecticides, delaying progress against this deadly disease. For these reasons, the identification of new drugs and vaccine targets is an urgent priority.

1.2. *Plasmodium* life cycle

Plasmodium parasites have a complex life cycle that requires two hosts, a vertebrate host, and a mosquito vector. In the vertebrate host, the *Plasmodium* life cycle includes two stages: the pre-erythrocytic stage, which includes all steps since sporozoite deposition under the skin of the vertebrate host until the release of the first generation of merozoites into the bloodstream; and the erythrocytic stage, also known as blood stage, that consists of infection of the host's red blood cells (RBCs)[4].

Plasmodium infection begins when, during a blood meal, an infected female *Anopheles* mosquito injects sporozoites under the skin of the vertebrate host[13] (Figure 1.2. A). Sporozoites, the salivary gland-resident and liver-infective forms of *Plasmodium* parasites,

then use gliding motility as the locomotion process to reach endothelial cells of a blood vessel and, subsequently, enter blood circulation[4,]. Most of the sporozoites leave the area of the bite and reach the bloodstream, while the remaining invade the lymphatic vessels or remain in the dermis[14].

Once in the bloodstream, the sporozoites target and travel to the liver[13]. The liver vasculature is composed by sinusoids, specialized blood vessels with fenestrated endothelial cells with protruding highly sulfated heparan sulfate proteoglycans (HSPGs). The targeting of the parasites to the liver is possibly due to an interaction between a positively charged *Plasmodium* surface protein, the circumsporozoite protein (CSP), and the negatively charged HSPGs[13,15]. The liver sinusoids are enriched in liver-resident macrophages called Kupffer cells, through which sporozoites cross the sinusoidal barrier to invade the hepatocytes[13,16]. A study employing animal models showed that two proteins of the rodent-infective parasite *P. berghei*, SPECT (sporozoite microneme protein essential for cell traversal) 1 and SPECT2, appear to be crucial in the process of cell traversal[13].

Having crossed the sinusoidal barrier, the sporozoites traverse several hepatocytes until they effectively invade a final one with formation of a parasitophorous vacuole (PV) (Figure 1.2. B), where the sporozoites differentiate into exo-erythrocytic forms (EEFs)[13,17,18]. Hepatocyte traversal leads to exocytosis of sporozoite's secretory organelles, named micronemes. Parasite micronemes release proteins, such as thrombospondin-related anonymous protein (TRAP), on the apical end of the parasite, which play a crucial role in sporozoite traversal and invasion[13,19]. Inside the PV, EEFs undergo a process called schizogony, characterized by extensive DNA replication, without cell division, and growth of organelles, such as mitochondria and apicoplast[13,20]. Three distinct *P. berghei* proteins are essential for parasite development and survival within the PV – upregulated in infective sporozoites (UIS) 3 and UIS4 and Pb36p[13].

Hepatic parasite schizogony culminates in the formation of thousands of individual merozoites (Figure 1.2. C), that are packed into vesicles called merosomes[13,20]. The fact that the merosome membrane is derived from the host hepatocyte plasma membrane allows it to overcome immune system defenses, such as Kupffer cells. The merosomes are then released from the infected hepatocytes into the bloodstream and, once in circulation, can travel to the lung capillaries (Figure 1.2. D) where they burst and release merozoites into the bloodstream (Figure 1.2. E). Merozoites will subsequently invade RBCs, initiating the erythrocytic stage of the *Plasmodium* life cycle[20,21].

Depending on the infecting *Plasmodium* species, the duration of the liver stage can range from 5 days in *P. falciparum* to 15 days in *P. malariae* in humans[2] and only 2 days for rodent-

infective parasites (*P. berghei* and *P. yoelli*)[20]. With *P. vivax* and *P. ovale*, the primary incubation period can be much longer, since they are capable of producing dormant forms, known as hypnozoites, that can persist in the liver until they are reactivated and initiate schizogony, culminating in blood infection, causing disease relapses[13,22].

Due to its asymptomatic nature, the liver stage of the *Plasmodium* life cycle is the most appealing stage for vaccination and prophylactic strategies since, if infection is blocked at this stage, there will be no pathology and disease.

Once in the bloodstream, merozoites can infect RBCs, following successive cycles of invasion, intracellular growth, proliferation, and re-invasion (Figure 1.2. F), initiating the symptomatic blood stage cycle, which is responsible for the clinical features and pathologies associated with malaria[2]. During invasion, a PV is formed around the parasite, by invagination of the host cell plasma membrane, to protect itself from the erythrocyte's cytoplasm and allow its development[23,24].

Inside the RBC, the merozoite goes through different morphological phases. The earliest form is known as ring-stage that rounds up and becomes more metabolically active coming to the trophozoite stage. At the trophozoite stage, the parasite increases in size, consumes erythrocyte's contents and modulates the surface of the infected RBC (iRBC). The next and final stage is known as schizont stage, in which parasite goes through a series of nuclear divisions, originating 16 – 32 new merozoites that are released into the bloodstream, being able to infect more RBCs[23,25]. Erythrocytic schizogony, depending on the *Plasmodium* species, consists of 24 (*P. knowlesi*), 48 (*P. falciparum*, *P. ovale*, *P. vivax*) or 72 (*P. malariae*) h asexual replication cycles, that are associated with the fever periodicity[26].

During the blood stage of infection, a small fraction of parasites differentiates into sexual forms, originating microgametocytes (males) or macrogametocytes (females), through a gametocytogenesis process (Figure 1.2. G)[2,25].

When a female *Anopheles* mosquito feeds on an infected vertebrate host, ingests the gametocytes, and becomes infected, continuing the *Plasmodium* life cycle (Figure 1.2. H)[2,25]. In the midgut lumen of the mosquito, the gametocytes maturate into gametes. Microgametes and macrogametes fuse, forming diploid zygotes that develop into ookinetes. Ookinetes penetrate the epithelium midgut in order to reach the basal lamina of the epithelium, where oocysts develop. The sporozoites are generated within oocysts. The accumulation of sporozoites leads to the rupture of the oocyst, releasing mature sporozoites that migrate into the mosquito's salivary glands (Figure 1.2. I)[25,27].

When the infected mosquito takes a blood meal, the sporozoites residing in the salivary glands will be injected into the skin of the vertebrate host, starting a new life cycle of the parasite (Figure 1.2. J)[25].

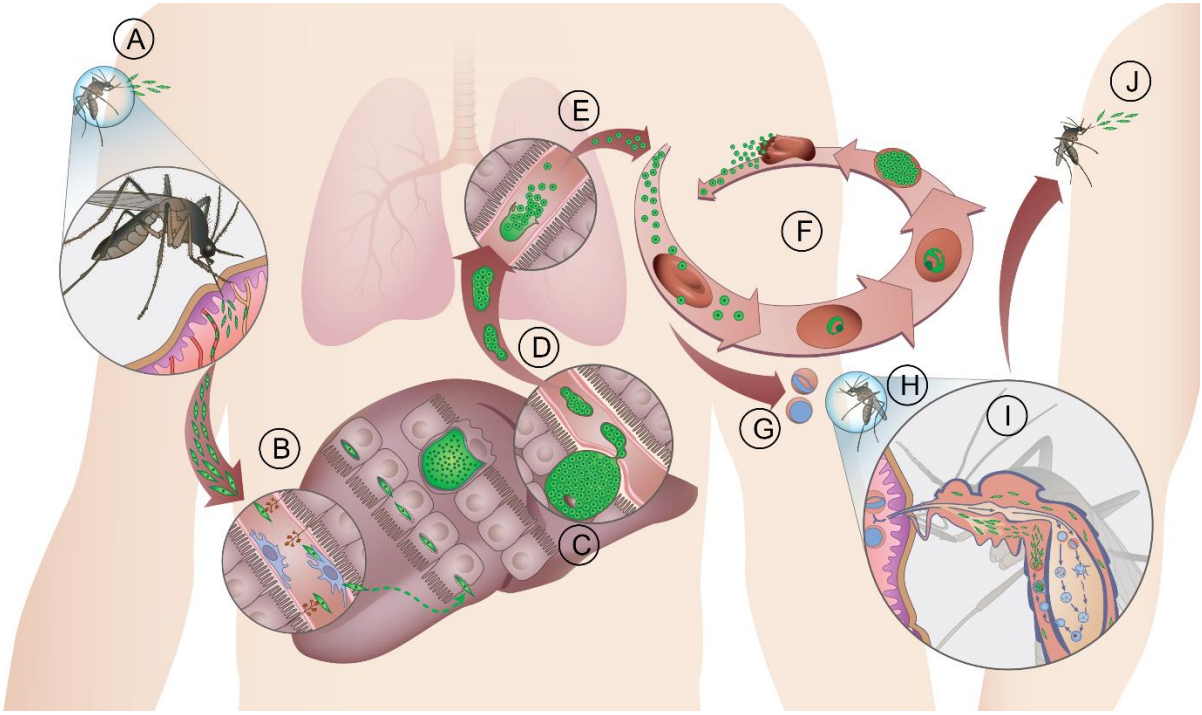

Figure 1.2. *Plasmodium* spp. life cycle. (A) During a blood meal, an infected female *Anopheles* mosquito injects sporozoites under the dermis of the vertebrate host that will migrate to the liver. **(B)** In the liver, sporozoites will traverse several hepatocytes until effectively invade a final one with the formation of a PV. **(C)** Inside the PV, sporozoites differentiate into EEFs culminating in the formation of thousands of individual merozoites. **(D)** The merosomes, where merozoites are accumulated, are released from the hepatocytes into the bloodstream and travel to the lung capillaries. **(E)** In the lungs, merosomes burst and release merozoites into the bloodstream. **(F)** Merozoites infect RBCs and undergo successive cycles of invasion, intracellular growth, proliferation, and re-invasion. **(G)** Some parasites differentiate into sexual forms, the gametocytes. **(H)** When a female *Anopheles* mosquito feeds on an infected vertebrate host, ingested the gametocytes, and became infected. **(I)** Inside the mosquito, the gametocytes mature into gametes that fuse, forming diploid zygotes. Zygotes mature into ookinetes that cross the epithelium midgut and differentiate into oocysts. The sporozoites, generated within oocysts, are released upon oocysts rupture, and invade the mosquito's salivary glands. **(J)** Sporozoites present in the salivary glands are inoculated into the host's skin, during a blood meal of the infected mosquito.

1.3. Clinical manifestation of malaria

Malarial-associated clinical symptoms occur during the erythrocytic stage of the *Plasmodium* life cycle, specifically on the asexual blood stage. The clinical manifestations of malaria depend on the infecting *Plasmodium* species, the health status of the individual, the quality of the diagnosis and, consequently, the efficacy of the treatment[2]. The symptoms associated with uncomplicated malaria are non-specific, being frequently mistaken with other pathologies: acute fever, chills, fatigue, headache, gastrointestinal symptoms, and muscle pain[2].

1.3.1. Severe malaria

Although most of malaria cases are uncomplicated, when the initial infection is not controlled, the disease can progress to severe malaria, eventually leading to death. Severe malaria is mainly caused by *P. falciparum* and affects mostly children, pregnant women, and immunocompromised individuals. The clinical features of severe malaria include severe anemia, renal complications, jaundice, pulmonary oedema with impaired respiratory function, and, ultimately, coma[2].

In Africa, there are three syndromes that dominate and that can occur separately or in combination: severe anemia caused by the destruction of iRBCs; cerebral malaria (CM) caused by the sequestration of iRBCs in the venules that adhere to the blood vessel wall and/or to other infected or noninfected RBCs, culminating in impairment of blood flow; and respiratory distress that presents metabolic acidosis largely reflecting tissue hypoxia[18].

The pathology associated with CM has been studied predominantly by *in vivo* infections of C57BL/6J mice with *P. berghei* ANKA (*Pb*A), a model known as experimental cerebral malaria (ECM)[28]. This ECM model mirrors some of the pathological features of human CM, such as immunological and neuropathological characteristics. ECM in *Pb*A-infected susceptible mice leads to neurological clinical signs such as paralysis, ataxia, deviation of the head, convulsion and/or coma[29]. Moreover, iRBC sequestration, higher production of pro-inflammatory cytokines, accumulation of $CD8^+$ T cells in the brain and up-regulation of the intercellular adhesion molecule-1 (ICAM-1) on the cerebral vasculature endothelium are some of the characteristic mechanisms of ECM[24,28,30].The time to onset of clinical signs is usually between 5- and 10-days post-infection and the rapid deterioration of the condition leads to animal death 4 or 5 h after the appearance of neurological signs[28].

1.4 Malaria diagnosis and treatment

Delay in diagnosis and, consequently, treatment of malaria are the main causes of death in several countries, so a prompt and correct diagnosis of the disease is essential for its control and elimination[1]. The current available tools for malaria diagnosis include microscopy of the patient's blood, rapid diagnostic tests (RDTs) and molecular techniques[31]. Microscopic visualization of patient's blood through thick and thin peripheral blood smears is still the gold standard method for malaria diagnosis: thick films are sensitive in detecting the presence of parasites, whereas thin films allow the identification of the infecting *Plasmodium* species and quantification of malaria parasites[31]. However, microscopic techniques show some limitations such as time consumption, expertise requirement and equipment maintenance[32]. Molecular

techniques such as polymerase chain reaction (PCR) are the most specific and sensitive diagnostic tests available, especially in cases of low parasitemia since it allows the identification of parasite's DNA[33]. However, PCR utility is limited by its complexity, high costs and the need of specialized technicians, making it difficult to be implemented in the field[34]. RDTs use immunochromatographic methods to quickly detect parasite antigens in lysed blood[35]. Despite having limited sensitivity and not allowing quantification of the parasite, RDTs are now the most widely used method for malaria diagnosis, especially in endemic areas, since they provide simple and rapid diagnosis, without needing high qualified staff and sophisticated equipment[36].

Malaria is a life-threatening disease, but if diagnosed early, it can be successfully treated. The use of artemisinin-based combination treatments (ACTs) is the current recommendation of the WHO for the treatment of uncomplicated malaria. ACTs combine the rapidly acting and rapidly eliminated artemisinin compounds with more slowly eliminated antimalarial drugs: artemisinin clears blood parasites and kills gametocytes, while the partner drug clears remaining parasites preventing development of drug resistance[37]. Primaquine is mainly used against dormant liver-stage hypnozoites, preventing relapses in *P. vivax* and *P. ovale*[38].

1.5. Malaria control

Over the past few decades, international efforts have been made to control, eliminate, and eradicate malaria. The key elements for malaria control are preventive and include vector control through the use of insecticides and employment of insecticide treated bed-nets (ITNs), to reduce the transmission from the mosquito vector to the human host; and use of effective drugs, as chemoprevention[2]. Thanks to these efforts, between 2004 and 2020, nearly 2.3 billion ITNs were distributed globally, and in 2020 alone about 229 million ITNs were delivered to malaria-endemic countries[1].

The use of antimalarial drugs as chemoprevention is recommended in high transmission areas and to risk groups. In many African countries, WHO advises intermittent preventive treatment (IPT) to women during pregnancy, which shows benefits on the health of the pregnant mother and the newborn[1,31]. Seasonal malaria chemoprevention (SMC) is a recommended strategy to protect children under 5 years of age in countries where malaria is highly seasonal, and transmission occurs only during a certain period[1,31]. A combination of measures, such as chemoprophylaxis and personal protective strategies to avoid mosquito bites are recommended to travelers from non-endemic countries[39]. The prophylactic drug recommended must take into account the travel destination, due to variability of *Plasmodium* species and its drug resistance, the length of stay and the traveler's health condition[39,40].

Effective treatment for malaria and vector control are essential keys in the fight against this disease, although the emergence resistance of the anopheline vector to insecticides and of the parasite to the antimalarial drugs represent a serious threat to global malaria control and elimination efforts[1,2].

Experts agree that malaria can only be eradicated with the crucial contribution of an effective vaccine, but the great antigenic variability presented by the parasite, amongst other factors, has made this task difficult. On 6th October 2021, the WHO recommended the use of the first vaccine against malaria, RTS,S (Mosquirix), in children living in regions with moderate-to-high transmission of *P. falciparum* malaria[41]. This subunit vaccine targets the *P. falciparum* circumsporozoite protein (CSP) present on the surface of sporozoites. The effectiveness of this vaccine was evaluated on a Phase III clinical study, showing that 4 doses of the vaccine provided a 25.9% and a 36.3% efficacy against clinical malaria in infants aged 6–12 weeks and in children aged 5–17 months, respectively[42]. Implementation of RTS,S demonstrates that a malaria vaccine is possible. Nevertheless, efforts must continue to develop a vaccine with higher efficacy and that protects against the remaining *Plasmodium* species capable of infecting humans.

1.6. Innate immunity elicited by liver stage *Plasmodium* infection

Vertebrates are constantly exposed to pathogens and, to prevent the development of infections, they have a complex immune system that recognizes and eliminates these invading microorganisms. Defense mechanisms can be divided into innate (or non-specific) and adaptive (or specific) immunity. The innate immune system represents the first line of defense against invading organisms and is mediated by external barriers and cellular components, including macrophages, dendritic cells (DCs), neutrophils, and natural killer (NK) cells. The adaptive immune system acts as a second line of defense, after being stimulated by the innate immune system, and offers protection against re-exposure to the same pathogen. Despite performing different functions mediated by several mechanisms with various cell groups, these two systems interact with each other to fight infection, that is, the components of the innate immune system influence the adaptive immune system and vice-versa[43,44].

The complex multistage and multiantigen life cycle, as well as the genetically diverse nature of *Plasmodium* parasites populations, constitute a major challenge for the host's immune system[45].

For many years it was thought that the parasites replicate within hepatocytes without being detected by the host's immune system, since the liver stage of *Plasmodium* infection is

clinically silent[13,46,47]. However, recent studies carried out in mice infected with *P. berghei* and *P. yoelli* demonstrate that the host can detect parasites by different receptors, triggering an immune response against them through the activation of signaling pathways and production of cytokines and chemokines[48,49]. Furthermore, a vast array of host-parasite interactions occurs during the hepatic stage of infection[50].

1.6.1 Interferon-mediated innate immune responses

Interferons (IFNs) are cytokines that were first described in 1957 as having the ability to interfere with viral replication, hence their name[51]. Interferons, being a large protein family, can be subdivided into three groups based on their functions and receptor employed[52]:

1) Type I IFNs, that consist of 13 subtypes of IFN-α in humans (14 in mice) and only one type of IFN-β, IFN-ω, IFN-κ, IFN-ε (with IFN-α and IFN-β being the most abundant). Type I IFNs are mainly produced by macrophages and DCs and are involved in innate and adaptive immune responses, playing important roles in protection and pathogenesis during *Plasmodium* infections[52,53];

2) Type II IFN, which consist of only one protein, IFN-γ, is produced by NK and T cells and contributes to parasite death and activation of immune cells[52];

3) Type III IFN (IFN-λ) was discovered in 2003[54] and activates intracellular signaling pathways and biological activities similar to type I IFNs, being co-produced with IFN-β, although using different receptors[52].

The introduction in this section focuses on the innate type-I IFN response as the first line of defense against liver infection.

The innate immune response is initiated when highly conserved molecules from pathogens called pathogen-associated molecular patterns (PAMPs) are recognized by the host through receptors called pathogen-recognition receptors (PRRs)[46]. The PAMPs-PRRs interaction triggers the activation of specific signaling pathways that stimulate antimicrobial responses, resulting in the production of type I IFNs[53]. The type I IFNs propagate the response between hepatocytes in an autocrine and paracrine manner through the activation of the heterodimeric transmembrane IFN-α/β receptor (IFNAR) in neighboring hepatocytes[47,53]. IFN-α and IFN-β bind to the IFNAR receptor, which is composed of two subunits, IFNAR1 (IFN-α/β receptor α chain) and IFNAR2 (IFN-α/β receptor β chain). In the canonical type I IFN signaling pathway, the IFNAR engagement activates the tyrosine kinase Janus kinase 1 (JAK1) and tyrosine kinase 2 (TYK2), two kinases associated with the IFNAR receptor, which phosphorylate the cytoplasmic transcription factors signal transducer and activator of transcription 1 (STAT1) and

STAT2. Tyrosine-phosphorylated STAT1 and STAT2 heterodimerize and translocate to the nucleus, where they attach to the IFN-regulatory factor 9 (IRF9) to form a trimolecular complex called IFN-stimulated gene factor 3 (ISGF3). Subsequently, in the nucleus, ISGF3 binds to consensus DNA sequences (TTTCNNTTTC), which are known as IFN-stimulated responses elements (ISREs), activating the transcription of various IFN-stimulated genes (ISGs)[52,53,55].

Although the IFN type II-mediated response to *Plasmodium* infection is the best studied, more recently it was demonstrated that *Plasmodium* also triggers type I IFN responses that play an important role in reducing parasite burden, inhibiting the development of exoerythrocytic forms of the parasite[56].

In 2014, Liehl *et al*. proposed that, during the asymptomatic development, the hepatocytes are capable of sensing the *Plasmodium* RNA, a previously unrecognized PAMP, through the melanoma differentiation-associated protein 5 (MDA5), a cytosolic retinoic acid-inducible gene (RIG)-I-like receptor[48]. Activated MDA5 recruits the adaptor molecule mitochondrial antiviral-signaling protein (MAVS), which phosphorylates the transcription factors interferon-regulatory factor 3 (IRF3) and IRF7, leading to the production of type I IFNs. Type I IFNs are released into the extracellular environment where they bind to the IFNAR on the surface of neighboring hepatocytes culminating in the induction of several ISGs. The ISG response leads to the production of chemokines by hepatocytes and recruitment of leukocytes to the liver[46,48,57]. Through the analysis of ISGs by microarrays in mice lacking IFNAR1 (*Ifnar1*$^{-/-}$), Liehl *et al*. identified hepatocytes as the primary source of ISG expression, since none of the genes were upregulated in the knockout mouse model in comparison to controls wild-type mice[48]. In addition, there was an increase in parasite liver load at 48h after *P. berghei* sporozoite injection in the absence of type I IFN-dependent signaling[48].

The type I IFN response is known to recruit immune cells to the site of infection[57]. Studies carried out by Liehl and Miller, and their respective colleagues, showed that the type I IFN pathway is important for the recruitment of leukocytes[48], particularly $CD8^+$ T cells and $CD49b^+$ $CD3^+$ NKT cells[49] in the liver following liver-stage infection and that the latter contribute to the elimination of liver stage parasites.

An important aspect of these studies is that the type I IFN response is not unique to one *Plasmodium* species, as the two studies were conducted independently with *P. berghei*[48] and *P. yoelli*[49].

In short, although the innate immune response to *Plasmodium* infection is not able to directly eliminate the parasites in the liver, it plays an essential role in activating and recruiting effector immune cells (e.g., $CD8^+$ T cells and NKT cells) that infiltrate in the liver to kill the infectious agent, and in preventing reinfections[48,49,58]. These findings contribute to a more complete

understanding of the innate immune response elicited by *Plasmodium* liver stage infection and how this response can limit parasite development in the liver and consequent infection of RBCs.

1.7. Immune evasion mechanisms of innate immunity during the pre-erythrocytic stage

Plasmodium parasites have a complex life cycle: they alternate between their mosquito and vertebrate hosts; depending on the stage of development, they can be extra- or intracellular; they present different forms and shapes; and they can infect different cell types during development. All these characteristics contribute to the parasite's ability to adapt to different hosts environments. Hence, during a *Plasmodium* infection, the vertebrate host displays various immune mechanisms to sense and fight the different forms of the parasite[46,59], while the latter has evolved strategies to escape host detection and/or to manipulate its defensive response to ensure survival and successful propagation.

During the pre-erythrocytic stage, *Plasmodium* parasites face strong innate immune responses from the host to limit the development of the liver stage. However, pre-erythrocytic parasites have developed a wide range of immune evasion strategies to escape host defenses during this stage of infection.

1.7.1. Strategies to overcome the skin barrier

The skin is the first barrier that sporozoites encounter after being deposited by the mosquito in the vertebrate host, acting as the first line of defense against *Plasmodium* parasites. To overcome this barrier, sporozoites have specialized proteins, such as SPECT1 and SPECT2, that are involved in motility and cell traversal ability, allowing their rapid migration to the blood vessels to avoid clearance by phagocytic cells. In fact, sporozoites deficient in the SPECT1 and SPECT2 proteins are immobilized in the dermis and subsequently destroyed by phagocytes, preventing their progression[60].

1.7.2. Modulation of Kupffer cells

Once in the bloodstream, sporozoites migrate to the liver where they must cross the sinusoidal cell layer to reach and invade hepatocytes. Studies employing intravital and electron microscopy techniques suggested that sporozoites do this through the Kupffer cells[61,62]. It is puzzling why these phagocytic cells do not kill sporozoites, despite being known to provide

innate immunity against microorganisms that invade hepatocytes. In fact, sporozoites evolved mechanisms to suppress the phagocytic function of Kupffer cells in order to actively penetrate them.

The CSP binds to the low-density lipoprotein receptor-related protein 1 (LRP-1) and proteoglycans on the Kupffer cell surface, increasing the levels of intracellular cyclic adenosyl mono-phosphate (cAMP) and exchange protein directly activated by cAMP (EPAC) which prevents the formation of reactive oxygen species (ROS) – a macrophage defense mechanism that can kill the parasite[63]. Additionally, the interaction between sporozoites and Kupffer cells downregulates the pro-inflammatory cytokines tumor necrosis factor alpha (TNF-α), interleukin-6 (IL-6), and monocyte chemoattractant protein 1 (MCP-1) and upregulates the anti-inflammatory cytokine IL-10 to ensure safe passage[64]. Moreover, in some cases, sporozoites induce Kupffer cell apoptosis[64].

1.7.3. Manipulation of hepatocytes

After successful crossing of the sinusoidal cell layer, sporozoites traverse several hepatocytes until they invade a final one with the formation of a PV, inside which sporozoites develop and differentiate into EEFs. The PV separates the sporozoite from the cytoplasm of the host cell, avoiding degradation by the endocytic/lysosome system[65].

Once inside the PV, sporozoites use different strategies to suppress hepatocyte function and inhibit cell death to ensure its survival and development. For instance, *Plasmodium* CSP promotes parasite proliferation by modulating the host inflammatory response[66]. CSP is released from the PV into hepatocyte cytoplasm through a protein export element denominated PEXEL (*Plasmodium* export element) motif. In the cytoplasm, CSP inhibits the nuclear factor kappa B (NF-κB) activation, preventing the transcription of pro-inflammatory genes regulated by this transcription factor[66]. Additionally, CSP inhibits protein synthesis in infected hepatocytes by binding ribosomes, blocking antigen presentation, which represent an immune evasion strategy[67]. Epiphanio *et al*. showed that *in vivo* liver infection with *P. berghei* and *P. yoelli* sporozoites induces the expression of the anti-inflammatory enzyme heme oxygenase-1 (HO-1) in hepatocytes. The up-regulation of HO-1 prevents inflammation, protecting the infected hepatocytes from an innate immune response, which allow the development of the parasite in the liver[68]. Furthermore, studies carried out with *P. berghei* have shown that parasites evade the attack of immune cells by actively inhibiting hepatocyte apoptosis during their development[69,70]. Sporozoite invasion interferes with hepatocyte regulatory pathways leading to up-regulation of mammalian target of rapamycin (mTOR) and down-regulation of

p53 and B-cell lymphoma 2 (Bcl-2), resulting in blockade of autophagy, cell cycle progression, and apoptosis, respectively[71,72].

In order to initiate the blood stage of infection, merozoites must exit hepatocytes, leaving them exposed to attack by hepatic phagocytes. To avoid host cell defenses, merozoites bud off from the hepatocytes in merosomes that are derived from the host cell membrane. In addition, merozoites inhibit the expression of phosphatidylserine on the surface of the merosome that function as a signal to phagocytes, preventing their recognition by phagocytic cells[73,74].

1.8. Genetic screening methods in malaria parasites

Plasmodium parasites have co-evolved with humans for centuries. Although powerful tools against malaria have been developed previously, such as highly effective insecticides to eliminate mosquito vectors or antimalarial drugs, like chloroquine, to control clinical malaria, *Plasmodium* parasites have always been able to adapt, escaping and developing resistance against these tools. *Plasmodium* parasites have evolved to express a diverse repertoire of molecules that modulate host-parasite interactions, contributing to immune evasion or modulation during infection, which warrant the parasite a chance to complete its development in the vertebrate host. Therefore, the identification of parasite molecules, and respective functions, that interact with the host's immune system and contribute to the outcome of *Plasmodium* liver stage infection is an urgent priority, with the ultimate goal of developing new targeted anti-malarial drugs and effective vaccines.

The understanding of the role of a particular *Plasmodium* protein during infection has evolved through the use of mutant parasites in which the encoding-gene is deleted or silenced using reverse genetic technologies[75,76]. However, initial attempts to apply reverse genetics in malaria research were not as successful as expected due to significant technical limitations, including: low rates of homologous recombination; the high content of adenine (A) and thymine (T) nucleotides, which makes genome manipulation difficult, since it makes *Plasmodium* genomic DNA unstable in *Escherichia coli* (model organism for genetic manipulation[77,78]); and the difficulties in introducing DNA into the parasite's nucleus while maintaining the host cell's integrity, as *Plasmodium* parasites spend most of their life cycle intracellularly[76,79,80].

In order to overcome these limitations, in 2006, Janse *et al.* reported a significant increase in transfection efficiency of the rodent-infective parasite *P. berghei* that strongly reduces the time, number of laboratory animals and amount of materials required to generate transfected parasites[80]. Despite the high A+T content in *P. berghei* (>77%), Pfender *et al.* were able to generate a representative genomic library covering most *P. berghei* genes in their entirety,

using a low-copy linear plasmid based on the bacteriophage N15[81], which replicates in *E. coli* as a linear, double-stranded DNA molecule[82]. Through the use of *lambda* phage recombinase-mediated engineering, a technology termed recombineering[83], it was possible to convert genomic DNA clones from this library into genetic modification vectors, which can be integrated into the *P. berghei* genome with efficiency due to their long homology arms[82].

1.8.1. The *Plasmo*GEM database

The genomes of malarial parasites contain many genes with unknown function due to the lack of efficient reverse genetic screening methods. Faced with the obstacles of experimental genetic approaches, Schwach and Bushell, along with their colleagues, launched, in 2015, the *Plasmodium* Genetic Modification (*Plasmo*GEM) database. This resource aims to provide the research community with a resource of vectors designed to manipulate the genome of *Plasmodium* parasites, as well as design tools that can be used in large-scale research projects[84].

The *Plasmo*GEM resource was created based on the recombineering technology[82] and contains knockout vectors that are quality controlled by next-generation sequencing[84]. Each vector carries a gene-specific molecular barcode of 10 – 11 nucleotides that can be used to identify individual vectors and transgenic parasites. Furthermore, all final *Plasmo*GEM vectors contain the *hdhfr-yfcu* marker that enables positive and negative selection *in vivo*[85]. The knockout vectors are transfected into *P. berghei* schizonts, the most suitable target cells for transfection of *P. berghei*, which are then injected into mice. The subsequent selection of genetically transformed parasites is based on the treatment of mice with drugs, namely by pyrimethamine, which selects for parasites expressing the *hdhfr-yfcu* marker [84,85].

Complex pools of barcoded *P. berghei* mutants can be generated by cotransfecting multiple gene knockout vectors in the same electroporation. Then, the pools can be injected into a single mouse and, employing a barcode sequencing approach (barseq) the number of barcodes can be counted and the growth rates of all mutants can be measured[86]. In this way, multiple *Plasmo*GEM vectors can be grouped into large pools of mutants to perform functional screens in malaria parasites using fewer mice. To analyze the growth curves derived from barcode counts, two parameters are considered: (1) the relative abundance of each barcode within the pool; and (2) the relative fitness of each mutant, i.e., the rate at which its abundance changes from day to day. Crossing these parameters, the competitive fitness of dozens of mutants can be measured during infection in the same mouse[84,86,87].

Currently, the *Plasmo*GEM database include a genomic library covering >90% of *P. berghei* genes and genome modification vectors for >2600 *P. berghei* genes[88], which can reduce the time and effort needed to modify parasite genes. The advantage of this approach is that each vector has a gene-specific molecular barcode, allowing the identification of individual mutants in the same mouse. Dropout screens that analyze which barcodes are lost between each stage of the *Plasmodium* life cycle make it possible to generate lists of candidate genes required for each stage.

The *Plasmo*GEM database in combination with barcode counting on a next-generation sequencer has already proven to be relevant for the identification of the essential genes and pathways required for the development of *Plasmodium*, both during the blood stage[87] and the liver stage[89]. In 2017, Bushell *et al*. measured competitive growth rates in mice of 2,578 barcoded *P. berghei* knockout mutants, representing more than 50% of the genome. They found that at a single stage of its complex life cycle, the asexual blood stage, *P. berghei* requires almost two-thirds of genes for optimal growth[87]. Later, in 2019, Stanway *et al.* generated pools of these blood stage-viable knockout mutants and analyzed their phenotypes throughout the entire parasite life cycle for the first time. Their findings provide interesting insights, including 1) the discovery of 461 genes required for efficient parasite transmission to mosquitoes through the liver stage and back into the bloodstream of mice; 2) the demonstration of a major reprogramming of parasite metabolism to achieve rapid growth in the liver; 3) the identification of essential metabolic pathways for parasite development[89].

These findings show the relevance of the applicability of the technique to fill existing gaps on the biology of the parasite, the physiology of the different stages of the life cycle, the interactions between host and *Plasmodium*, among others. Therefore, the technique may have a wide use in the different areas of study of *Plasmodium* infection, particularly in the immune response. For instance, pools of *P. berghei* knockout mutants may be combined with mice genetically modified for immune ablation to allow the identification not only of parasite genes that are targets of specific immune responses, but also of genes related to immune resistance/immune evasion mechanisms.

The rapid evolution of resistance to blood-stage drugs, including the current frontline antimalarial treatment, artemisinin, contributes greatly to the challenge of controlling malaria. The identification of genes with pivotal roles in the development of the liver stage, as well as in evasion of the host's immune system, is particularly important, since these genes may be potential drug and vaccine targets of the pre-erythrocytic stage of the parasite development, preventing the establishment of clinical disease.

1.9. Experimental models for malaria research

Although humans are the ideal system to investigate infection by *Plasmodium* and malaria disease, their use is not always possible due to ethical and practical limitations and, therefore, a variety of experimental models that can reproduce aspects of human disease are available for research, both for *in vitro* and *in vivo* studies[4].

Despite several advantages of using cell lines (mainly easy maintenance and propagation in the laboratory and a well-defined genome), their applicability becomes limiting, since they cannot replicate the *in vivo* environment, especially with regard to the host's immune response[90,91]. On the other hand, mouse models are useful to investigate host-parasite interactions as a whole, allowing to unravel the pathogenesis of the disease, as well as the subsequent responses of the immune system to fight the infection[4,90]. As such, and because there is a wide variety of models available, mouse models remain the closest tool to replicate the human disease, having been regularly used in the study and development of antimalarial drugs and vaccines[24,30,90]. Four species of rodent malaria parasites (*P. berghei*, *P. yoelii*, *P. chabaudi*, *P. vinckei*), each including multiple strains, have been used to study human disease *in vivo*, since that their basic biology is highly conserved with human-infectious *Plasmodium*[24,30,90]. *P. berghei* and *P. yoelii* have been the most commonly used models for liver stage *Plasmodium* infection research[4,92]. The large diversity of mouse and parasite species and strains available makes it possible to establish numerous host-parasite combinations that allow to assess different pathways and outcomes of infection and, subsequently, the progress of the disease[24,90,93]. Furthermore, it is also possible to genetically modify mice and parasites in order to manipulate and test specific conditions, helping to decipher host-parasite interactions, particularly the immune response[24,90].

At Instituto de Medicina Molecular João Lobo Antunes (iMM JLA, Lisbon)'s, Prudêncio Lab, *P. berghei*, which naturally infects rodents and does not pose a health concern for humans, is the experimental parasite model most used to study malaria. Analysis of the combination of this parasite with different mouse strains suggest that C57BL/6J mice present the highest susceptibility to *P. berghei* hepatic infection and, therefore, C57BL/6J-*P. berghei* is the preferred system to investigate liver stage infection[93]. Besides, it constitutes the most appropriate model to study the pathogenesis of experimental cerebral malaria (ECM)[24,28,30].

Objectives

2. Objectives

The clinically silent nature of the liver-stage of *Plasmodium* infection led to the assumption that parasites infect and replicate within the liver without being detected by the host immune system[13]. Nonetheless, it has been reported that the host can sense the parasites during this stage of infection and, subsequently, mount an anti-parasitic response. This response is mediated by the type I IFN pathway which recruits inflammatory cells, leading to a reduction in parasite load[48,94]. Although the parasite is known to have the ability to modulate the host's immune response, the identity of parasite proteins that are able to hinder the establishment of a protective immune response to ensure its survival remains poorly understood.

We hypothesize that specific *Plasmodium* molecules may modulate the ability of the parasite to evade and/or escape immunity in the liver under different immune conditions. To validate this, we combine the use of a transgenic rodent model of immune ablation with a high-throughput genetic screening tool based on pools of *P. berghei* knockout mutants. Thus, the main goal of this thesis is to identify *Plasmodium* molecules that interact with the host's innate immune system and contribute to the outcome of the liver stage of *Plasmodium* infection.

To this end, we established the following aims:

1. Validate the reproducibility of the methodology employed.
2. Identify and quantify specific transgenic knockout mutant parasites capable of completing liver stage development in either wild-type or *Ifnar1*$^{-/-}$ mice, in which type I IFN response is abolished.
3. Provide insights on specific parasite proteins that are directly involved in parasite evasion and/or modulation of the type I IFN response in the host liver.

Materials and Methods

3. Materials and Methods

3.1. Use of rodents

Mice were housed under specific-pathogen-free (SPF) conditions and in a 12-hour light/dark cycle, with food and water *ad libitum*, in the animal house facility of Instituto de Medicina Molecular João Lobo Antunes (iMM JLA), a licensed establishment that complies with the European Directive 2010/63/EU on the protection of animals used for scientific purposes. All *in vivo* experiments were approved by iMM JLA's Animal Care and Ethics Committee guidelines (ORBEA – Órgão Responsável pelo Bem-Estar Animal) and were performed in strict compliance with the guidelines of the Federation of European Laboratory Animal Science Associations (FELASA).

C57BL/6J wild-type (WT) mice, aged eight to ten weeks-old, and BALB/c, aged six to ten weeks-old, were purchased from Charles River Laboratories. IFNAR1 knockout (KO) mice (*Ifnar1*$^{-/-}$) on the C57BL/6J background, in which the type-I IFN response is ablated, were bred in the animal house facility of iMM JLA under SPF conditions and were used at six to ten weeks-old.

3.2. Use of mosquitoes

Anopheles stephensi mosquitoes were bred at the insectary facility of iMM JLA in conditions of 27 °C and 80% humidity and in a 12-h light/dark cycle. Mosquitoes were fed on mice infected with *P. berghei* parasites to obtain the sporozoites (spz). Following infection with *P. berghei* parasites, mosquitoes were maintained at 21 °C at 80% humidity in a 12-h light/dark cycle. All mosquitoes were supplied with 10% glucose solution (filter sterilized, supplemented with para-aminobenzoic acid – PABA) and for dissection were anaesthetized on ice.

3.3. Parasites

Generation and transmission of transgenic parasite pools

To perform infectious challenge of the mice, pools of barcoded *P. berghei* KO mutants kindly provided by Dr. Ellen Bushell, our collaborator at MIMS, in the Umeå University, Sweden, were used. For the generation of these KO parasite pools, 192 KO vectors were assigned to vector pools, creating a total of 2 pools of vectors, each one with 96 KO vectors. KO vectors were transfected into *P. berghei* schizonts and these transfected schizonts were injected into

BALB/c mice and selected by pyrimethamine following previously described procedures[86,89]. Identification numbers for all vectors included in this study are listed in Supplementary Table 1 (Annexes) and can be used to access details of each vector design, primer, and barcode sequences through the *Plasmo*GEM database at https://plasmogem.umu.se/pbgem/[84]. Infected blood was collected in complete schizont medium (RPMI 1640 supplemented with 25mM L-glutamine, 25mM HEPES, 10mM $NaHCO_3$, 100 U/mL penicillin/streptomycin and 25% fetal bovine serum) and shipped to the host laboratory where, for subsequent expansion and transmission, it was intravenously injected to various BALB/c mice (Figure 3.1). When parasitemia reached 5%, a blood sample was stored for further sequencing, and ~150 *Anopheles stephensi* mosquitoes were allowed to feed on anesthetized mice in order to generate spz. Mosquitoes were monitored until KO mutant spz were present in the mosquito salivary glands (~21 days). At the end of this task, KO mutant spz covering all the targetable *P. berghei* genes were produced and subsequently employed as the challenge agent for mice for subsequent barseq sequencing to identify and quantify specific transgenic parasite KO mutants present at each stage of the life cycle and under differential innate immune pressure.

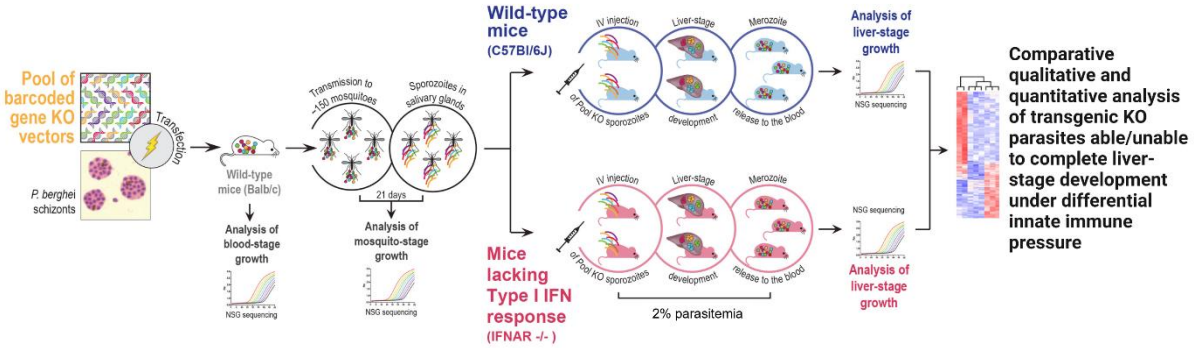

Figure 3.1. Schematic representation of a high-throughput gene knockout barseq screen. Pools of barcoded *Plasmo*GEM KO vectors were transfected into *P. berghei* schizonts by electroporation and injected into pyrimethamine-treated mice for transfectant parasites selection. Infected mice, from which a blood sample was collected for further sequencing, were used to infect *Anopheles stephensi* mosquitoes. At day 21 post-infection, spz of KO parasite pools were isolated from infected mosquito salivary glands and intravenously injected into both WT and *Ifnar1*$^{-/-}$ mice, as well as stored for later sequencing. Blood from infected mice was collected for barcode sequencing. DNA samples were used for sequencing by an Illumina platform to determine the barcode counts and to do a qualitative and quantitative analysis of transgenic KO parasites at each stage of the life cycle.

3.4. Sporozoite collection

On day 21 after mosquito infection, the salivary glands of infected Anopheles *stephensi* mosquitoes were hand-dissected and collected in non-supplemented Roswell Park Memorial Institute 1640 (RPMI 1640; Gibco) medium, in order to obtain spz. The salivary glands were mechanically homogenized to release the spz and filtered through a 40 µm strainer. Sporozoites were then counted in a Neubauer chamber using a ZEISS Primovert inverted

microscope and the concentration was adjusted with non-supplemented RPMI medium to have 30,000 spz/200 µL.

3.5. *In vivo* infection of mice

For all the inoculations, mice were previously anaesthetized using isoflurane (IsoFlo®; Zoetis) and freshly collected *P. berghei* spz diluted in RPMI 1640 were inoculated.

WT and *Ifnar1*$^{-/-}$ mice were infected with 30,000 spz of *P. berghei* KO mutants by retro-orbital intravenous injection. Vials of 150,000 – 200,000 spz were stored at -80 °C for sequencing.

Experimental groups consisted of five mice housed together.

3.6. Assessment of parasitemia

The presence of blood stage parasites was monitored daily between days 3 and 12 post-infection and parasitemia was determined by methanol-fixed and Giemsa-stained thin blood smears on a ZEISS Axio Lab.A1 microscope and expressed as percentage of infected red blood cells (iRBCs). When parasitemia reached 2.0%, mice were sacrificed by isoflurane overdose (Figure 3.2) and blood was collected by cardiac puncture using sodic heparin (5000 U.I./mL; B. Braun) as an anticoagulant, for parasite genomic DNA (gDNA) extraction.

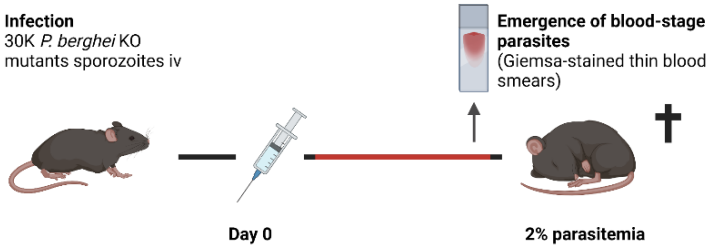

Figure 3.2. Schematic representation of the mouse infection daily monitoring. Mice infection with KO parasite mutants and assessment of parasitemia. Created with BioRender.com

3.7. Preparation of direct amplification libraries for barcode counting by Illumina sequencing

3.7.1. Genomic DNA sampling

The isolation of parasite gDNA from mice blood was performed using a phenol-chloroform extraction method.

A total of 300 µL of infected blood was diluted in 500 µL of 1x phosphate-buffered saline (PBS) and centrifuged at 2,348 rcf, at 4 °C, for 10 min to precipitate the RBCs. The pellet was resuspended in 2 mL of Ammonium-Chloride-Potassium (ACK) solution (0.15 M NH_4Cl, 0.01 M $KHCO_3$, 0.001 M EDTA) for 15 min on ice to lyse the RBCs and subsequently centrifuged for 5 min at 500 rcf, at 4 °C, finishing with 1 min at 2,348 rcf. The supernatant was carefully removed, and the pellet was frozen in liquid nitrogen and stored at -80 °C until the blood of all experimental mice was sampled.

The pellet of each sample was resuspended in a total volume of 992 µL with 700 µL of TNE buffer (10 mM Tris pH 8.0, 5 mM EDTA pH 8.0, 100 mM NaCl), 100 µL 10% SDS, 190 µL dH_2O and 2 µL RNase (100 mg/mL) (NZYTech) and then incubated for 10 min at 37 °C. After this incubation, 20 µL of proteinase K (10 mg/mL) was added to each sample that was incubated at 37 °C for 30 min to digest proteins. The digested mix was decanted into a 2 mL Phase Lock Gel Light Tube (QuantaBio) and 700 µL buffered phenol:chloroform:isoamylalcohol (25:24:1) (Sigma-Aldrich/Merck) was added and subsequently inverted vigorously several times to mix and centrifuged for 5 min at 16,000 rcf, at room temperature (RT). The aqueous upper phase was decanted into a new 2 mL Phase Lock Gel Light Tube, without disturbing the cloudy mid-layer, and 700 µL chloroform:isoamylalcohol (24:1) (Sigma-Aldrich/Merck) was added and again inverted vigorously several times to mix and centrifuged for 5 min at 16,000 rcf at RT. The aqueous upper phase was decanted to a clean 2 mL tube, without disturbing the cloudy mid-layer, and 900 µL 100% isopropanol was added to precipitate DNA overnight at 4 °C. The next day, the precipitated DNA was centrifuged at 15,871 rcf, at 4 °C, for 30 min and all supernatant was carefully removed and allowed to air dry. To finish this gDNA extraction method, 102 µL dH_2O was added to all samples.

The concentration of DNA in each sample was assessed by measurement of absorbance at 260 nm on a NanoDrop 2000 spectrophotometer.

3.7.2 Preparation of barcoded (“indexed”) sequencing libraries

Each of the extracted gDNA samples contains a mixture of unique barcodes assigned to single KO lines, that were counted through Illumina sequencing in order to determine the abundance of each gene KO parasite and compare between different experimental conditions. For that, Illumina sequencing libraries were prepared using a nested PCR approach, i.e., an approach that involves two sequential amplification reactions and therefore, two different pairs of primers to amplify a target sequence[95]. First, 5 µL of each DNA sample served as template for a PCR reaction using Advantage® 2 Polymerase Mix (Takara) with primers 91 and 97, which bind to

constant annealing sites flanking each barcode. Amplification of the barcodes was performed using the following program: 5 min at 95 °C for initial denaturation, followed by 35 cycles of 30 sec at 95 °C, 20 sec at 55 °C and 8 sec at 68 °C, finishing with 10 min at 68 °C. For sample-specific indexing, 2.5 µL of the first amplicon (~150 bp) served as template for a second PCR reaction using one generic oligonucleotide (PE 1.0) and one of a set of 30 sample-specific indexing oligonucleotides (Table 3.1), allowing multiplexing up to 30 samples in one run of a MiSeq instrument. To introduce Illumina indexes, the following program was performed: 2 min at 95 °C for initial denaturation, followed by 10 cycles of 30 sec at 95 °C, 15 sec at 68 °C and 8 sec at 68 °C, finishing with 5 min at 68 °C. A water control was used throughout the entire experiment to ensure that reagents were not contaminated.

After each PCR reaction, the amplified PCR products were analyzed by gel electrophoresis on a 2% agarose gel stained with GelRed® Nucleic Acid Stain (Biotium) and revealed on Amersham ImageQuant 800.

The resulting libraries consisting of 240 bp long amplicons containing sample-specific indexes were cleaned to purify the DNA, using NZYDNA Clean-up 96 well plate kit (NZYTech), according to the manufacturer's instructions. After that, the libraries were sent to our collaborators at MIMS that quantified them using Qubit HS Kit and pooled equal amounts (125 ng) of each sequencing library. Libraries were sequenced using MiSeq Reagent Kit v2 (300 cycle) from Illumina (MS-102-2002).

Table 3.1 | List of oligonucleotides used for barcode sequencing.

Oligo name	Sequence 5' → 3'
Primer 91	TCGGCATTCCTGCTGAACCGCTCTTCCGATCTGTAATTCGTGCGCGTCAG
Primer 97	ACACTCTTTCCCTACACGACGCTCTTCCGATCTCCTTCAATTTCGATGGGTAC
PE 1.0	AATGATACGGCGACCACCGAGATCTACACTCTTTCCCTACACGACGCTCTTCCGATC*T
iPCRindex1	CAAGCAGAAGACGGCATACGAGATTGCTAATCACTGAGATCGGTCTCGGCATTCCTGCTGAACCG CTCTTCCGATC*T
iPCRindex2	CAAGCAGAAGACGGCATACGAGATTAGGGGGATTCGAGATCGGTCTCGGCATTCCTGCTGAACCG CTCTTCCGATC*T
iPCRindex3	CAAGCAGAAGACGGCATACGAGATAGTTTCCCAGGGAGATCGGTCTCGGCATTCCTGCTGAACCG CTCTTCCGATC*T
iPCRindex4	CAAGCAGAAGACGGCATACGAGATCCTGGGAGGTAGAGATCGGTCTCGGCATTCCTGCTGAACCG CTCTTCCGATC*T
iPCRindex5	CAAGCAGAAGACGGCATACGAGATATACCACAAATGAGATCGGTCTCGGCATTCCTGCTGAACCG CTCTTCCGATC*T
iPCRindex6	CAAGCAGAAGACGGCATACGAGATGATCTCTCGGGGAGATCGGTCTCGGCATTCCTGCTGAACCG CTCTTCCGATC*T
iPCRindex7	CAAGCAGAAGACGGCATACGAGATACCCTATACTCGAGATCGGTCTCGGCATTCCTGCTGAACCG CTCTTCCGATC*T
iPCRindex8	CAAGCAGAAGACGGCATACGAGATCTCAATTAAGAGAGATCGGTCTCGGCATTCCTGCTGAACCG CTCTTCCGATC*T
iPCRindex9	CAAGCAGAAGACGGCATACGAGATCGACAGAACGTGAGATCGGTCTCGGCATTCCTGCTGAACCG CTCTTCCGATC*T
iPCRindex10	CAAGCAGAAGACGGCATACGAGATTCGCCATTATGGAGATCGGTCTCGGCATTCCTGCTGAACCG CTCTTCCGATC*T

iPCRindex11	CAAGCAGAAGACGGCATACGAGATATGTTCCGGCCGAGATCGGTCTCGGCATTCCTGCTGAACCG CTCTTCCGATC*T
iPCRindex12	CAAGCAGAAGACGGCATACGAGATTCTTGAAGTGAGAGATCGGTCTCGGCATTCCTGCTGAACCG CTCTTCCGATC*T
iPCRindex13	CAAGCAGAAGACGGCATACGAGATGAAGGCCAGCTGAGATCGGTCTCGGCATTCCTGCTGAACCG CTCTTCCGATC*T
iPCRindex14	CAAGCAGAAGACGGCATACGAGATCCAATGTGCAGGAGATCGGTCTCGGCATTCCTGCTGAACCG CTCTTCCGATC*T
iPCRindex15	CAAGCAGAAGACGGCATACGAGATATCGAAGGACCGAGATCGGTCTCGGCATTCCTGCTGAACCG CTCTTCCGATC*T
iPCRindex16	CAAGCAGAAGACGGCATACGAGATTCGGGTGCGAAGAGATCGGTCTCGGCATTCCTGCTGAACCG CTCTTCCGATC*T
iPCRindex17	CAAGCAGAAGACGGCATACGAGATGTAATTTACGGGAGATCGGTCTCGGCATTCCTGCTGAACCG CTCTTCCGATC*T
iPCRindex18	CAAGCAGAAGACGGCATACGAGATATATCGACTACGAGATCGGTCTCGGCATTCCTGCTGAACCG CTCTTCCGATC*T
iPCRindex19	CAAGCAGAAGACGGCATACGAGATTGATTCTTACAGAGATCGGTCTCGGCATTCCTGCTGAACCG CTCTTCCGATC*T
iPCRindex20	CAAGCAGAAGACGGCATACGAGATACGGCGGGCCTGAGATCGGTCTCGGCATTCCTGCTGAACC GCTCTTCCGATC*T
iPCRindex21	CAAGCAGAAGACGGCATACGAGATCTTGCGTGGAGGAGATCGGTCTCGGCATTCCTGCTGAACCG CTCTTCCGATC*T
iPCRindex22	CAAGCAGAAGACGGCATACGAGATTAATCAAAGACGAGATCGGTCTCGGCATTCCTGCTGAACCG CTCTTCCGATC*T
iPCRindex23	CAAGCAGAAGACGGCATACGAGATGGCGGGCTCTAGAGATCGGTCTCGGCATTCCTGCTGAACC GCTCTTCCGATC*T
iPCRindex24	CAAGCAGAAGACGGCATACGAGATCCTCCATTTCTGAGATCGGTCTCGGCATTCCTGCTGAACCG CTCTTCCGATC*T
iPCRindex25	CAAGCAGAAGACGGCATACGAGATAACCAGCGCTGGAGATCGGTCTCGGCATTCCTGCTGAACCG CTCTTCCGATC*T
iPCRindex26	CAAGCAGAAGACGGCATACGAGATTATTCGTCAACGAGATCGGTCTCGGCATTCCTGCTGAACCG CTCTTCCGATC*T
iPCRindex27	CAAGCAGAAGACGGCATACGAGATGCGCTGATGCAGAGATCGGTCTCGGCATTCCTGCTGAACCG CTCTTCCGATC*T
iPCRindex28	CAAGCAGAAGACGGCATACGAGATCTCATATGGCTGAGATCGGTCTCGGCATTCCTGCTGAACCG CTCTTCCGATC*T
iPCRindex29	CAAGCAGAAGACGGCATACGAGATACAGGGGCAGGGAGATCGGTCTCGGCATTCCTGCTGAACC GCTCTTCCGATC*T
iPCRindex30	CAAGCAGAAGACGGCATACGAGATGGTTTTATACCGAGATCGGTCTCGGCATTCCTGCTGAACCG CTCTTCCGATC*T

* asterisk denotes phosphorothioate bond between the penultimate and final base pair.

3.8. Barcode counting

Our collaborators at MIMS extracted the barcode sequences from the sequencer output and counted the total number of barcodes for each gene, for each mouse. Raw reads from the sequencer were separated based on their sample which was identified through the index tag. Each sample contains a mixture of unique barcodes assigned to single KO lines that were counted and then transformed into gene IDs.

At the host laboratory, the data were analyzed and any mutant with a number of counts below 50 in the sample were excluded from subsequent analysis. The abundance of each barcode in each sample was calculated using DESeq approach[96], in order to be able to compare read counts between different samples:

- ***r*** is the raw count of barcode ***b*** in sample ***S***;
- for each barcode ***b***, the geometric mean ***m*** of the raw counts for all the samples for that gene was calculated;
- for each sample ***S***, the normalization factor ***N*** was calculated as the median of the values ***r'***, where ***r'*** = $\frac{r}{m}$;
- the normalized counts ***n*** for each barcode ***b*** in the sample ***S*** were obtained by $\frac{r}{N}$.

3.9. Gene ontology analysis

Gene ontology (GO) terms related to biological processes, molecular function, and cell component and interpro domains were downloaded from PlasmoDB at https://plasmodb.org/plasmo/app.

3.10. Statistical analysis

Results are expressed as mean ± standard error of the mean (SEM). Statistical analyses were performed using the GraphPad Prism 9 software. Comparisons between two different groups were performed using the Mann-Whitney test. *P*-values less than 0.05 were considered statistically significant.

Results and Discussion

4. Results and Discussion

4.1. A high-throughput barcode-based sequencing approach for targeting *P. berghei* genes

Rodent malaria parasites possess compact genomes of 18–30 Mb, which encode an average of 5,500 genes. However, nearly 50% of the genes in the *Plasmodium* genomes have unknown functions due to the lack of efficient reverse genetic screening methods. To respond to these difficulties, our collaborators at Laboratory for Molecular Infection Medicine Sweden - MIMS (Umeå University, Sweden) developed an innovative method for reverse genetic screening of the *P. berghei* genome and created an open-access *Plasmodium* genetic modification resource, *Plasmo*GEM, which includes *P. berghei* knockout (KO) vectors tagged with gene-specific molecular barcodes, which allow for the generation of pools of *P. berghei* KO mutants[84,86]. Here, we propose to use this high-throughput genetic screening tool to investigate *Plasmodium* molecules that interact with the host's innate immune system and contribute to the outcome of the liver stage of *Plasmodium* infection.

The development of this project relied on the collaboration with our partners, who prepared the pools of barcoded *P. berghei* KO mutants used to perform infectious challenge of the mice (Figure 4.1. A). The detailed experimental procedure has been described in the material and methods section. Briefly, 192 barcoded *Plasmo*GEM vectors were assigned to vector pools, creating a total of 2 pools of vectors, each containing 96 KO vectors. To generate pools of mutant parasites, the *Plasmo*GEM vectors were transfected by electroporation into purified *P. berghei* schizonts, and the transfection mixture was immediately injected intravenously into BALB/c mice. After 24 hours of infection, mice were placed under selective drug pressure to eliminate wild-type parasites, while allowing transfected parasites to thrive[86,89]. Infected blood was collected, cryopreserved, and shipped to iMM JLA. At the host laboratory, blood infected with KO parasites was intravenously injected into two BALB/c mice. When parasitemia reached 5%, blood samples from each mouse were collected to establish the starting composition of mutants and ~150 *Anopheles stephensi* mosquitoes were allowed to feed on anesthetized mice. At day 21 post-infection, sporozoites (spz) of KO parasite pools were isolated from infected mosquito salivary glands and intravenously injected into both C57BL/6J (WT) and *Ifnar1*$^{-/-}$ mice, as well as stored for later genetic sequencing to determine the composition of mutant parasite pools in salivary glands. At 2% parasitemia, blood from spz-infected mice was collected to establish the composition of the mutant pool, allowing assessment of parasite development in the liver (Figure 4.1. B). The parasite gDNA from the samples collected

throughout the experiment was isolated and used for nested PCR of vector barcodes, with an index primer used to tag each sample for individual identification, and subsequent sequencing by an Illumina platform for barcode counting analysis. The barcode sequencing and subsequent counting of the barcode sequences using a Perl script was conducted by our collaborators at MIMS.

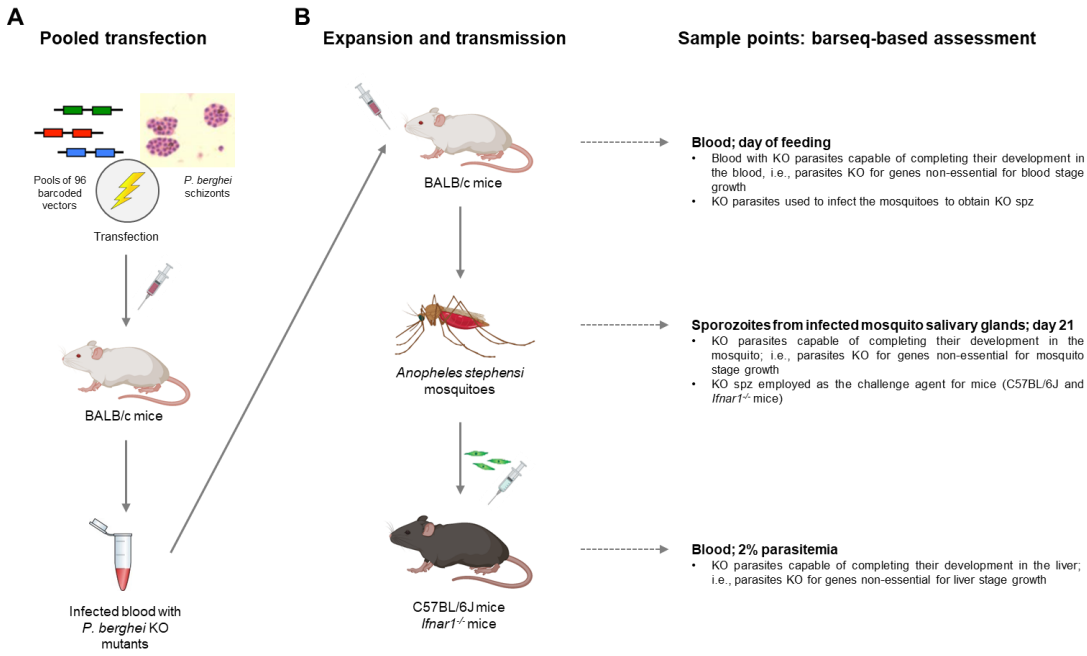

Figure 4.1. Schematic representation of a parasite gene KO screen using a barcode-based sequencing assay. (A) Pooled transfection by our collaborators at MIMS. Pools of barcoded *Plasmo*GEM KO parasites were transfected into *P. berghei* schizonts by electroporation. Transfectant parasites were intravenously injected into BALB/c and selected by pyrimethamine from day one post-infection. Infected blood was collected, cryopreserved, and shipped to the host laboratory. **(B)** Expansion and transmission of transgenic parasite pools in the host laboratory. Infected blood with *P. berghei* KO mutants was injected to two BALB/c mice, which were used to infect female *Anopheles stephensi* mosquitoes. On day 21 post-infection, spz of KO parasite pools were isolated from infected mosquito salivary glands and injected intravenously into both C57BL/6J and *Ifnar1*$^{-/-}$ mice. At 2% parasitemia, blood from spz-infected mice was collected for barcode sequencing. Barcode counts determined by DNA barcoding sequence were used to do a qualitative and quantitative analysis of mutant KO parasites at either the blood, the mosquito, and the liver stages of infection. Created with BioRender.com

The 192 genes selected as targets to produce *P. berghei* KO mutants for this study, were previously phenotypically characterized as being either essential or partially redundant (92, 48%), or non-essential (100, 52%) to complete liver stage development[89]. Based on this previous characterization, we established two phenotype designations for the assessment of impact in parasite liver stage development that are used throughout the study (Figure 4.2):

1) compromised liver development: includes genes that are predicted as essential or partially redundant for completion of the parasite's development in the liver;

2) regular liver development: includes genes that are predicted as non-essential for completion of the parasite's development in the liver.

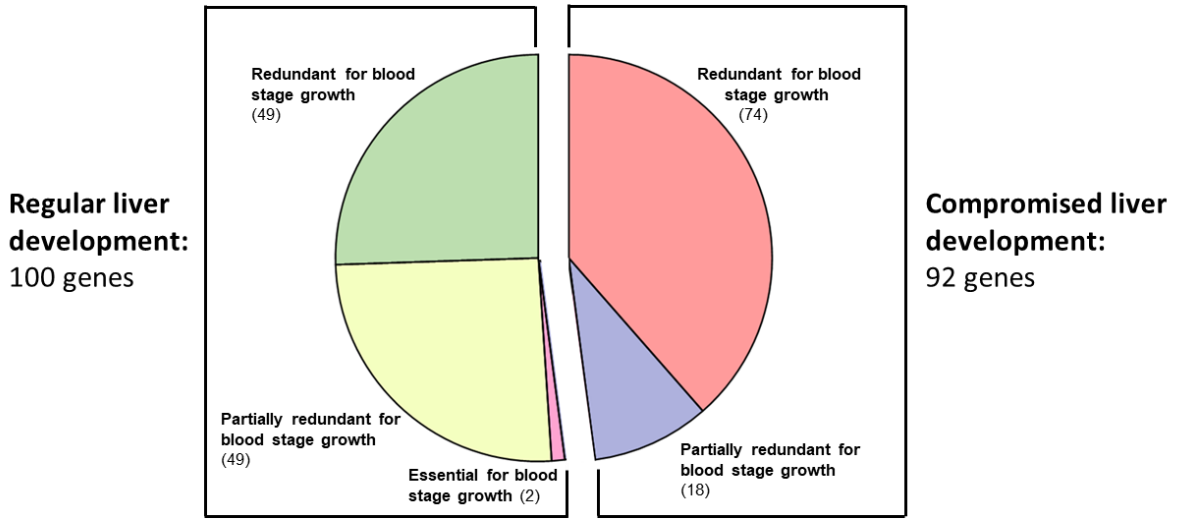

Figure 4.2. Liver stage phenotypes. Frequency distribution of liver stage growth phenotypes for targeted *P. berghei* genes that at the blood stage are redundant, partially redundant, or essential for normal growth[87].

4.2. Validating DNA barcode sequencing for analysis of gene KO mutants

Before screening large numbers of genes, we first assessed the biological and technical replicability of the barcoding sequencing analysis. Until now, in experiments employing this technique, the transfected barcoded parasites were immediately injected into the mouse, carrying out the experiment from start to finish, without interruption[86,87,89]. So, we sought to determine if it would be possible to cryopreserve blood infected with mutant parasites, ship it to another laboratory and use it in *in vivo* experiments, without compromising the viability of the transfected parasites. Furthermore, we asked whether the final composition of KO parasite in the pool would be different if we performed the expansion of the transfected parasite in various BALB/c mice and, consequently, their transmission to different mosquito batches.

To test this hypothesis, a pool of 96 KO mutant parasites was produced and blood carrying these parasites was divided into two vials (A and B) that were used to initiate an experiment with two technical replicates. Each vial was used to infect two BALB/c mice simultaneously, which were then used to feed approximately 150 *Anopheles stephensi* mosquitoes. The spz collected from salivary glands from each group of mosquitoes were injected into 5 C57BL/6J mice (Figure 4.3).

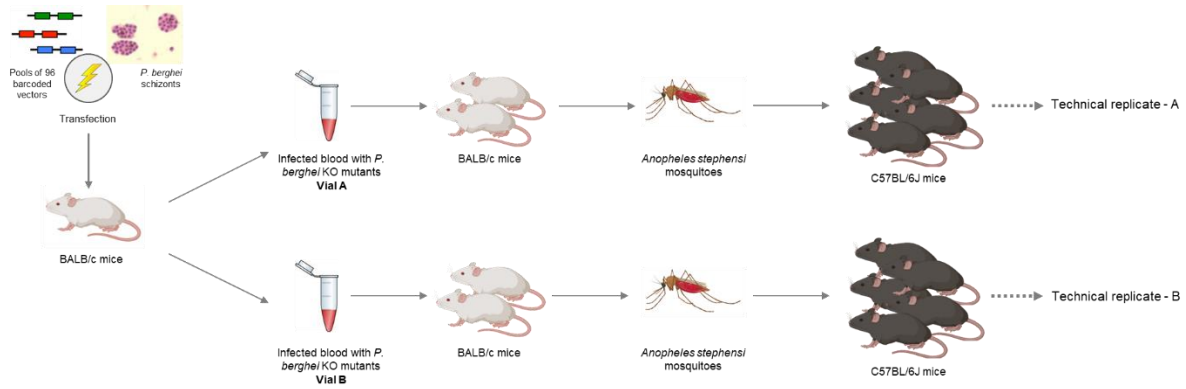

Figure 4.3. Schematic representation of the experimental design used to assess reproducibility of KO parasite life cycle development by barcode sequencing. For each experiment, two BALB/c mice were injected with blood infected with the same pool of vectors. Created with BioRender.com

4.2.1. Mice parasitemia

An initial comparison between the two technical replicates was made by daily monitoring the presence of blood stage parasites after they had been infected with 30,000 KO spz. In each of the two technical replicates, mice reached at least 2% parasitemia on day 5 post infection and were euthanized for blood collection (Figure 4.4). Furthermore, we ensured that the overall parasitemia at the time of blood collection was not significantly different so that this would not influence our analysis.

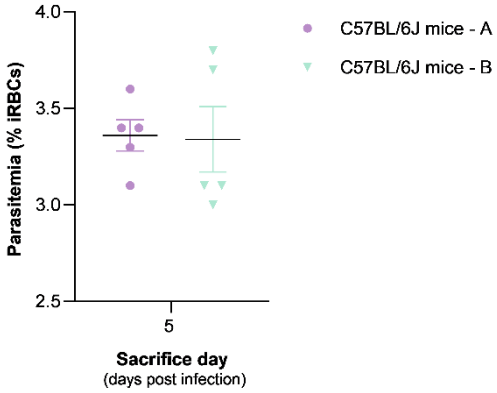

Figure 4.4. Mice parasitemia at the time of blood collection. % of parasitemia in both groups of mice (n=5 mice per group) on the day of sacrifice, assessed by Giemsa-stained thin blood smears. Symbols represent the individual values of each mouse and data are expressed as means ± SEM.

4.2.2. Quality control assessment of barcode sequencing results

Barcode sequences were extracted from the sequencer output and the total number of barcodes for each gene, for each sample, was counted. The number of reads obtained for the

different KO parasites was very diverse with some presenting >20000 reads while other <20, representing potential misread sequences. To determine the minimum cut-off number of reads to be considered for ensuing analysis, warranting the high quality of the sequencing data without losing significant information, we performed a distribution analysis.

Different numbers of reads cut-offs were established and the % of mutant parasites identified at each cut-off was determined. We found no significant difference in the % of parasites covered for the cut-offs of 50, 100 and 500 counts (Figure 4.5), although a higher number of counts <20 were detected, indicating that potentially, below a threshold of 50 counts, the probability of inclusion of misreading errors is higher. Thus, we established a cut-off of 50 counts that we assume is sufficient to ensure the technical quality of the analysis and, therefore, any barcode/mutant parasite with a number of reads below 50 in a specific sample was excluded from subsequent analysis.

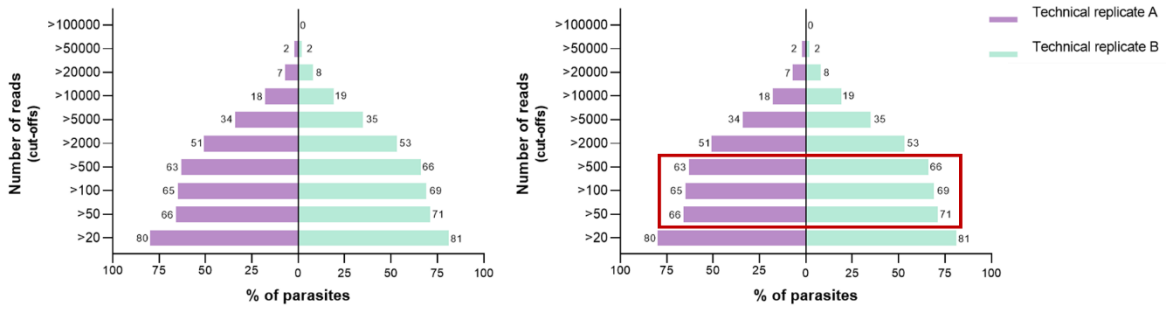

Figure 4.5. A lower threshold limit of 50 reads has established as quality control for barcode sequencing. Different cut-offs for the number of counts were established and the % of parasite mutants detected at each cut-off was evaluated.

4.2.3. Overall quantitative assessment of KO parasites pool composition across various life cycle stage transitions and different technical replicates

Having established a quality control cut-off for sequencing reads, we were able to determine with high confidence the presence or absence of a specific KO parasite in each sample. Collectively, we could subsequently identify differences in the pool of parasites between the various life cycle stages, as well as between technical replicates.

Of the 96 vectors used for transfection, we identified 55 KO parasites in the blood of BALB/c mice (Figure 4.6. A), representing a 42.7% loss of KO parasites in each of two replicate experiments (Figure 4.6. B). We hypothesize that such loss of KO parasites is due to the freezing process that the blood infected with the transfected parasites underwent to allow its shipment between laboratories. One possible way to confirm this hypothesis in the future is to barcode sequence the mutant parasite pool present in the blood before freezing and

immediately after thawing, providing us with a better insight into whether KO parasites are lost during the freezing process. However, we predict that such hypothesis is unlikely to be correct because our results indicate that the pool composition of parasites present in A and B is very similar (86.4% overlap). Therefore, the fact that the KO parasites lost during the freezing process are practically the same between the two technical replicates (Figure 4.6. C) suggests that the loss of parasites was not random, as would be expected if it was caused by the freezing process. Next, we hypothesized that the genes targeted in the KO parasites lost in this stage transition were essential genes for blood-stage growth, which would result in the death of the mutant parasite at this stage. However, these target genes were characterized as non-essential for completing parasite development in the blood in previous studies, which does not support this hypothesis[87]. Additionally, it is also possible that different vectors integrate into the parasite's genome with different efficiency (integration efficiency depends on the length of vectors homology arms and recombination rate)[86]. Hence, we could not confidently determine whether an absence of barcodes for a particular mutant was due to the inability of this mutant to grow or due to the inability of the vector to integrate into the genome.

The mutant parasites identified in the blood of BALB/c mice and in the spz isolated from the salivary glands of mosquitoes are the same. Thus, as no mutant parasites were lost, we assume that none of the target genes used in the experiment are essential for parasite development in the mosquito (Figure 4.6 C).

In the blood of C57BL/6J mice (which allow the assessment of parasite development in the liver), 42 mutant parasites were identified in replicate A and 44 mutant parasites in replicate B (Figure 4.6. A), representing a loss of 24% and 20% of parasites, respectively, during the transition from sporozoite to blood stage form and across liver stage development (Figure 4.6. B). Although we have identified 5 mutant parasites unique to replicate A and 7 mutant parasites unique to replicate B, the difference in the composition of the parasite pools is not significant, since there is a 76% overlap between the two replicates (Figure 4.6. C). Therefore, we conclude that the two technical replicates, A and B, are not significantly different in terms of KO parasite identity and are therefore similar in that regard.

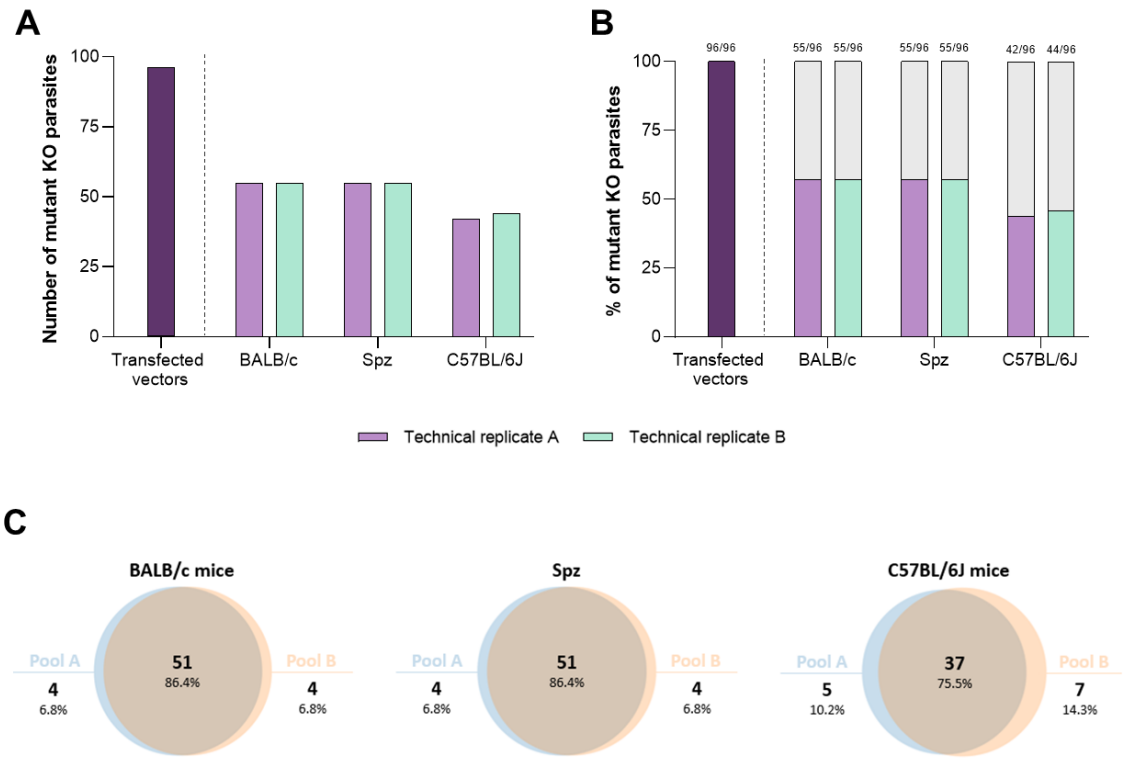

Figure 4.6. Comparative analysis of KO parasites present at various life cycle stages indicates no significant differences between the technical replicates. The number **(A)** and the % **(B)** of total distinct mutant KO parasites observed at each stage of the life cycle for each of the technical replicates. **(C)** Venn diagram of the comparative analysis between the mutant parasites identified in replicates A (blue) and B (orange) for the three sample points (BALB/c mice, spz and C57BL/6J mice).

4.2.4. Qualitative assessment of KO parasites capable to completing various life cycle stage transitions in different technical replicates

Having shown that there are no significant differences in the total number of distinct KO parasites composing the parasite pools identified in the two replicates at various life cycle stages, we questioned if there were differences in the developmental profile of the KO parasites identified for both replicates. To answer this question two parameters were evaluated and compared between the two replicates: 1) the frequency of each KO parasite in the blood of the various infected C57BL/6J mice at the end of the experimental procedure, which we expect should reflect the ability of the KO parasite to survive the various life cycle stage transitions analyzed; 2) the abundance of each KO parasite at the various life cycle stages analyzed, which should reflect the capacity of the parasite to replicate at each life cycle stage.

We first evaluated the number of C57BL/6J mice in which each mutant parasite was identified in the blood after injected with 30,000 mutant spz to determine the frequency of each mutant parasite in the samples (mice positive for the mutant parasite/mice injected with mutant spz).

Here, we focused our analysis on mutant parasites present in both replicates (37 mutant parasites). We concluded that overall, the average frequency of mutant parasites in the blood of C57BL/6J mice is similar between the two technical replicates (Figure 4.7. A). When considering each mutant parasite individually, the frequency of each mutant parasite is similar for the two technical replicates (Figure 4.7. B).

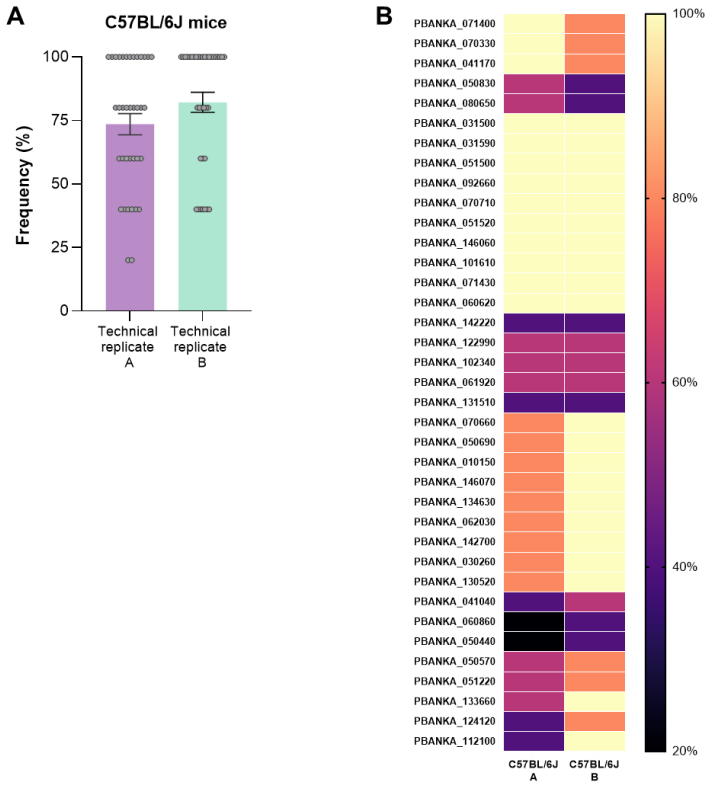

Figure 4.7. Frequency of KO parasites among mice from technical replicate group A and B. C57BL/6J mice were infected with 30,000 *P. berghei* KO spz and the frequency of each mutant parasite was measured for each technical replicate. **(A)** Frequency of mutant parasites in the blood of C57BL/6J mice in the two technical replicates (n=5 per group). Dots represent the individual values of each mutant parasite and data are expressed as means ± SEM. **(B)** Heat map representing the frequency (%) of each mutant parasite (rows) in each group of mice (columns).

Next, we evaluated the abundance of the mutant parasites in each life cycle stage, considering only the parasites that appear in both technical replicates (BALB/c mice, 51 KO parasites; spz, 51 KO parasites; C57BL/6J mice, 37 KO parasites). Thus, in an overall context, the average abundance of mutant parasites at each life-cycle stage is similar between the two technical replicates (Figure 4.8. A). Looking at each mutant parasite individually, the abundance of each mutant parasite is similar for the two technical replicates, and for all three sample points (Figure 4.8. B).

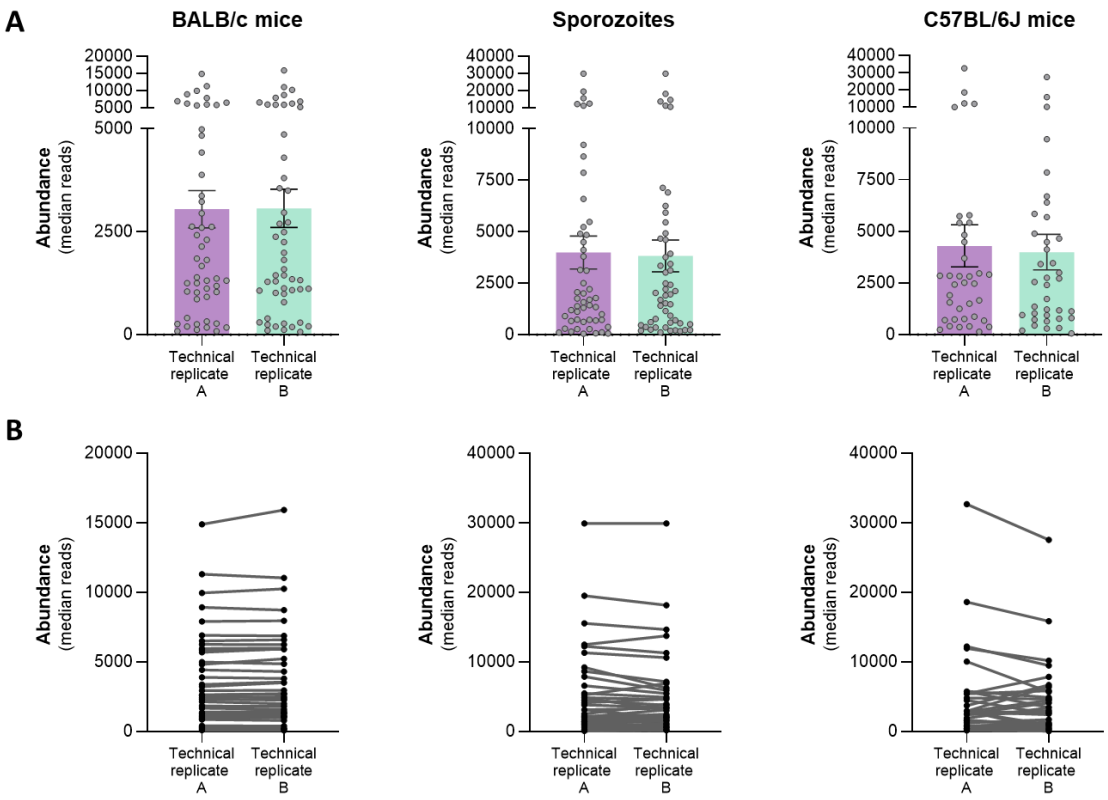

Figure 4.8. Abundance of KO parasites in samples from technical replicate A and B. (A) Abundance of mutant parasites in BALB/c mice, spz and C57BL/6J mice in the two technical replicates (BALB/c mice, n=2; spz, n=1; C57BL/6J mice, n=5). Dots represent the individual values of each mutant parasite and data are expressed as means ± SEM. **(B)** Abundance of each parasite in both technical replicates, for the same samples presented in (A). Each line represents the same parasite in the two replicates.

Based on these results, we can infer that: 1) it is possible to send cryopreserved blood with transfected parasites to another laboratory, in order to be injected into mice for the development of *in vivo* experiments; 2) there are no differences in the final composition of KO parasites when comparing KO parasites pools amplified in different sets of passage mice and through different mosquitoes batches, which shows the replicability of the technique.

4.3. Exploring the role of *Plasmodium* genes in evasion and/or modulation of the host's type I IFN response during liver stage parasite development

When a *P. berghei*-infected mosquito bites a host, it injects spz that enter the blood circulation and travel to the liver[13,97]. Inside this organ, spz infect hepatocytes and, over the course of the following 2 days develop and form thousands of merozoites that will infect red blood cells (RBCs)[13,98]. For many years it was thought that the parasites develop within hepatocytes without being recognized by the host immune system, due to the asymptomatic nature of *Plasmodium* infection[13]. However, in 2014, Liehl *et al*. and Miller *et al*. reported that the host

can mount an anti-parasitic response mediated by the type I IFN pathway during the liver-stage infection to control *Plasmodium* infection at this stage[48,49]. The parasite expresses a diverse repertoire of essential, partially redundant, or redundant genes, which moderate host-parasite interactions, not only scavenging nutrients but also evading and modulating the host's immune system to ensure survival[89,99–101]. While, it is clear that some parasite molecules help averting the host's responses, including autophagy and NF-κB signaling[66,99], the identity of the parasite proteins that contribute to the modulation of the host's immune responses remains unknown. The recent development of high-throughput genetic screening tools by our partners at MIMS opens the possibility to identify and characterize not only parasite genes that are targets of specific immune responses and whose absence or mutation weakens the host protective capacity, but also genes related to immune resistance/ immune evasion mechanisms whose absence increases the efficiency of the immune responses.

Having validated the reproducibility of the technique, we expanded the screen to cover 192 KO vectors with the aim of identifying *Plasmodium* molecules that interact with the host's innate immune system and contribute to the outcome of the liver stage of *Plasmodium* infection. If a particular gene is important for interacting with the host immune system, then the KO mutant parasite for that gene will be lost from the pool of mutants in the immunocompetent host. Therefore, the WT mice C57BL/6J and their corresponding immunodeficient mice *Ifnar1*$^{-/-}$, in which type I IFN response is ablated, were used for screening of 192 genes. In particular, this allows to identify from within the pool of KO mutants used for challenge, individual KO mutants that were previously described as unable to complete liver stage development and regain the capacity to complete liver stage development when administered to mice with ablated type-I IFN response.

4.3.1. Mice parasitemia

We investigated the impact of type I IFN response deficiency on KO *P. berghei* parasites development. To this end, WT and *Ifnar1*$^{-/-}$ mice were infected with 30,000 spz of *P. berghei* KO mutants by retro-orbital intravenous injection. The presence of blood stage parasites was monitored daily by methanol-fixed and Giemsa-stained thin blood smears and, at 2% parasitemia, mice were euthanized, and blood was collected by cardiac puncture for gDNA extraction and subsequent barcode sequencing. Although some *Ifnar1*$^{-/-}$ mice reached 2% parasitemia earlier than the WT mice (13%), most WT and *Ifnar1*$^{-/-}$ mice reached 2% parasitemia at a similar time, around day 5 post infection. Therefore, there was no significant difference independently of their background (Figure 4.9. A). Furthermore, we ensured that

the overall parasitemia at the time of sacrifice was not significantly different so as to not influence our analysis (Figure 4.9. B).

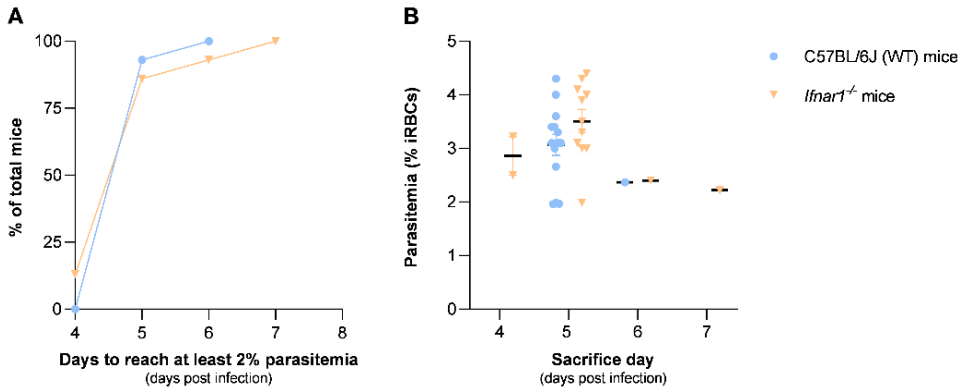

Figure 4.9. KO parasites grew similarly in both mouse strains. (A) Days that WT and *Ifnar1*$^{-/-}$ mice took to reach 2% parasitemia following infection with 30,000 spz of *P. berghei* KO mutants (n=15 mice per group). **(B)** % of parasitemia in WT and *Ifnar1*$^{-/-}$ mice on the day of sacrifice, assessed by Giemsa-stained thin blood smears. Symbols represent the individual values of each mouse and data are expressed as means ± SEM.

4.3.2 Overall quantitative assessment of KO parasites pool composition

When a target gene is essential for parasite development at a specific life cycle stage, KO parasites should not be able to survive, and consequently the corresponding barcodes should not be detected upon sequencing. Therefore, genes with no evidence at each stage of the life cycle can be considered as essential genes for parasite development at that particular stage. Thus, sequencing data were used to determine the presence and abundance of each baaq rcode for each sample. We initially focused on identifying the KO parasites present in the different sample points, allowing us to study the different stages of the parasite's life cycle (BALB/c mice for the blood stage, spz for the mosquito stage and C57BL/6J and *Ifnar1*$^{-/-}$ mice for the liver stage). This first analysis can give us information about the phenotype of the parasite and consequent importance of the target gene at each stage of the life cycle.

The pool of selected 192 genes targeted in this study was previously characterized for their phenotype during the liver stage and assembled as to include an approximately equal number of KO targets previously show to result in either a compromised liver development (92 genes, 48% of the pool) or not impacting parasite liver development (100 genes, 52% of the pool)[89] (Figure 4.10. C).

From the 192 genes targeted, 109 KO parasites were identified in the blood of BALB/c mice after transfection (Figure 4.10. A), reflecting a 43% loss of potential KO parasites (Figure 4.10. B). We could hypothesize that the parasites were lost in the process of freezing/thawing the infected blood, but as we noted earlier in the analysis of the replicability of the technique, this

is unlikely. An alternative hypothesis would be that the absence of the parasite in the blood could be because the target genes are essential for development in the blood. However, these genes were previously characterized as non-essential for completing development in the blood, except for only one gene (PBANKA_0315400) which was characterized as essential for blood stage[87]. The lack of barcodes for these mutants can also be explained due to the inability of the vector to integrate into the genome. Further studies are needed to understand whether the inability of the mutants to grow was a one-off in this study or whether this result would be repeated.

The pool of total KO parasites identified in the spz collected from the salivary glands of mosquitoes is the same as that identified in the blood of BALB/c mice. Since there was no loss of mutant parasites between these two stages, it suggests that the target genes used in the experiment do not have an essential or non-redundant function during the development of the parasite in the mosquito (Figure 4.10. A and B). The 109 KO parasites present in the spz and subsequently injected into C57BL/6J and *Ifnar1*$^{-/-}$ mice include 66 (61%) mutant parasites with compromised liver development and 43 (39%) mutant parasites with regular liver development (Figure 4.10. C).

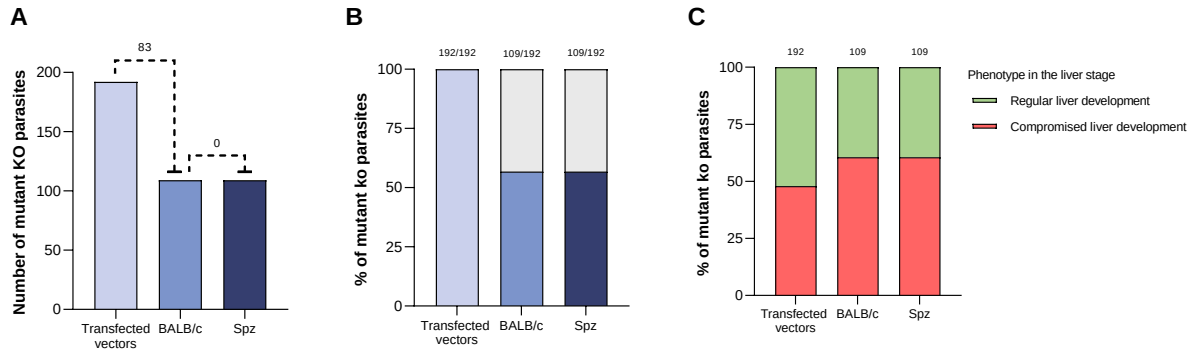

Figure 4.10. Analysis of KO parasite survival dynamics across life cycle stage transitions. The number **(A)** and the % **(B)** of total different mutant KO parasites observed at the blood stage (BALB/c mice) and the mosquito stage (spz) of the parasite life cycle. **(C)** The % of mutant parasites for the two sample points regarding their liver stage phenotype (green for regular liver development and red for compromised liver development).

To identify *Plasmodium* genes that interact with the host's innate immune system, 30,000 mutant spz were injected into at least 5 WT and 5 *Ifnar1*$^{-/-}$ mice, covering a pool of 109 KO parasites. Eighty-eight KO parasites were subsequently identified in the blood of mice (Figure 4.11. A), representing a 19% loss of parasites (Figure 4.11. B). These 21 lost genes were identified as likely essential for parasite growth in the liver regardless of host immune status as there was no evidence of their corresponding barcodes in parasites circulating in the blood of any of the mice (Figure 4.11. C). Of the 21 KO parasites that are absent from blood stage, only 2 (9.52%) had been previously described as presenting a regular liver development, while

the remaining 19 KO parasites (90.47%) absent from any of the mice had a previously described compromised liver development phenotype (Figure 4.11. D and Table 4.1)[89].

We identified 3 mutant parasites that did not grow in C57BL/6J WT mice but grew in immunodeficient *Ifnar1*$^{-/-}$ mice, as well as 6 mutant parasites that are exclusively present in the blood of WT mice (Figure 4.11. C). Although 9 mutant parasites are present uniquely in either WT or *Ifnar1*$^{-/-}$ mice, 89.8% of the parasites were present in the blood of both groups of mice (Figure 4.11. C). Thus, our data suggests that only a very small fraction of genes have an essential function in parasite liver development in WT versus *Ifnar1*$^{-/-}$ mice. The 79 KO parasites common to both groups of mice include 41 (52%) mutant parasites with compromised liver development and 38 (48%) mutant parasites with regular liver development (Figure 4.11. D). Importantly, the inability of 3 mutant parasites to grow in immunocompetent mice, C57BL/6J, suggests that these genes are crucial for liver stage parasite growth in the presence of an intact immune system, whereas they are redundant in immunodeficient mice, *Ifnar1*$^{-/-}$. Therefore, we consider them an important group of genes for studying host-parasite interactions in *Plasmodium*, since they may be a target of the type I IFN response.

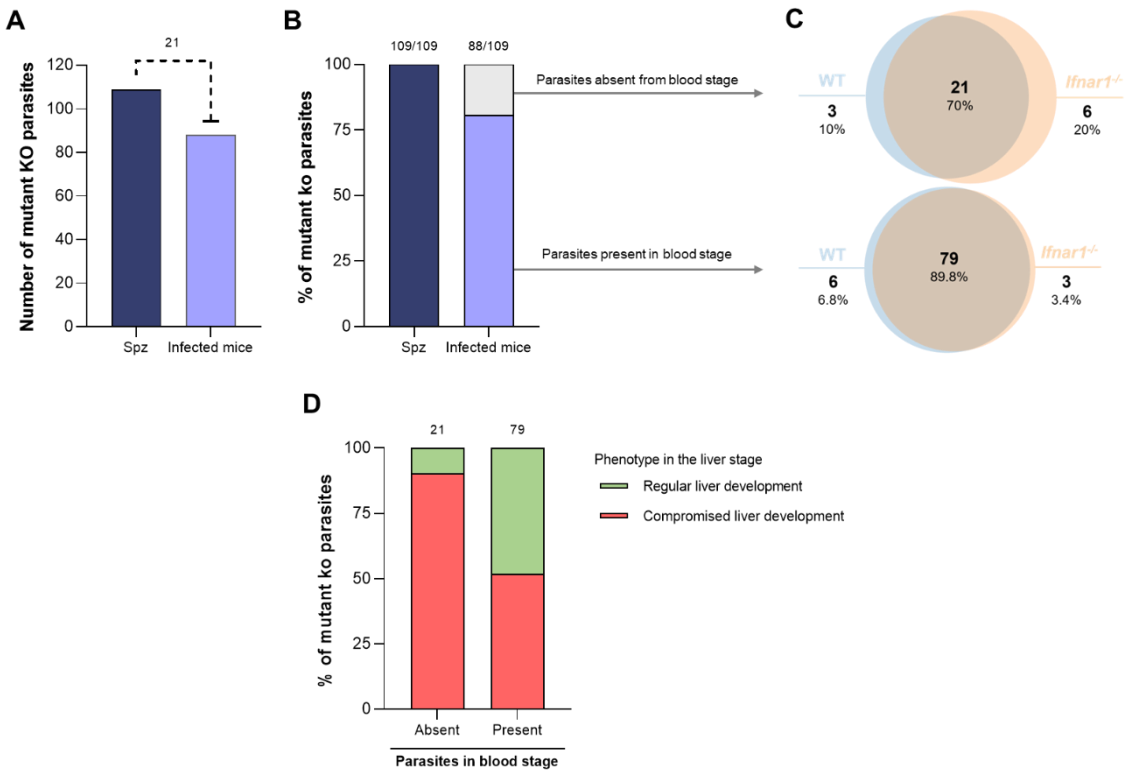

Figure 4.11. Comparative analysis of KO parasite survival dynamics between WT and *Ifnar1*$^{-/-}$ mice. The number **(A)** and the % **(B)** of total different mutant KO identified in the spz collected from the salivary glands of mosquitoes and in the blood of the infected mice (n≥5 mice per group). **(C)** Venn diagram demonstrating the intersection of all mutant parasites absent (upper row) or present (lower row) in the blood stage in both WT and *Ifnar1*$^{-/-}$ mice. **(D)** The % of KO parasites with regular (green) or compromised (red) liver development that are absent or present in the blood stage.

Table 4.1 | Likely essential genes for liver stage growth in *Plasmodium* infection.

Gene ID	Gene name	Previously described phenotype in the liver stage[89]	WT mice	*Ifnar1*$^{-/-}$ mice
PBANKA_142880	SDHB	Compromised liver development	0	0
PBANKA_112510	FabB/FabF	Compromised liver development	0	0
PBANKA_082430	-	Compromised liver development	0	0
PBANKA_051100	HCS1	Compromised liver development	0	0
PBANKA_112810	PL	Compromised liver development	0	0
PBANKA_141050	MCAT	Compromised liver development	0	0
PBANKA_071490	aLipDH	Compromised liver development	0	0
PBANKA_071120	-	Regular liver development	0	0
PBANKA_050500	-	Compromised liver development	0	0
PBANKA_100520	-	Compromised liver development	0	0
PBANKA_050120	UIS4	Compromised liver development	0	0
PBANKA_010110	PALM	Compromised liver development	0	0
PBANKA_134650	DEH	Compromised liver development	0	0
PBANKA_100220	P36p	Compromised liver development	0	0
PBANKA_112780	-	Compromised liver development	0	0
PBANKA_133820	FabZ	Compromised liver development	0	0
PBANKA_100630	PLP1	Compromised liver development	0	0
PBANKA_020830	NPT1	Regular liver development	0	0
PBANKA_082090	ELO-A	Compromised liver development	0	0
PBANKA_102460	LISP1	Compromised liver development	0	0
PBANKA_030820	-	Compromised liver development	0	0

4.3.3. KO parasites respond differently to different immune pressures

In an initial comparative analysis, we showed that the innate immune status of the host did not significantly influence the pool of mutants capable to complete liver stage development, as 89.8% of the parasite KO tested were present in the blood of both C57BL/6J WT and *Ifnar1*$^{-/-}$ mice. Although most of the parasites were identified in the blood of the mice, this first analysis does not provide detailed information on the abundance of the parasites present at this stage. Therefore, in a second approach, we sought to investigate the behaviour of the parasites, as individual mutants may respond differently to different host immune environments. To this end, we evaluated and compared the frequency and abundance of each mutant parasite between the two groups of mice to assess their ability to survive and capacity to replicate, respectively.

4.3.3.1. Analysis of KO parasites presently uniquely in either of the mouse strains tested

Firstly, we focused our attention on the 9 parasites that are unique to one of the two groups of mice, as they are the most relevant and may give more information about the interaction of

these genes with the innate immune system (Table 4.2). The 3 mutant parasites that did not grow in WT mice but did grow in *Ifnar1*$^{-/-}$ mice were considered the most interesting group of genes to study the interaction of *Plasmodium* with the type I IFN immune response. We hypothesize that these parasites are KO for genes related to mechanisms of resistance/evasion to the type I IFN immune response, whose absence increases the efficacy of immune responses and, therefore, the parasites are only able to develop in immunodeficient mice *Ifnar1*$^{-/-}$, in which type I IFN response is ablated. One of these likely essential genes for liver stage parasite growth in the presence of an intact immune system is novel and is annotated only as conserved *Plasmodium* protein of unknown function. Another, the ABCB4 gene encodes a multidrug resistance (MDR) protein located in the apicoplast. This protein belongs to the B subfamily of the ATP Binding Cassette (ABC) transporters, which export a wide range of compounds, including some of pharmaceutical interest. Previous studies showed contradictory data regarding this gene: some refer to this gene as being dispensable for the development of the parasite in the blood[87,89], while others show that the ABCB4 gene has an essential role during blood stage growth/multiplication, validating them as potential targets for antimalarial drugs[102,103]. Thus, more studies are needed to clarify the role of this gene in parasite development. Pb115 is another interesting gene among this group, because KO parasites for this gene were previously described as unable to complete liver stage development. Our results indicate the KO parasite regains capacity to complete liver stage development when administered to mice with ablated type-I IFN response and do so with high frequency as this KO parasite is present in most *Ifnar1*$^{-/-}$ infected mice. A study conducted by Liu *et al.* with *P. berghei* showed that Pb115 is expressed in both asexual and sexual stages of the malaria parasites[104]. Deletion of Pb115 did not affect asexual multiplication and gametocyte development, but led to defects in ookinete formation, resulting in transmission failure to the mosquitoes. Despite the very low fertilization rates in KO Pb115 parasites, KO spz were equally infective to mice as the WT spz. These findings suggest that Pb115 plays a critical role in gamete fertilization, as both male and female gametes require this protein for gamete recognition and attachment, highlighting the transmission-blocking vaccines potential of this protein. Nevertheless, we found no previous reports of links between PB115 and the type I IFN response.

Regarding the 6 KO parasites that were present in immunocompetent mice but not in *Ifnar1*$^{-/-}$, 5 of them already had a previously described phenotype in the liver[89], so their presence in the blood of WT mice was not expected. Also, the low frequency and abundance of these parasites raises the possibility that this may be a stochastic escape event. We focused our attention on the PBANKA_010740 gene, which is the only in this group that was previously described as not essential for liver stage growth and the only one with a considerable frequency in mice, although its abundance decreases relative to spz. Malaria parasites have to adapt to the

different environments they encounter during their life cycle, and this adaptation is associated with reconfiguration of metabolism. In 2016, Srivastava *et al.* studied metabolic pathways to examine whether any of them were essential for parasite growth at different stages[105]. Mutant *P. berghei* parasites lacking the ornithine amino transferase (OAT), a putative GABA/glutamate transaminase which can recycle glutamate, grew only slightly less quickly than wild type parasites during asexual blood stages. The authors also evaluated metabolic pathways during mosquito stage development and observed that KO parasites for the OAT gene displayed a significant reduction in oocyst numbers but were able to produce spz in mosquito salivary glands, completing transmission through the mosquito and generating blood stage asexual forms with the same kinetics as the parental wild-type line[105].

After a literature search, we could not find previous reports that suggested a clear link between these genes and the type 1 IFN response during the liver stage infection. The data obtained suggest that this is most likely a stochastic effect, as the genes listed were not expected to be identified, since: 1) the identified parasites show low frequency and abundance values in the blood of the mice; 2) about 67% of the parasites already have a phenotype in the liver described and therefore have impaired liver development; 3) most parasites decrease their abundance in the blood relative to spz.

Table 4.2 | Mutant parasites present exclusively in C57BL/6J WT or *Ifnar1*$^{-/-}$ mice and their frequency and abundance at each *Plasmodium* life cycle stage (BALB/c mice for the blood stage, spz for the mosquito stage and WT and *Ifnar1*$^{-/-}$ mice for the liver stage). Complete table is presented in Annexes, Supplementary Table 2.

Gene ID	Gene name	Product description	Previously described phenotype in the liver stage[89]	Sporozoites		WT mice		*Ifnar1*$^{-/-}$ mice	
				Freq.	Abund.	Freq.	Abund.	Freq.	Abund.
PBANKA_010740	OAT	Ornithine aminotransferase, putative	Regular liver dev.	100%	548.46	40%	460.63	Absent	Absent
PBANKA_071750	CBP20	Nuclear cap-binding protein subunit 2, putative	Compromised liver dev.	100%	175.15	20%	421.98	Absent	Absent
PBANKA_090980	-	RNA-binding protein, putative	Compromised liver dev.	100%	626.76	20%	285.44	Absent	Absent
PBANKA_082100	-	Chaperone, putative	Compromised liver dev.	100%	81.06	20%	77.86	Absent	Absent
PBANKA_093290	G3PDH	Glycerol-3-phosphate dehydrogenase, putative	Compromised liver dev.	100%	14975.69	10%	114.05	Absent	Absent
PBANKA_070700	LipB	Lipoate-protein ligase B	Compromised liver dev.	100%	12996.84	10%	38.05	Absent	Absent
PBANKA_040120	ABCB4	ABC transporter B family member 4, putative	Regular liver dev.	100%	167.56	Absent	Absent	11%	375.87
PBANKA_030770	-	Conserved *Plasmodium* protein, unknown function	Regular liver dev.	100%	958.24	Absent	Absent	40%	68.73
PBANKA_093100	Pb115	MFS domain-containing protein P115	Compromised liver dev.	100%	138.24	Absent	Absent	40%	170.80

Abbreviations are as follows: Dev. - development; Freq. – frequency; Abund. – abundance.

4.3.3.2. Qualitative assessment of KO parasites present in the blood of both C57BL/6J and *Ifnar1*$^{-/-}$ mice

We next focused our analysis in the 79 parasites that were present in the blood of both WT and *Ifnar1*$^{-/-}$ mice, but which show striking differences in their frequency among the various mice infected and/or abundance, as indicated by the number of reads sequenced. Regarding frequency, as indicated by the number of mice in which each mutant parasite was identified, the average frequency of mutant parasites in the blood of C57BL/6J and *Ifnar1*$^{-/-}$ mice is similar (Figure 4.12. A). Looking at each mutant parasite individually, the frequency of each mutant parasite is similar between both groups of mice, except for two parasites (PBANKA_080650 and PBANKA_020760) that show a difference in frequency of more than 50% (Figure 4.12. B). Regarding the overall relative abundance of all KO parasites detected in both groups of mice, the average abundance of mutant parasites in the blood is similar between WT and *Ifnar1*$^{-/-}$ mice (Figure 4.12. C) and the same could be observed in an individual KO analysis, with no significant differences in the abundance for each KO parasite observed between the two mice models studied (Figure 4.12. D).

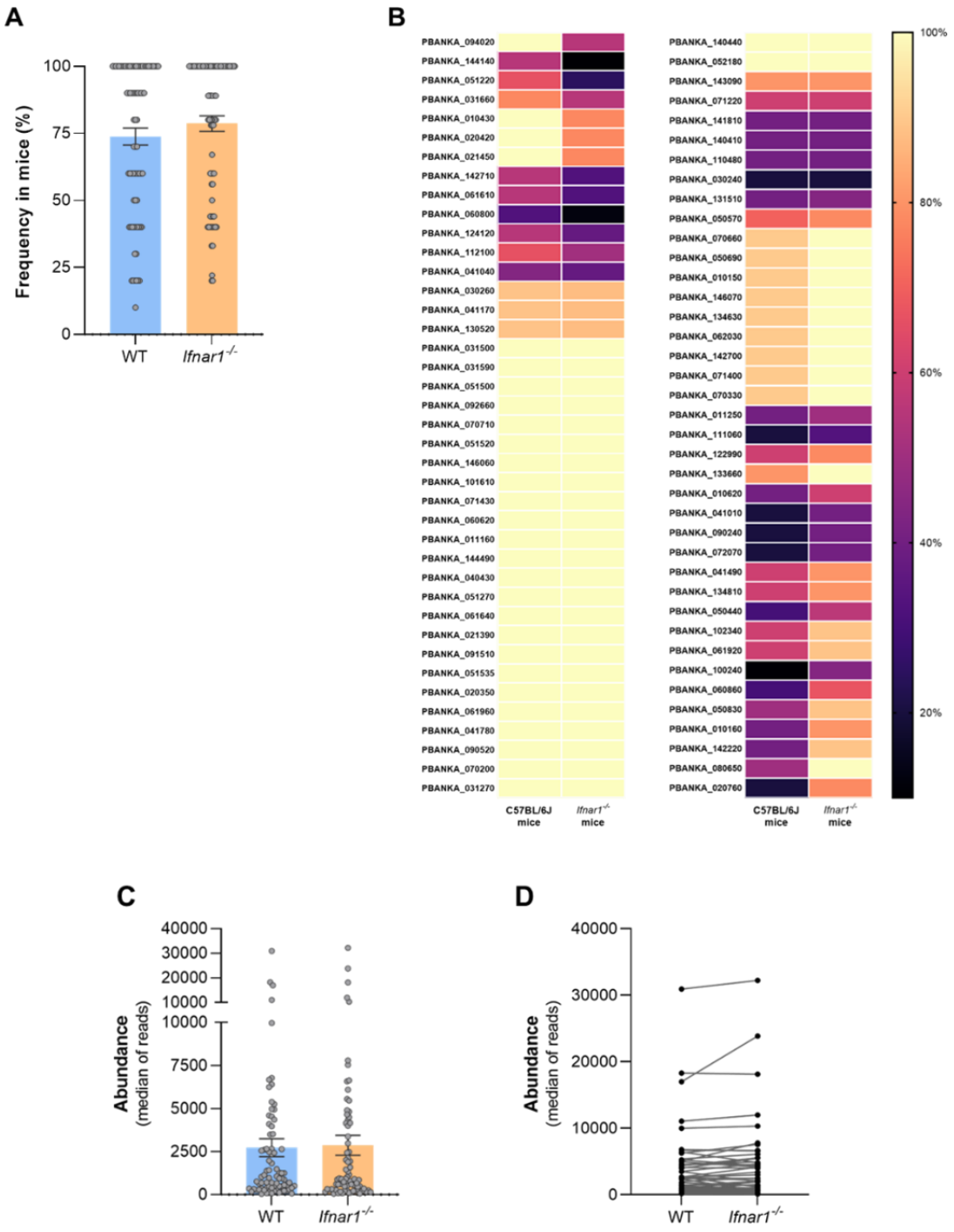

Figure 4.12. Analysis of the frequency and abundance of KO parasites in WT and *Ifnar1*$^{-/-}$ mice. C57BL/6J and *Ifnar1*$^{-/-}$ mice were infected with 30,000 *P. berghei* KO spz and the frequency and abundance of each mutant parasite was measured for each group of mice. **(A)** Frequency of mutant parasites in the blood of WT and *Ifnar1*$^{-/-}$ mice. **(B)** Heat map representing the frequency (%) of each mutant parasite (rows) in each group of mice (columns). **(C)** Abundance of mutant parasites in the blood of WT and *Ifnar1*$^{-/-}$ mice. **(D)** Abundance of each parasite in each group of mice. Each line represents the same parasite in the two mouse models. Dots represent the individual values of each mutant parasite and data are expressed as means ± SEM (n≥5 mice per group).

The results of the analysis of the KO parasites present in the two experimental groups suggest that genes with different behaviors between the study groups can be identified, such as: a) parasites with higher frequency and abundance in WT or *Ifnar1*$^{-/-}$ mice; b) parasites with higher

frequency in WT mice, but higher abundance in *Ifnar1*$^{-/-}$ mice, or vice versa; and c) parasites with no significant difference in frequency, but with a significant difference in abundance, or vice versa. (Figure 4.13).

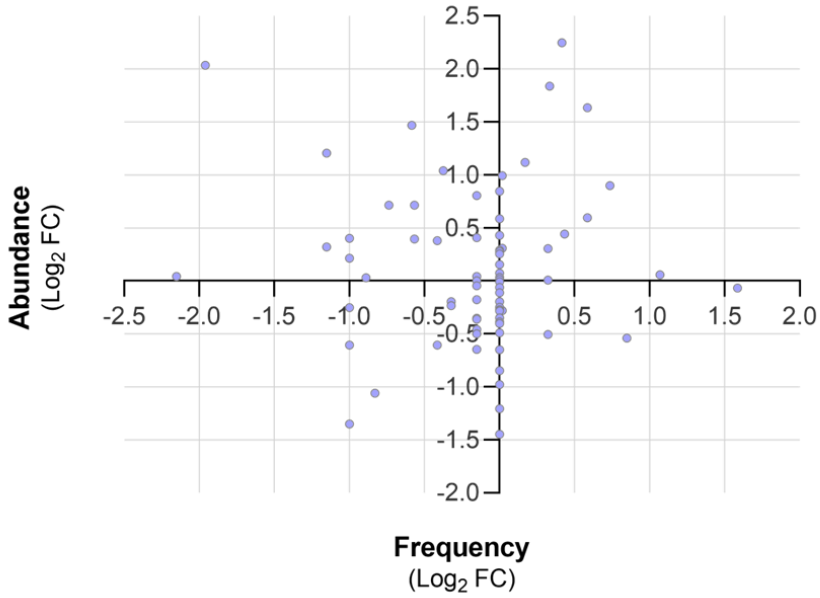

Figure 4.13. KO parasites show different behaviours between WT and *Ifnar1*$^{-/-}$ mice regarding their frequency and abundance in the blood. Positive log_2FC values for parasites that are prominent in WT mice and negative log_2FC values for higher frequency and abundance in *Ifnar1*$^{-/-}$ mice. Dots represent the log_2FC values of each mutant parasite.

Overall, we identified 16 KO parasites with an increased potential to complete the life stage transition in WT mice, 31 in *Ifnar1*$^{-/-}$ mice and 32 parasites whose immune status of the mice did not influence their survival. Considering the relative abundance of the various KO parasites, 41 parasites had a higher capacity to replicate in WT mice, 37 parasites in *Ifnar1*$^{-/-}$ mice and 1 parasite had the same abundance in the blood of both mice models. Despite this evidence, as we mentioned before (Fig 4.12), most observed differences in KO parasite frequency and abundance are not significant, except for a few cases highlighted below.

An important aspect to take into consideration for analysis is the previously reported liver phenotype of the various KO parasites that appear most frequently/abundantly in each experimental group. Considering the 16 KO parasites that have the highest survival ability in WT mice, 9 (56%) have been reported to present a compromised liver development and the remaining 7 (44%) to have a normal liver development. Of the 31 KO parasites with the highest frequency in *Ifnar1*$^{-/-}$ mice, 17 (55%) have been reported to present a compromised liver development and the remaining 14 (45%) to have normal liver development (Figure 4.14. A). However, as expected, KO parasites for genes not essential for normal liver development have

a higher frequency in both animal models (Figure 4.14. C). Looking at the capacity of the KO parasites to replicate in the blood, of the 41 parasites with the highest abundance in WT mice, 20 (49%) have a described liver phenotype and 21 (51%) have normal liver development. Of the 37 parasites with the highest capacity to replicate in the immunocompromised mice, 20 (54%) have a described phenotype in the liver and 17 (46%) have normal liver development (Figure 4.14. B). Regardless of the immune status of the mice, the abundance of KO parasites that had previously been reported to have a regular liver development is higher than that of KO parasites that had previously been reported to have a compromised liver stage development (Figure 4.14. D).

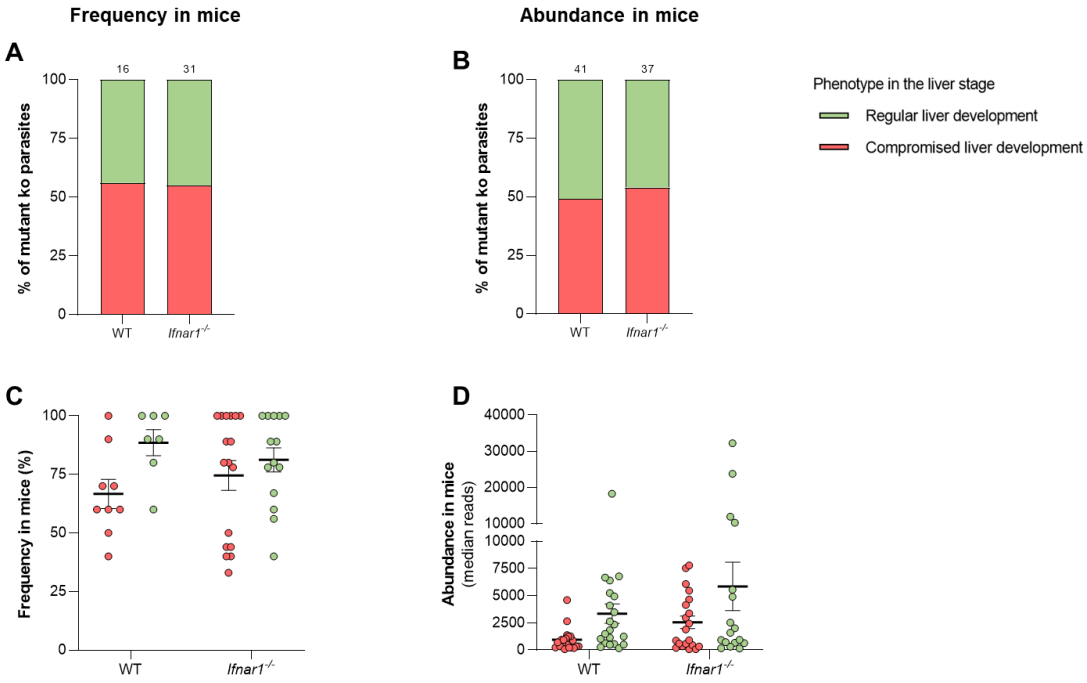

Figure 4.14. Analysis of predicted liver stage phenotype for parasites that show high frequency and abundance in WT and *Ifnar1*$^{-/-}$ mice. The % mutant KO parasites with regular or compromised liver development, regarding the parasites with the highest ability to survive **(A)** and the highest capacity to replicate **(B)** in WT and *Ifnar1*$^{-/-}$ mice. Frequency **(C)** and abundance **(D)** of the parasites with regular or compromised liver development that appear more frequently and abundantly in each group of mice. Dots represent the individual values of each mutant parasite and data are expressed as means ± SEM (n≥5 mice per group).

We next sought to investigate possible interactions of some of these genes with the type I IFN response. From the list of genes obtained, we selected for our literature research those that we considered to be most relevant for the study (Table 4.3), which include those with the highest frequency and/or abundance in immunocompromised mice, namely those that were previously described as unable to complete liver stage development and recover the capacity to complete liver stage development when administered to mice with ablated type-I IFN response.

Firstly, we focused our attention on the KO parasites that, besides appearing in more than 70% of the *Ifnar1*$^{-/-}$ mice, have a difference of at least 49% in their frequency compared to WT mice (PBANKA_142220, PBANKA_080650, PBANKA_020760). The differences in the ability to survive of the PBANKA_142220 and PBANKA_080650 parasites coincide with the previously described liver phenotype, and therefore their higher frequency in *Ifnar1*$^{-/-}$ mice validates their observed phenotype. Interestingly, despite their higher ability to survive in *Ifnar1*$^{-/-}$ mice, their capacity to replicate in the blood is higher in WT mice. *Ifnar1*$^{-/-}$ mice showed a 2.31-fold reduction in the abundance of the parasite KO for the CDF gene compared to infected WT mice. Massive zinc fluxes are essential for the infection cycle of *Plasmodium* parasites, namely during their development within the host erythrocyte. Restriction of zinc availability leads to the disruption of parasite mitochondrial function and inhibits parasite growth[106]. The cation diffusion facilitator (CDF) family protein might participate in the transport of heavy metal ions[106,107]. Kenthirapalan *et al.* revealed that CDF may also play roles during sexual blood-stage development and mouse-to-mosquito transition, as substantial reductions in male gamete exflagellation and ookinete formation were detected for KO parasites[108]. However, no function during the hepatic stage was found. The PBANKA_080650 parasite showed a 1.16-fold reduction in its abundance in the *Ifnar1*$^{-/-}$ mice when compared to WT mice. Triosephosphate isomerase is an important glycolytic enzyme[109]. In *Plasmodium*, where glycolysis is the sole source of ATP in asexual stages [110], the parasite cannot afford inhibition of its critical enzyme triosephosphate isomerase. Drugs that specifically inhibit *Plasmodium* triosephosphate isomerase may hold promise for use in anti-malarial therapies. Despite the relevance of this enzyme in asexual parasite stages, specific functions for the liver stage were not previously described. The abundance of PBANKA_020760 parasite in *Ifnar1*$^{-/-}$ mice had a 4.10-fold reduction when compared to WT mice. First, we should note that the presence of this gene at this stage of the study is strange, since it was previously characterized as being essential to blood stage growth and, therefore, it would be expected that we had lost this parasite during KO parasite expansion in BALB/c mice. The proteins of *Plasmodium* are strikingly rich in asparagine, which is an amino acid that have a significant influence on immune responses of the host such as the function of innate immune cells (e.g., macrophage), the activation and differentiation of T cells, the production of antibodies by B cells as well as playing a role in pathogen survival and infection[111]. A study carried out in *P. berghei*, showed that deletion of asparagine synthetase delays the asexual- and liver-stage development with substantial reduction in the formation of ookinetes, oocysts and sporozoites in mosquitoes[112]. A different study based on a conserved *Plasmodium* asparagine-rich protein demonstrated that this protein is specifically expressed in sporozoites and liver stages and that gene disruption in *P. berghei* results in complete loss of sporozoite infectivity to rodents, due to early developmental arrest after invasion of hepatocytes[113]. Notably, although related to asparagine

metabolism, the gene target in these studies are different from the one revealed by our screen, and no orthologous genes have been identified for our target gene. Further studies targeting the PBANKA_020760 gene and its corresponding KO parasite are needed to clarify these aspects and unravel its function/s during parasite development.

The parasites PBANKA_050830 and PBANKA_041010 have a higher frequency in *Ifnar1*$^{-/-}$ mice, although the difference for WT mice is less than 50%, but unlike the parasites detailed previously, they also have a higher abundance in *Ifnar1*$^{-/-}$ mice. The parasite KO for the OMG1 gene showed a ~2.10-fold increase in its abundance in the *Ifnar1*$^{-/-}$ mice when compared to WT mice. OMG1 is a target gene of AP2-Z (an AP2 transcription factor expressed in zygotes). Recently, Nishi *et al.* demonstrated that OMG1 is important for zygote/ookinete development by showing that: 1) ookinete maturation was delayed in OMG1 KO; and 2) the number of oocysts in the midgut of infected mosquitoes was significantly reduced[114].

The PBANKA_041010 parasite showed a 2.53-fold increase in its abundance in the *Ifnar1*$^{-/-}$ mice when compared to WT mice and relates to the ubiquitylation process. The ubiquitin system has been shown to be particularly important in the survival and spread of human malaria parasites and is possibly involved in mechanisms of drug resistance[115]. E3 ligase is one of the three enzymes involved in the ubiquitylation process[116]. In a study carried out with *P. falciparum*, E3 ligase inhibitors blocked the development of *P. falciparum* parasite at the trophozoite and schizont stages, suggesting the role of ubiquitin functions in the intraerythrocytic development of malaria parasite[117]. No data were found on a possible role of this gene during liver development.

The KO parasites for PBANKA_140440 and PBANKA_071220, the immune status of the mice appears to not interfere with the ability of the parasite to survive, as they have the same frequency in both mice, but their ability to replicate is higher in the *Ifnar1*$^{-/-}$ mice. Unexpectedly, despite the KO parasite for this gene had been described has leading to a compromised liver development, the PBANKA_140440 parasite was able to infect all WT mice, but since it is only annotated as a conserved *Plasmodium* protein of unknown function, it is not possible for us to make assumptions about its interaction with the type I IFN response. The parasite KO for the PBLP gene showed a 2.72-fold increase in its abundance in the *Ifnar1*$^{-/-}$ mice when compared to WT mice. A study carried out on *P. yoelii* parasites showed that *Plasmodium* BEM46-like protein (PBLP) has an important role in modulating maturation of the invasive stages, including in intra-erythrocytic and exo-erythrocytic stage merozoite development as well as oocyst formation and sporozoite maturation[118]. *P. yoelii* parasites knocked out for PBLP show defects in the development of all invasive stages: 1) KO parasites formed fewer merozoites during schizogony, which results in decreased parasitemia; 2) KO parasites formed fewer oocysts

resulting in a reduction in the number of developed spz in infected mosquitoes; 3) KO parasites showed decreased infectivity in hepatocytes *in vitro*; and 4) mice infected with KO spz exhibited a delay in the onset of blood-stage patency. This latter annotation may explain the reduced abundance of the parasite in WT mice when compared to *Ifnar1*$^{-/-}$ mice in our study, suggesting a possible interaction between the PBLP gene and the type I IFN response.

Table 4.3 | Mutant parasites highlighted for their different behaviour between WT and *Ifnar1*$^{-/-}$ mice. Complete table is presented in Annexes, Supplementary Table 2.

Gene ID	Gene name	Product description	Previous described phenotype	WT mice		*Ifnar1*$^{-/-}$ mice		Delta WT/IFNAR	
				Freq.	Abund.	Freq.	Abund.	Freq.	Abund.
PBANKA_142220	CDF	Cation diffusion facilitator family protein, putative	Compromised liver dev.	40%	2663.16	89%	1154.32	-49%	2.31
PBANKA_080650	-	Triosephosphate isomerase, putative	Compromised liver dev.	50%	705.52	100%	608.04	-50%	1.16
PBANKA_020760	-	Asparagine-rich antigen, putative	Regular liver dev.	20%	2343.16	78%	571.63	-58%	4.10
PBANKA_050830	OMG1	Ookinete maturation gene OMG1	Regular liver dev.	50%	763.78	89%	1592.30	-39%	0.48
PBANKA_041010	-	E3 ubiquitin-protein ligase, putative	Regular liver dev.	20%	66.18	40%	168.71	-20%	0.39
PBANKA_140440	-	Conserved *Plasmodium* protein, unknown function	Compromised liver dev.	100%	393.43	100%	908.96	0%	0.43
PBANKA_071220	PBLP	BEM46-like protein, putative	Regular liver dev.	60%	269.69	60%	734.84	0%	0.37

Abbreviations are as follows: Dev. - development; Freq. – frequency; Abund. – abundance.

Although we did not find information that would allow us to establish a direct link between the genes studied and the type I IFN response, the outcomes of this study highlight that KO parasites for different genes respond differently to different immune pressures and therefore this methodology can be used to unveil genes that play a crucial role in the interaction with the host immune system. More experiments must be carried out to clarify the role of these genes in the observed phenotype.

Concluding remarks and future perspectives

5. Concluding remarks and future perspectives

Malaria is an infectious disease that remains a leading cause of mortality and morbidity worldwide and is therefore a major health concern for the World Health Organization. The outcome of this disease depends on a wide variety of factors, including parasite species and strain, host immune responses, host and parasite metabolic pathways, and host and parasite genetic polymorphisms. Understanding the mechanisms by which the vertebrate host and parasite interact can be useful for the urgent development of effective vaccines and novel therapeutic interventions in malaria[119,120].

For many years, the pathogenic blood stages have been the main focus of malaria research, and most of the antimalarial drugs available on the market primarily target the blood stage of *Plasmodium* infection. Nevertheless, *P. falciparum* has rapidly and repeatedly developed resistance to all available blood-stage drugs, including the current first-line antimalarial, artemisinin[121]. Furthermore, until a few years ago, the liver stage of *Plasmodium* infection was largely overlooked, and its asymptomatic nature led to the assumption that parasites were undetected within this organ by the host's immune system[13]. Nonetheless, this notion was disproved in 2014 by Liehl *et al*. and Miller *et al*. who reported that the host can mount an immune response mediated by the type I IFN pathway which recruits inflammatory cells to control *Plasmodium* infection during the liver stage[48,49]. Targeting the pre-erythrocytic stage of the parasite has the considerable advantage that successful drug treatment prevents the appearance of any clinical symptoms of the disease.

The *Plasmodium* parasite has the ability to modulate the host's immune response. However, the parasite proteins that play a role in this process remain unknown, partly due to difficulties in manipulating the AT-rich *Plasmodium* genome by reverse genetic technology. We proposed to use a high-throughput genetic screening tool based on pools of *P. berghei* KO mutants[84,86] to identify *Plasmodium* molecules that interact with the host's innate immune system, namely the type I IFN response, and contribute to the outcome of the liver stage of *Plasmodium* infection.

Pools of barcoded *P. berghei* KO mutants based on 192 KO vectors were prepared by our collaborators at MIMS and blood infected with these pools was frozen and sent to us. Our first task was to verify that this procedure is feasible and that freezing and thawing the infected blood does not significantly impact the experimental design. Using a pool of 96 KO mutants we designed an experiment with two technical replicates and followed the development of the parasite throughout its life cycle. We found that most of the mutants lost were the same for both replicates (Figure 4.6) and that the frequency (Figure 4.7) and abundance (Figure 4.8) values for the KO parasites were similar between the two replicates at the different stages of

the life cycle. Therefore, we have shown that it is possible to ship frozen blood infected with KO parasites and have validated the reproducibility of the experimental design.

Subsequently, using immunocompetent and immunodeficient mice, we screened 192 genes to identify *Plasmodium* proteins that interact with the host's innate immune system, namely the type I IFN response. The data revealed that 21 of these genes were likely essential for parasite growth in the liver regardless of host immune status as there was no evidence of their corresponding barcodes in parasites circulating in the blood of any of the mice (Figure 4.11. D and Table 4.1). On the other hand, 89.8% of the parasites were present in the blood of both groups of mice, 3 mutant parasites did not grow in C57BL/6J WT mice but grew in immunodeficient *Ifnar1*$^{-/-}$ mice and 6 mutant parasites were exclusively present in the blood of WT mice (Figure 4.11. C). Mutants which did not grow or had exhibited reduced growth in the C57BL/6J model of experimental cerebral malaria but grew well in immunodeficient mice *Ifnar1*$^{-/-}$, represent one of the most interesting groups of genes for studying host-parasite interactions.

We next sought to investigate whether any of the 9 genes uniquely present in one of the animal models (Table 4.2) had a previously described interaction with the type I IFN response. After an extensive literature review, we did not find a link between these genes and the type I IFN response during the liver stage infection. Consequently, we focused on the 79 parasites that appear in the blood of both WT and *Ifnar1*$^{-/-}$ mice and pursued an in-depth comparative analysis of their frequency and abundance in the blood of the two groups of mice. We reduced the list of 79 parasites to 7 KO parasites that we considered most relevant for our study because they presented a higher frequency and/or abundance in *Ifnar1*$^{-/-}$ mice than in WT mice, some of which were previously described as having impaired development in the liver (Table 4.3). Again, we did not find previously published evidence of an interaction between the studied genes and the type I IFN response.

In summary, in the present work we were not able to fully achieve our main objective of identifying *P. berghei* genes that directly interact with the type I IFN response in the host liver. This failure can be justified by the following reasons:

- Over 1170 genes of the *P. berghei* genome can be assessed for their role during liver stage development. However, in this study was restricted to a small group of only 192 genes, covering merely 16.4% of the available genes.
- It is possible that the type I IFN response alone does not represent a sufficient immune pressure to identify *Plasmodium* genes that interact with the host immune system and contribute to the outcome of the liver stage of *Plasmodium* infection.

Nevertheless, we validated the proposed experimental design for its applicability in immune studies, since so far it had only been applied in studies of the parasite's development throughout its life cycle, for example in the identification of genes essential for normal parasite development in the blood[87] and genes involved in metabolic processes during liver development[89]. Our experimental work confirmed that the barcode-based NGS sequencing approach[84] is indeed suitable for detecting KO mutants responding differently to different immune pressures, validating the use of this approach to study the effects of immune pressure on parasite development. Furthermore, we provided proof-of-concept that there may be genes that are crucial for interacting with the host immune system but that are functionally redundant in immunodeficient environments.

Future experiments should follow all the 1170 genes available to identify their role during liver stage development and begin the process of functionally testing candidates for immune-system dependent phenotypes. If it remains impossible to identify genes that interact with the type I IFN response, we should consider that, despite being the first-line of defense against liver infection, the type I IFN response may not be sufficient for the identification of *Plasmodium* genes that contribute to the modulation of the host's innate immune system, and may even depend on other types of immune responses. In this case, other animal models should be considered, such as those with impaired function of γδ T cells, whose activation in the liver has recently been shown to play an important role in the severity of malaria[122].

Elucidating the mechanisms by which the host innate immune system responds to and/or is manipulated by *Plasmodium* infection will lead to the discovery of potential targets that may ultimately be of value for malaria control interventions.

References

6. References

1. World Health Organization (WHO). World Malaria Report 2021 (2021).
2. White, N. J. Malaria. *Manson's Tropical Diseases: Twenty-Third Edition* 532-600.e1 (2014) doi:10.1016/B978-0-7020-5101-2.00044-3.
3. Basu, S. & Sahi, P. K. Malaria: An Update. (2017) doi:10.1007/s12098-017-2332-2.
4. Prudêncio, M., Mota, M. M. & Mendes, A. M. A toolbox to study liver stage malaria. *Trends Parasitol* **27**, 565–574 (2011).
5. Nadjm, B. & Behrens, R. H. Malaria: An Update for Physicians. *Infect Dis Clin North Am* **26**, 243–259 (2012).
6. Collins, W. E. & Jeffery, G. M. Plasmodium malariae: Parasite and disease. *Clinical Microbiology Reviews* vol. 20 Preprint at https://doi.org/10.1128/CMR.00027-07 (2007).
7. Fei, A. A. *et al.* Plasmodium knowlesi malaria: current research perspectives. (2018) doi:10.2147/IDR.S148664.
8. Brasil, P. *et al.* Outbreak of human malaria caused by Plasmodium simium in the Atlantic Forest in Rio de Janeiro: a molecular epidemiological investigation. *Lancet Glob Health* **5**, e1038–e1046 (2017).
9. Dolby, K. et al. Malaria 1990–2009. Portf. Rev. 8 (2012).
10. Greenwood, B. M., Bojang, K., Whitty, C. J. & Targett, G. A. Malaria. *The Lancet* **365**, 1487–1498 (2005).
11. Worrall, E., Basu, S. & Hanson, K. Is malaria a disease of poverty? A review of the literature. *Tropical Medicine and International Health* **10**, 1047–1059 (2005).
12. About Malaria | RBM. Available at: https://endmalaria.org/about-malaria/what-malaria.
13. Prudêncio, M., Rodriguez, A. & Mota, M. M. The silent path to thousands of merozoites: The Plasmodium liver stage. *Nature Reviews Microbiology* vol. 4 Preprint at https://doi.org/10.1038/nrmicro1529 (2006).
14. Amino, R. *et al.* Quantitative imaging of Plasmodium transmission from mosquito to mammal. *Nat Med* **12**, (2006).
15. Coppi, A. *et al.* Heparan Sulfate Proteoglycans Provide a Signal to Plasmodium Sporozoites to Stop Migrating and Productively Invade Host Cells. *Cell Host Microbe* **2**, (2007).
16. Tavares, J. *et al.* Role of host cell traversal by the malaria sporozoite during liver infection. *Journal of Experimental Medicine* **210**, (2013).
17. Mota, M. M. *et al.* Migration of Plasmodium sporozoites through cells before infection. *Science (1979)* **291**, (2001).
18. Cowman, A. F., Healer, J., Marapana, D. & Marsh, K. Malaria: Biology and Disease. *Cell* vol. 167 Preprint at https://doi.org/10.1016/j.cell.2016.07.055 (2016).

19. Risco-Castillo, V. *et al.* Malaria Sporozoites Traverse Host Cells within Transient Vacuoles. *Cell Host Microbe* **18**, 593–603 (2015).
20. Lindner, S. E., Miller, J. L. & Kappe, S. H. I. Malaria parasite pre-erythrocytic infection: preparation meets opportunity. (2012) doi:10.1111/j.1462-5822.2011.01734.x.
21. Baer, K., Klotz, C., Kappe, S. H. I., Schnieder, T. & Frevert, U. Release of Hepatic Plasmodium yoelii Merozoites into the Pulmonary Microvasculature. doi:10.1371/journal.ppat.0030171.
22. Baird, J. K. Malaria caused by Plasmodium vivax: recurrent, difficult to treat, disabling, and threatening to life-averting the infectious bite preempts these hazards. doi:10.1179/2047772413Z.000000000179.
23. Cowman, A. F. & Crabb, B. S. Invasion of Red Blood Cells by Malaria Parasites. *Cell* **124**, 755–766 (2006).
24. Zuzarte-Luis, V., Mota, M. M. & Vigário, A. M. Malaria infections: What and how can mice teach us. *J Immunol Methods* **410**, (2014).
25. Josling, G. A. & Llinás, M. Sexual development in Plasmodium parasites: Knowing when it's time to commit. *Nature Reviews Microbiology* vol. 13 Preprint at https://doi.org/10.1038/nrmicro3519 (2015).
26. Sato, S. Plasmodium—a brief introduction to the parasites causing human malaria and their basic biology. *Journal of Physiological Anthropology* vol. 40 Preprint at https://doi.org/10.1186/s40101-020-00251-9 (2021).
27. Smith, R. C. & Barillas-Mury, C. Plasmodium Oocysts: Overlooked Targets of Mosquito Immunity. *Trends Parasitol* **32**, 979–990 (2016).
28. Brian De Souza, J., Hafalla, J. C. R., Riley, E. M. & Couper, K. N. Cerebral malaria: Why experimental murine models are required to understand the pathogenesis of disease. *Parasitology* vol. 137 Preprint at https://doi.org/10.1017/S0031182009991715 (2010).
29. Rénia, L. *et al.* Cerebral malaria Mysteries at the blood-brain barrier. *Virulence* vol. 3 Preprint at https://doi.org/10.4161/viru.19013 (2012).
30. Simwela, N. V. & Waters, A. P. Current status of experimental models for the study of malaria. *Parasitology* vol. 149 Preprint at https://doi.org/10.1017/S0031182021002134 (2022).
31. Varo, R., Chaccour, C. & Bassat, Q. Update on malaria. *Med Clin (Barc)* **155**, 395–402 (2020).
32. Payne', D. *Use and limitations of light microscopy for diagnosing malaria at the primary health care level*. *Bulletin of the World Health Organization* vol. 66 (1988).
33. Tangpukdee, N., Duangdee, C., Wilairatana, P. & Krudsood, S. Malaria diagnosis: a brief review. (2009) doi:10.3347/kjp.2009.47.2.93.

34. Hänscheid, T. & Grobusch, M. P. How useful is PCR in the diagnosis of malaria? *Trends Parasitol* **18**, 395–398 (2002).
35. Moody, A. Rapid diagnostic tests for malaria parasites. *Clinical Microbiology Reviews* vol. 15 Preprint at https://doi.org/10.1128/CMR.15.1.66-78.2002 (2002).
36. Varo, R., Balanza, N., Mayor, A. & Bassat, Q. Diagnosis of clinical malaria in endemic settings. *Expert Review of Anti-Infective Therapy* vol. 19 Preprint at https://doi.org/10.1080/14787210.2020.1807940 (2021).
37. Health Organization World (WHO). *Guidelines for malaria*. https://www.who.int/publications/i/item/guidelines-for-malaria (2022).
38. Chu, C. S. & White, N. J. Management of relapsing Plasmodium vivax malaria. (2016) doi:10.1080/14787210.2016.1220304.
39. Schwartz, E. Prophylaxis of Malaria. *Open Journal System MEDITERRANEAN JOURNAL OF HEMATOLOGY AND INFECTIOUS DISEASES Mediterr J Hematol Infect Dis* **4**, 201 (2012).
40. Genton, B. & D'Acremont, V. Malaria Prevention in Travelers. *Infect Dis Clin North Am* **26**, 637–654 (2012).
41. Historic RTS,S/AS01 recommendation can reinvigorate the fight against malaria. (2021).
42. Nadeem, A. Y., Shehzad, A., Islam, S. U., Al-Suhaimi, E. A. & Lee, Y. S. Mosquirix™ RTS, S/AS01 Vaccine Development, Immunogenicity, and Efficacy. (2022) doi:10.3390/vaccines10050713.
43. Mayer, G. Innate (Non-specific) Immunity. in *Microbiology and Immunology On-line* (ed. Hunt, R. C.) (2017).
44. McComb, S., Thiriot, A., Akache, B., Krishnan, L. & Stark, F. Introduction to the Immune System. in *Methods in Molecular Biology* vol. 2024 (2019).
45. Riley, E. M. & Stewart, V. A. Immune mechanisms in malaria: New insights in vaccine development. *Nature Medicine* vol. 19 Preprint at https://doi.org/10.1038/nm.3083 (2013).
46. Gowda, D. C. & Wu, X. Parasite Recognition and Signaling Mechanisms in Innate Immune Responses to Malaria. *Frontiers in Immunology* vol. 9 Preprint at https://doi.org/10.3389/fimmu.2018.03006 (2018).
47. Götz, A. *et al.* Innate Immunity to Malaria. in *Malaria: Immune Response to Infection and Vaccination* (eds. Mota, M. M. & Rodrigues, A.) 3–25 (2017). doi:10.1007/978-3-319-45210-4.
48. Liehl, P. *et al.* Host-cell sensors for Plasmodium activate innate immunity against liver-stage infection. *Nat Med* **20**, (2014).

49. Miller, J. L., Sack, B. K., Baldwin, M., Vaughan, A. M. & Kappe, S. H. I. Interferon-Mediated Innate Immune Responses against Malaria Parasite Liver Stages. *Cell Rep* **7**, 436–447 (2014).
50. Silvie, O., Mota, M. M., Matuschewski, K. & Prudêncio, M. Interactions of the malaria parasite and its mammalian host. *Current Opinion in Microbiology* vol. 11 Preprint at https://doi.org/10.1016/j.mib.2008.06.005 (2008).
51. Virus interference. I. The interferon. *Proc R Soc Lond B Biol Sci* **147**, (1957).
52. Borden, E. C. *et al.* Interferons at age 50: Past, current and future impact on biomedicine. *Nature Reviews Drug Discovery* vol. 6 Preprint at https://doi.org/10.1038/nrd2422 (2007).
53. Ivashkiv, L. B. & Donlin, L. T. Regulation of type I interferon responses. *Nature Reviews Immunology* vol. 14 Preprint at https://doi.org/10.1038/nri3581 (2014).
54. Kotenko, S. v. *et al.* IFN-λs mediate antiviral protection through a distinct class II cytokine receptor complex. *Nature Immunology* vol. 4 Preprint at https://doi.org/10.1038/ni875 (2003).
55. Majoros, A. *et al.* Canonical and non-canonical aspects of JAK-STAT signaling: Lessons from interferons for cytokine responses. *Frontiers in Immunology* vol. 8 Preprint at https://doi.org/10.3389/fimmu.2017.00029 (2017).
56. Gomes, P. S., Bhardwaj, J., Rivera-Correa, J., Freire-De-Lima, C. G. & Morrot, A. Immune escape strategies of malaria parasites. *Frontiers in Microbiology* vol. 7 Preprint at https://doi.org/10.3389/fmicb.2016.01617 (2016).
57. He, X., Xia, L., Tumas, K. C., Wu, J. & Su, X. Z. Type I Interferons and Malaria: A Double-Edge Sword Against a Complex Parasitic Disease. *Frontiers in Cellular and Infection Microbiology* vol. 10 Preprint at https://doi.org/10.3389/fcimb.2020.594621 (2020).
58. Liehl, P. *et al.* Innate Immunity Induced by Plasmodium Liver Infection Inhibits Malaria Reinfections. (2015) doi:10.1128/IAI.02796-14.
59. Long, C. A. & Zavala, F. Immune Responses in Malaria. *Cold Spring Harb Perspect Med* **7**, a025577 (2017).
60. Amino, R. *et al.* Host Cell Traversal Is Important for Progression of the Malaria Parasite through the Dermis to the Liver. *Cell Host Microbe* **3**, (2008).
61. Frevert, U. *et al.* Intravital observation of plasmodium berghei sporozoite infection of the liver. *PLoS Biol* **3**, (2005).
62. Baer, K. *et al.* Kupffer cells are obligatory for Plasmodium yoelii sporozoite infection of the liver. *Cell Microbiol* **9**, (2007).
63. Usynin, I., Klotz, C. & Frevert, U. Malaria circumsporozoite protein inhibits the respiratory burst in Kupffer cells. *Cell Microbiol* **9**, (2007).

64. Klotz, C. & Frevert, U. Plasmodium yoelii sporozoites modulate cytokine profile and induce apoptosis in murine Kupffer cells. *Int J Parasitol* **38**, (2008).
65. Thieleke-Matos, C. *et al.* Host cell autophagy contributes to Plasmodium liver development. *Cell Microbiol* **18**, (2016).
66. Singh, A. P. *et al.* Plasmodium Circumsporozoite Protein Promotes the Development of the Liver Stages of the Parasite. *Cell* **131**, (2007).
67. Frevert, U. *et al.* Malaria circumsporozoite protein inhibits protein synthesis in mammalian cells. *EMBO Journal* **17**, (1998).
68. Epiphanio, S. *et al.* Heme Oxygenase-1 Is an Anti-Inflammatory Host Factor that Promotes Murine Plasmodium Liver Infection. *Cell Host Microbe* **3**, (2008).
69. Leirião, P. *et al.* HGF/MET signalling protects Plasmodium-infected host cells from apoptosis. *Cell Microbiol* **7**, (2005).
70. van de Sand, C. *et al.* The liver stage of Plasmodium berghei inhibits host cell apoptosis. *Mol Microbiol* **58**, (2005).
71. Hanson, K. K. *et al.* Torins are potent antimalarials that block replenishment of Plasmodium liver stage parasitophorous vacuole membrane proteins. *Proc Natl Acad Sci U S A* **110**, (2013).
72. Kaushansky, A. *et al.* Malaria parasite liver stages render host hepatocytes susceptible to mitochondria-initiated apoptosis. *Cell Death Dis* **4**, (2013).
73. Sturm, A. *et al.* Manipulation of host hepatocytes by the malaria parasite for delivery into liver sinusoids. *Science (1979)* **313**, (2006).
74. Cowman, A. F. & Kappe, S. H. I. Malaria's stealth shuttle. *Science* vol. 313 Preprint at https://doi.org/10.1126/science.1132940 (2006).
75. Carvalho, T. G. & Ménard, R. Manipulating the Plasmodium genome. *Current Issues in Molecular Biology* vol. 7 Preprint at https://doi.org/10.21775/cimb.007.039 (2005).
76. Gardiner, D. L., Skinner-Adams, T. S., Spielmann, T. & Trenholme, K. R. Malaria transfection and transfection vectors. *Trends in Parasitology* vol. 19 Preprint at https://doi.org/10.1016/S1471-4922(03)00187-9 (2003).
77. Lee, S. Y. High cell-density culture of Escherichia coli. *Trends Biotechnol* **14**, 98–105 (1996).
78. Cornelis, P. Expressing genes in different Escherichia coli compartments. *Curr Opin Biotechnol* **11**, 450–454 (2000).
79. de Koning-Ward, T. F., Janse, C. J. & Waters, A. P. The development of genetic tools for dissecting the biology of malaria parasites. *Annual Review of Microbiology* vol. 54 Preprint at https://doi.org/10.1146/annurev.micro.54.1.157 (2000).
80. Janse, C. J. *et al.* High efficiency transfection of Plasmodium berghei facilitates novel selection procedures. *Mol Biochem Parasitol* **145**, 60–70 (2006).

81. Godiska, R. *et al.* Linear plasmid vector for cloning of repetitive or unstable sequences in Escherichia coli. *Nucleic Acids Res* **38**, (2010).
82. Pfander, C. *et al.* A scalable pipeline for highly effective genetic modification of a malaria parasite. *Nat Methods* **8**, (2011).
83. Zhang, Y., Muyrers, J. P. P., Testa, G. & Stewart, A. F. DNA cloning by homologous recombination in Escherichia coli. *Nat Biotechnol* **18**, (2000).
84. Schwach, F. *et al.* PlasmoGEM, a database supporting a community resource for large-scale experimental genetics in malaria parasites. *Nucleic Acids Res* **43**, D1176–D1182 (2015).
85. Janse, C. J., Ramesar, J. & Waters, A. P. High-efficiency transfection and drug selection of genetically transformed blood stages of the rodent malaria parasite Plasmodium berghei. *Nat Protoc* **1**, 346–356 (2006).
86. Gomes, A. R. *et al.* A Genome-Scale Vector Resource Enables High-Throughput Reverse Genetic Screening in a Malaria Parasite. *Cell Host Microbe* **17**, 404–413 (2015).
87. Bushell, E. *et al.* Functional Profiling of a Plasmodium Genome Reveals an Abundance of Essential Genes. *Cell* **170**, 260-272.e8 (2017).
88. PlasmoGEM resource overview | PlasmoGEM. Available at: https://plasmogem.umu.se/pbgem/resource.
89. Stanway, R. R. *et al.* Genome-Scale Identification of Essential Metabolic Processes for Targeting the Plasmodium Liver Stage. *Cell* **179**, 1112-1128.e26 (2019).
90. Wykes, M. N. & Good, M. F. What have we learnt from mouse models for the study of malaria? *European Journal of Immunology* vol. 39 Preprint at https://doi.org/10.1002/eji.200939552 (2009).
91. LeRoux, M., Lakshmanan, V. & Daily, J. P. Plasmodium falciparum biology: analysis of in vitro versus in vivo growth conditions. *Trends in Parasitology* vol. 25 Preprint at https://doi.org/10.1016/j.pt.2009.07.005 (2009).
92. Tarun, A. S. *et al.* Quantitative isolation and in vivo imaging of malaria parasite liver stages. *Int J Parasitol* **36**, 1283–1293 (2006).
93. Scheller, L. F., Wirtz, R. A. & Azad, A. F. Susceptibility of different strains of mice to hepatic infection with Plasmodium berghei. *Infect Immun* **62**, (1994).
94. Miller, J. L., Sack, B. K., Baldwin, M., Vaughan, A. M. & Kappe, S. H. I. Interferon-Mediated Innate Immune Responses against Malaria Parasite Liver Stages. *Cell Rep* **7**, 436–447 (2014).
95. Levin, R. E., Ekezie, F.-G. C. & Sun, D.-W. DNA-Based Technique: Polymerase Chain Reaction (PCR). *Modern Techniques for Food Authentication* 527–616 (2018) doi:10.1016/B978-0-12-814264-6.00014-1.

96. Anders, S. & Huber, W. Differential expression analysis for sequence count data. *Genome Biol* **11**, (2010).
97. Mota, M. M. & Rodriguez, A. Migration through host cells: The first steps of Plasmodium sporozoites in the mammalian host. *Cellular Microbiology* vol. 6 Preprint at https://doi.org/10.1111/j.1462-5822.2004.00460.x (2004).
98. Frevert, U. Sneaking in through the back entrance: The biology of malaria liver stages. *Trends in Parasitology* vol. 20 Preprint at https://doi.org/10.1016/j.pt.2004.07.007 (2004).
99. Real, E. *et al.* Plasmodium UIS3 sequesters host LC3 to avoid elimination by autophagy in hepatocytes. *Nat Microbiol* **3**, (2017).
100. Albuquerque, S. S. *et al.* Host cell transcriptional profiling during malaria liver stage infection reveals a coordinated and sequential set of biological events. *BMC Genomics* **10**, (2009).
101. Mancio-Silva, L. *et al.* Nutrient sensing modulates malaria parasite virulence. *Nature* **547**, (2017).
102. Rijpma, S. R. *et al.* Vital and dispensable roles of Plasmodium multidrug resistance transporters during blood- and mosquito-stage development. *Mol Microbiol* **101**, (2016).
103. Sayers, C. P., Mollard, V., Buchanan, H. D., McFadden, G. I. & Goodman, C. D. A genetic screen in rodent malaria parasites identifies five new apicoplast putative membrane transporters, one of which is essential in human malaria parasites. *Cell Microbiol* **20**, (2018).
104. Liu, F. *et al.* An MFS-Domain Protein Pb115 Plays a Critical Role in Gamete Fertilization of the Malaria Parasite Plasmodium berghei. *Front Microbiol* **10**, (2019).
105. Srivastava, A. *et al.* Stage-Specific Changes in Plasmodium Metabolism Required for Differentiation and Adaptation to Different Host and Vector Environments. *PLoS Pathog* **12**, (2016).
106. Marvin, R. G. *et al.* Fluxes in 'free' and total zinc are essential for progression of intraerythrocytic stages of plasmodium falciparum. *Chem Biol* **19**, (2012).
107. Martin, R. E., Ginsburg, H. & Kirk, K. Membrane transport proteins of the malaria parasite. *Molecular Microbiology* vol. 74 Preprint at https://doi.org/10.1111/j.1365-2958.2009.06863.x (2009).
108. Kenthirapalan, S., Waters, A. P., Matuschewski, K. & Kooij, T. W. A. Functional profiles of orphan membrane transporters in the life cycle of the malaria parasite. *Nat Commun* **7**, (2016).
109. Maithal, K., Ravindra, G., Balaram, H. & Balaram, P. Inhibition of Plasmodium falciparum triose-phosphate isomerase by chemical modification of an interface

cysteine: Electrospray ionization mass spectrometric analysis of differential cysteine reactivities. *Journal of Biological Chemistry* **277**, (2002).

110. Mehta, M., Sonawat, H. M. & Sharma, S. Glycolysis in Plasmodium falciparum results in modulation of host enzyme activities. *J Vector Borne Dis* **43**, (2006).
111. Ren, W. *et al.* Amino acids as mediators of metabolic cross talk between host and pathogen. *Frontiers in Immunology* vol. 9 Preprint at https://doi.org/10.3389/fimmu.2018.00319 (2018).
112. Nagaraj, V. A. *et al.* Asparagine requirement in Plasmodium berghei as a target to prevent malaria transmission and liver infections. *Nat Commun* **6**, (2015).
113. Silvie, O., Goetz, K. & Matuschewski, K. A sporozoite asparagine-rich protein controls initiation of Plasmodium liver stage development. *PLoS Pathog* **4**, (2008).
114. Nishi, T., Kaneko, I., Iwanaga, S. & Yuda, M. Identification of a novel AP2 transcription factor in zygotes with an essential role in Plasmodium ookinete development. *PLoS Pathog* **18**, (2022).
115. Hamilton, M. J., Lee, M. & le Roch, K. G. The ubiquitin system: An essential component to unlocking the secrets of malaria parasite biology. *Molecular BioSystems* vol. 10 Preprint at https://doi.org/10.1039/c3mb70506d (2014).
116. Laney, J. D. & Hochstrasser, M. Substrate targeting in the ubiquitin system. *Cell* vol. 97 Preprint at https://doi.org/10.1016/S0092-8674(00)80752-7 (1999).
117. Jain, J., Jain, S. K., Walker, L. A. & Tekwani, B. L. Inhibitors of ubiquitin E3 ligase as potential new antimalarial drug leads. *BMC Pharmacol Toxicol* **18**, (2017).
118. Groat-Carmona, A. M. *et al.* A Plasmodium α/β-hydrolase modulates the development of invasive stages. *Cell Microbiol* **17**, (2015).
119. Langhorne, J. & Duffy, P. E. Expanding the antimalarial toolkit: Targeting host-parasite interactions. *Journal of Experimental Medicine* vol. 213 143–153 Preprint at https://doi.org/10.1084/jem.20151677 (2016).
120. Acharya, P., Garg, M., Kumar, P., Munjal, A. & Raja, K. D. Host-parasite interactions in human malaria: Clinical implications of basic research. *Front Microbiol* **8**, (2017).
121. Blasco, B., Leroy, Di. & Fidock, D. A. Antimalarial drug resistance: Linking Plasmodium falciparum parasite biology to the clinic. *Nature Medicine* vol. 23 Preprint at https://doi.org/10.1038/nm.4381 (2017).
122. Chora, Â. F. *et al.* Interplay between liver and blood stages of Plasmodium infection dictates malaria severity via γδ T cells and IL-17-promoted stress erythropoiesis. *Immunity* (2023) doi:10.1016/j.immuni.2023.01.031.

Annexes

7. Annexes

Supplementary Table 1 | Gene identification numbers (ID), *Plasmo*GEM vector IDs, gene name and product of the vectors used in the experiments.

GeneID	*Plasmo*GEM ID	Gene name	Product
PBANKA_031500	PbGEM-010777		rRNA methyltransferase, putative
PBANKA_031590	PbGEM-010877		pseudouridine synthase, putative
PBANKA_051500	PbGEM-015561	P25	ookinete surface protein P25
PBANKA_070660	PbGEM-234257		conserved Plasmodium protein, unknown function
PBANKA_092660	PbGEM-121290	GCN20	protein GCN20, putative
PBANKA_050690	PbGEM-230990	PLSCR	phospholipid scramblase, putative
PBANKA_010150	PbGEM-226693		conserved Plasmodium protein, unknown function
PBANKA_146070	PbGEM-258996	DPAP2	dipeptidyl aminopeptidase 2
PBANKA_070710	PbGEM-021287	IMC1i	inner membrane complex protein 1i
PBANKA_051520	PbGEM-086151	MORN1	MORN repeat-containing protein 1, putative
PBANKA_146060	PbGEM-071005		uroporphyrinogen-III synthase, putative
PBANKA_101610	PbGEM-036651	RF1	peptide chain release factor 1, putative
PBANKA_134630	PbGEM-059519	UIS19	CPW-WPC family protein
PBANKA_071430	PbGEM-022313	HSP20	small heat shock protein HSP20
PBANKA_060620	PbGEM-087185		41-3 protein, putative
PBANKA_093290	PbGEM-032706	G3PDH	glycerol-3-phosphate dehydrogenase, putative
PBANKA_062030	PbGEM-019862		conserved protein, unknown function
PBANKA_142700	PbGEM-066015	PPM7	protein phosphatase PPM7
PBANKA_070700	PbGEM-088924	LipB	lipoate-protein ligase B
PBANKA_071400	PbGEM-022265	DMC1	meiotic recombination protein DMC1
PBANKA_070330	PbGEM-233516		conserved protein, unknown function
PBANKA_133660	PbGEM-058133		conserved protein, unknown function
PBANKA_030260	PbGEM-009087		3'-5' exonuclease, putative
PBANKA_142220	PbGEM-065359	CDF	cation diffusion facilitator family protein, putative
PBANKA_122990	PbGEM-050692		conserved protein, unknown function
PBANKA_142880	PbGEM-111006	SDHB	succinate dehydrogenase [ubiquinone] iron-sulfur subunit, mitochondrial, putative
PBANKA_041170	PbGEM-230293		HSP20-like chaperone, putative
PBANKA_130520	PbGEM-053796		serine/threonine protein kinase, putative
PBANKA_102340	PbGEM-096918	GR	glutathione reductase, putative
PBANKA_050830	PbGEM-014629		conserved Plasmodium protein, unknown function
PBANKA_061920	PbGEM-019700	PSOP1	secreted ookinete protein, putative
PBANKA_112510	PbGEM-043599	FabB/FabF	3-oxoacyl-acyl-carrier protein synthase, putative

PBANKA_050570	PbGEM-230776	ROK1	ATP-dependent RNA helicase ROK1, putative
PBANKA_080650	PbGEM-090509		triosephosphate isomerase, putative
PBANKA_060860	PbGEM-018233		zinc finger protein, putative
PBANKA_131510	PbGEM-055230	Sir2b	transcriptional regulatory protein sir2b
PBANKA_112100	PbGEM-099377		conserved Plasmodium protein, unknown function
PBANKA_124120	PbGEM-052197		conserved Plasmodium protein, unknown function
PBANKA_051220	PbGEM-015197	PPO	protoporphyrinogen oxidase, putative
PBANKA_041040	PbGEM-012290	GSK3	glycogen synthase kinase 3, putative
PBANKA_082430	PbGEM-026560		conserved Plasmodium protein, unknown function
PBANKA_141810	PbGEM-064794		ACDC domain-containing protein, putative
PBANKA_060800	PbGEM-018144	PBGD	porphobilinogen deaminase
PBANKA_071220	PbGEM-235245	PBLP	BEM46-like protein, putative
PBANKA_050440	PbGEM-014061		conserved Plasmodium protein, unknown function
PBANKA_020760	PbGEM-082330		asparagine-rich antigen, putative
PBANKA_030240	PbGEM-083023		5'-3' exonuclease, putative
PBANKA_111060	PbGEM-041538		conserved Plasmodium protein, unknown function
PBANKA_100240	PbGEM-034599	DPAP3	dipeptidyl aminopeptidase 3, putative
PBANKA_140410	PbGEM-062848	S2P	site-2 protease S2P
PBANKA_051100	PbGEM-015012	HCS1	biotin--protein ligase 1
PBANKA_112810	PbGEM-099883	PL	phospholipase
PBANKA_141050	PbGEM-063795	MCAT	malonyl CoA-acyl carrier protein transacylase, putative
PBANKA_040120	PbGEM-230537	ABCB4	ABC transporter B family member 4, putative
PBANKA_071490	PbGEM-022409	aLipDH	dihydrolipoyl dehydrogenase, apicoplast, putative
PBANKA_011250	PbGEM-227922	MFR1	major facilitator superfamily-related transporter, putative
PBANKA_010740	PbGEM-006127	OAT	ornithine aminotransferase, putative
PBANKA_071120	PbGEM-021894		ubiquitin-like protein, putative
PBANKA_050500	PbGEM-085541		dihydrolipoamide acyltransferase, putative
PBANKA_011160	PbGEM-267395	ROP14	rhoptry protein ROP14, putative
PBANKA_144490	PbGEM-258539		vacuolar transporter chaperone, putative
PBANKA_040430	PbGEM-228846		P-loop containing nucleoside triphosphate hydrolase, putative
PBANKA_051270	PbGEM-275114		conserved Plasmodium protein, unknown function
PBANKA_061640	PbGEM-278858		conserved protein, unknown function
PBANKA_021390	PbGEM-227253		dynein light chain, putative
PBANKA_091510	PbGEM-332595	CDC50B	LEM3/CDC50 family protein, putative
PBANKA_051535	PbGEM-232086	OTU	OTU-like cysteine protease, putative
PBANKA_020350	PbGEM-267803	SELB	selenocysteine-specific elongation factor, putative
PBANKA_010430	PbGEM-266515		cyclin dependent kinase binding protein, putative
PBANKA_100520	PbGEM-293248		conserved Plasmodium protein, unknown function

PBANKA_050120	PbGEM-329235	UIS4	early transcribed membrane protein
PBANKA_061960	PbGEM-264780	PELO	protein pelota homolog, putative
PBANKA_041780	PbGEM-273282		conserved protein, unknown function
PBANKA_090520	PbGEM-287586	CAP93	oocyst capsule protein Cap93
PBANKA_020420	PbGEM-267883		tubulin-specific chaperone a, putative
PBANKA_010110	PbGEM-266100	PALM	liver merozoite formation protein
PBANKA_021450	PbGEM-269163	IMP2	IMP1-like protein, putative
PBANKA_070200	PbGEM-330539		conserved protein, unknown function
PBANKA_094020	PbGEM-241251	DNA2	DNA replication ATP-dependent helicase/nuclease DNA2, putative
PBANKA_031270	PbGEM-229846		DEAD/DEAH box helicase, putative
PBANKA_140440	PbGEM-339451		conserved Plasmodium protein, unknown function
PBANKA_041490	PbGEM-272922		dynein intermediate light chain, putative
PBANKA_134810	PbGEM-249387		AMMECR1 domain-containing protein, putative
PBANKA_143090	PbGEM-322203		SUN domain-containing protein, putative
PBANKA_010620	PbGEM-327715	SAS6	spindle assembly abnormal protein 6
PBANKA_052180	PbGEM-233197	RRF2	ribosome-recycling factor, putative
PBANKA_010160	PbGEM-226701	JmjC2	JmjC domain-containing protein 2, putative
PBANKA_031660	PbGEM-328723	Pb235	reticulocyte binding protein, putative
PBANKA_134650	PbGEM-264324	DEH	3-hydroxyacyl-CoA dehydratase DEH
PBANKA_100220	PbGEM-292744	P36p	6-cysteine protein P52
PBANKA_071750	PbGEM-265044	CBP20	nuclear cap-binding protein subunit 2, putative
PBANKA_110480	PbGEM-245297	ALP2b	actin-like protein, putative
PBANKA_041010	PbGEM-230013		E3 ubiquitin-protein ligase, putative
PBANKA_142710	PbGEM-321755	AQP2	aquaporin, putative
PBANKA_112780	PbGEM-248353		DnaJ protein, putative
PBANKA_144140	PbGEM-258076	PCNA2	proliferating cell nuclear antigen 2
PBANKA_133820	PbGEM-252132	FabZ	beta-hydroxyacyl-ACP dehydratase, putative
PBANKA_090980	PbGEM-288170		RNA-binding protein, putative
PBANKA_100630	PbGEM-293440	PLP1	perforin-like protein 1
PBANKA_030770	PbGEM-270187		conserved Plasmodium protein, unknown function
PBANKA_090240	PbGEM-287226		conserved Plasmodium protein, unknown function
PBANKA_061610	PbGEM-234590		prefoldin subunit 3, putative
PBANKA_020830	PbGEM-229203	NPT1	novel putative transporter 1
PBANKA_082090	PbGEM-239778	ELO-A	elongation of fatty acids protein, putative
PBANKA_072070	PbGEM-331075		regulator of chromosome condensation, putative
PBANKA_093100	PbGEM-290856	Pb115	MFS domain-containing protein P115
PBANKA_102460	PbGEM-334115	LISP1	liver specific protein 1
PBANKA_030820	PbGEM-270259		apicoplast beta-ketoacyl-acyl carrier protein synthase III precursor, putative

PBANKA_082100	PbGEM-239805		chaperone, putative
PBANKA_112690	PbGEM-099789	PK4	eukaryotic translation initiation factor 2-alpha kinase
PBANKA_010770	PbGEM-006154	ZIP1	zinc transporter ZIP1
PBANKA_020580	PbGEM-082161	eIK2	eukaryotic translation initiation factor 2-alpha kinase 2
PBANKA_040110	PbGEM-084034	SRPK1	serine/threonine protein kinase, putative
PBANKA_062250	PbGEM-020158		exonuclease I, putative
PBANKA_031480	PbGEM-010745		conserved protein, unknown function
PBANKA_070940	PbGEM-021641		conserved Plasmodium protein, unknown function
PBANKA_030500	PbGEM-009429	SERA2	serine repeat antigen 2
PBANKA_131720	PbGEM-055524	NTH	NAD(P) transhydrogenase
PBANKA_051880	PbGEM-016150		U2 snRNA/tRNA pseudouridine synthase, putative
PBANKA_061140	PbGEM-018598	PANK2	pantothenate kinase 2, putative
PBANKA_040230	PbGEM-011169	BCKDH-E2	lipoamide acyltransferase component of branched-chain alpha-keto acid dehydrogenase complex, putative
PBANKA_132950	PbGEM-057165	PPKL	protein phosphatase containing kelch-like domains
PBANKA_030230	PbGEM-009046	AspAT	aspartate aminotransferase, putative
PBANKA_071560	PbGEM-022521	RPT3	26S protease regulatory subunit 6B, putative
PBANKA_110420	PbGEM-122074	BCKDHB	2-oxoisovalerate dehydrogenase subunit beta, mitochondrial, putative
PBANKA_061430	PbGEM-018972	SufS	cysteine desulfurase
PBANKA_041030	PbGEM-012274	RPN12	26S proteasome regulatory subunit RPN12, putative
PBANKA_061880	PbGEM-019636	DDX31	ATP-dependent DNA helicase DDX31, putative
PBANKA_093850	PbGEM-033491		succinate--CoA ligase [ADP-forming] subunit alpha, putative
PBANKA_091820	PbGEM-093581		phosphoacetylglucosamine mutase, putative
PBANKA_061040	PbGEM-087402	ATP4	non-SERCA-type Ca2+ -transporting P-ATPase, putative
PBANKA_031240	PbGEM-083773	RPB2	DNA-directed RNA polymerase II subunit RPB2, putative
PBANKA_090140	PbGEM-092506		ATP synthase subunit delta, mitochondrial, putative
PBANKA_021140	PbGEM-082644	DNMT	DNA (cytosine-5)-methyltransferase, putative
PBANKA_070410	PbGEM-088775	UBE4B	ubiquitin conjugation factor E4 B, putative
PBANKA_040760	PbGEM-084472	AS	asparagine synthetase [glutamine-hydrolyzing]
PBANKA_111100	PbGEM-098813		RNA pseudouridylate synthase, putative
PBANKA_122030	PbGEM-102772	PARE	prodrug activation and resistance esterase, putative
PBANKA_030860	PbGEM-083434		asparagine--tRNA ligase, putative
PBANKA_030960	PbGEM-010018		SRR1-like protein
PBANKA_030370	PbGEM-228022	RAD2	DNA repair protein RAD2, putative
PBANKA_051210	PbGEM-231655		methyltransferase, putative
PBANKA_030850	PbGEM-228946	TKL1	tyrosine kinase-like protein, putative
PBANKA_062270	PbGEM-235866		mago nashi protein homologue, putative
PBANKA_051780	PbGEM-232532	SLY1	Sec1 family protein, putative
PBANKA_031540	PbGEM-230276	PRP45	pre-mRNA-processing protein 45, putative

PBANKA_143620	PbGEM-257004	SET10	histone-lysine N-methyltransferase, H3 lysine-4 specific, putative
PBANKA_144690	PbGEM-256413	LPD1	dihydrolipoyl dehydrogenase, mitochondrial, putative
PBANKA_123820	PbGEM-261556		DnaJ protein, putative
PBANKA_133180	PbGEM-249676	DER1-1	derlin-1, putative
PBANKA_030170	PbGEM-227680		5'-3' exonuclease, putative
PBANKA_030420	PbGEM-228077		DNA-directed RNA polymerase III subunit RPC10, putative
PBANKA_020650	PbGEM-228772	RAB5c	ras-related protein Rab-5C, putative
PBANKA_030840	PbGEM-228889	ALG14	UDP-N-acetylglucosamine transferase subunit ALG14, putative
PBANKA_070370	PbGEM-233612	DBP10	ATP-dependent RNA helicase DBP10, putative
PBANKA_071510	PbGEM-235843		ubiquitin, putative
PBANKA_051660	PbGEM-232294	LRR1	leucine-rich repeat protein
PBANKA_051980	PbGEM-265292	ACT	acetyl-CoA transporter, putative
PBANKA_144110	PbGEM-265660	HAD2	haloacid dehalogenase-like hydrolase, putative
PBANKA_020510	PbGEM-265404		mitochondrial carrier protein, putative
PBANKA_040840	PbGEM-264140		phosphoglycerate mutase, putative
PBANKA_010920	PbGEM-265388	SPT5	transcription elongation factor SPT5, putative
PBANKA_070220	PbGEM-264356		translation initiation factor eIF-2B subunit alpha, putative
PBANKA_010730	PbGEM-266931	CCT6	T-complex protein 1 subunit zeta, putative
PBANKA_062180	PbGEM-279650	COQ3	ubiquinone biosynthesis O-methyltransferase, putative
PBANKA_051630	PbGEM-232246		DER1-like protein, putative
PBANKA_051820	PbGEM-275858	SDHA	flavoprotein subunit of succinate dehydrogenase, putative
PBANKA_090660	PbGEM-287762	CPO	coproporphyrinogen-III oxidase, putative
PBANKA_030470	PbGEM-269819	SERA5	serine repeat antigen 5
PBANKA_135750	PbGEM-317331	LipA	lipoyl synthase
PBANKA_060120	PbGEM-276866		dynein heavy chain, putative
PBANKA_062140	PbGEM-279586		RNA-binding protein, putative
PBANKA_061680	PbGEM-234694	ARP6	actin-related protein ARP6, putative
PBANKA_052040	PbGEM-232916	DYN2	dynamin-like protein, putative
PBANKA_051990	PbGEM-276178		conserved Plasmodium protein, unknown function
PBANKA_061570	PbGEM-330283		dynein heavy chain, putative
PBANKA_041710	PbGEM-329163		conserved protein, unknown function
PBANKA_121810	PbGEM-336595	Cap380	oocyst capsule protein Cap380
PBANKA_020790	PbGEM-268387		conserved Plasmodium protein, unknown function
PBANKA_020900	PbGEM-328099		protein E140, putative
PBANKA_040830	PbGEM-328971		phd finger protein, putative
PBANKA_010820	PbGEM-327787		protein KIC6, putative
PBANKA_093380	PbGEM-291216		conserved Plasmodium protein, unknown function
PBANKA_050720	PbGEM-274330		conserved Plasmodium protein, unknown function

PBANKA_091910	PbGEM-289441	PV1	parasitophorous vacuolar protein 1
PBANKA_030450	PbGEM-328427		conserved Plasmodium protein, unknown function
PBANKA_145980	PbGEM-341067		conserved Plasmodium protein, unknown function
PBANKA_020290	PbGEM-228217		transcription initiation factor TFIIB, putative
PBANKA_010520	PbGEM-227028	PTB	polypyrimidine tract-binding protein, putative
PBANKA_041590	PbGEM-273050		conserved protein, unknown function
PBANKA_040670	PbGEM-229398		activator of Hsp90 ATPase, putative
PBANKA_051140	PbGEM-231569	nPrx	peroxiredoxin, putative

Supplementary Table 2 | Frequency and abundance for genes included in the screen.

Gene ID	Gene name	Product description	Previously described phenotype in the liver stage	BALB/c mice		Sporozoites		WT mice		*Ifnar1*$^{-/-}$ mice	
				Frequency	Abundance	Frequency	Abundance	Frequency	Abundance	Frequency	Abundance
PBANKA_031500	-	rRNA methyltransferase, putative	Regular liver dev.	100%	15611.142	100%	29662.904	100%	30904.079	100%	32216.918
PBANKA_031590	-	pseudouridine synthase, putative	Regular liver dev.	100%	9892.623	100%	18677.682	100%	16981.634	100%	23834.074
PBANKA_051500	P25	ookinete surface protein P25	Regular liver dev.	100%	6196.693	100%	11659.247	100%	11053.345	100%	11973.635
PBANKA_070660	-	conserved Plasmodium protein, unknown function	Regular liver dev.	100%	3411.707	100%	7682.149	90%	9968.144	100%	10300.249
PBANKA_092660	GCN20	protein GCN20, putative	Compromised liver dev.	100%	4233.847	100%	6845.574	100%	4970.620	100%	7790.693
PBANKA_050690	PLSCR	phospholipid scramblase, putative	Regular liver dev.	100%	2478.957	100%	3187.330	90%	6401.271	100%	4820.046
PBANKA_010150	-	conserved Plasmodium protein, unknown function	Regular liver dev.	100%	6468.676	100%	5977.509	90%	6780.325	100%	6580.915
PBANKA_146070	DPAP2	dipeptidyl aminopeptidase 2	Compromised liver dev.	100%	5906.391	100%	7835.921	90%	5387.607	100%	6087.911
PBANKA_070710	IMC1i	inner membrane complex protein 1i	Regular liver dev.	100%	4970.783	100%	3935.615	100%	4949.879	100%	4144.996
PBANKA_051520	MORN1	MORN repeat-containing protein 1, putative	Regular liver dev.	100%	2622.641	100%	3589.980	100%	4358.098	100%	5552.546
PBANKA_146060	-	uroporphyrinogen-III synthase, putative	Compromised liver dev.	100%	7835.436	100%	10880.386	100%	2552.550	100%	3380.139
PBANKA_101610	RF1	peptide chain release factor 1, putative	Compromised liver dev.	100%	3809.647	100%	4349.966	100%	4599.622	100%	4501.844
PBANKA_134630	UIS19	CPW-WPC family protein	Compromised liver dev.	100%	6828.858	100%	4688.942	90%	3973.579	100%	5459.666
PBANKA_071430	HSP20	small heat shock protein HSP20	Regular liver dev.	100%	4826.716	100%	6015.722	100%	4537.877	100%	4903.088

PBANKA_060620	-	41-3 protein, putative	Regular liver dev.	100%	2919.148	100%	2231.321	100%	3489.477	100%	1940.379
PBANKA_093290	G3PDH	glycerol-3-phosphate dehydrogenase, putative	Compromised liver dev.	100%	10879.061	100%	14975.693	10%	114.045	0%	0.000
PBANKA_062030	-	conserved protein, unknown function	Compromised liver dev.	100%	2605.056	100%	2074.464	90%	2472.155	100%	2472.155
PBANKA_142700	PPM7	protein phosphatase PPM7	Compromised liver dev.	100%	2035.541	100%	2512.637	90%	2658.558	100%	4158.851
PBANKA_070700	LipB	lipoate-protein ligase B	Compromised liver dev.	100%	8716.261	100%	12996.844	10%	38.050	0%	0.000
PBANKA_071400	DMC1	meiotic recombination protein DMC1	Regular liver dev.	100%	2267.983	100%	1577.791	90%	1979.570	100%	2525.938
PBANKA_070330	-	conserved protein, unknown function	Regular liver dev.	100%	1302.317	100%	771.794	90%	1423.620	100%	2013.810
PBANKA_133660	-	conserved protein, unknown function	Compromised liver dev.	100%	2454.826	100%	1836.102	80%	2600.841	100%	2977.250
PBANKA_030260	-	3'-5' exonuclease, putative	Regular liver dev.	100%	1055.315	100%	1945.102	90%	2641.689	89%	2131.911
PBANKA_142220	CDF	cation diffusion facilitator family protein, putative	Compromised liver dev.	100%	5732.316	100%	2573.199	40%	2663.155	89%	1154.324
PBANKA_122990	-	conserved protein, unknown function	Compromised liver dev.	100%	1788.405	100%	1314.883	60%	1385.152	78%	673.864
PBANKA_142880	SDHB	succinate dehydrogenase [ubiquinone] iron-sulfur subunit, mitochondrial, putative	Compromised liver dev.	100%	5815.707	100%	5159.572	0%	0.000	0%	0.000
PBANKA_041170	-	HSP20-like chaperone, putative	Regular liver dev.	100%	1112.431	100%	726.734	90%	555.491	89%	674.555
PBANKA_130520	-	serine/threonine protein kinase, putative	Compromised liver dev.	100%	1335.974	100%	1388.404	90%	1276.797	89%	641.875
PBANKA_102340	GR	glutathione reductase, putative	Compromised liver dev.	100%	1599.471	100%	4098.218	60%	358.689	89%	218.725
PBANKA_050830	-	ookinete maturation gene OMG1	Regular liver dev.	100%	813.336	100%	622.660	50%	763.780	89%	1592.303
PBANKA_061920	PSOP1	secreted ookinete protein, putative	Regular liver dev.	100%	1061.074	100%	694.820	60%	1036.930	89%	789.120
PBANKA_112510	FabB/FabF	3-oxoacyl-acyl-carrier protein synthase, putative	Compromised liver dev.	100%	3301.442	100%	3201.253	0%	0.000	0%	0.000
PBANKA_050570	ROK1	ATP-dependent RNA helicase ROK1, putative	Regular liver dev.	100%	1218.882	100%	1722.786	70%	494.084	78%	634.611
PBANKA_080650	-	triosephosphate isomerase, putative	Compromised liver dev.	100%	224.470	100%	590.493	50%	705.524	100%	608.040
PBANKA_060860	-	zinc finger protein, putative	Regular liver dev.	100%	1405.666	100%	726.471	30%	1140.832	67%	913.737
PBANKA_131510	Sir2b	transcriptional regulatory protein sir2b	Compromised liver dev.	100%	306.384	100%	205.910	40%	1065.807	44%	609.621
PBANKA_112100	-	conserved Plasmodium protein, unknown function	Compromised liver dev.	100%	1238.360	100%	930.834	70%	879.091	56%	245.744
PBANKA_124120	-	conserved Plasmodium protein, unknown function	Compromised liver dev.	100%	1078.633	100%	713.545	60%	684.433	44%	503.875

PBANKA_051220	PPO	protoporphyrinogen oxidase, putative	Compromised liver dev.	100%	1306.640	100%	1671.903	70%	88.038	33%	84.515
PBANKA_041040	GSK3	glycogen synthase kinase 3, putative	Compromised liver dev.	100%	989.207	100%	1014.340	50%	240.272	44%	110.604
PBANKA_082430	-	conserved Plasmodium protein, unknown function	Compromised liver dev.	100%	1628.271	100%	246.184	0%	0.000	0%	0.000
PBANKA_141810	-	ACDC domain-containing protein, putative	Compromised liver dev.	50%	793.126	100%	433.264	40%	499.422	40%	593.788
PBANKA_060800	PBGD	porphobilinogen deaminase	Compromised liver dev.	100%	1037.335	100%	1890.726	40%	50.073	22%	72.837
PBANKA_071220	PBLP	BEM46-like protein, putative	Regular liver dev.	50%	158.063	100%	94.684	60%	269.692	60%	734.836
PBANKA_050440	-	conserved Plasmodium protein, unknown function	Regular liver dev.	100%	268.754	100%	547.996	30%	509.778	56%	499.705
PBANKA_020760	-	asparagine-rich antigen, putative	Regular liver dev.	100%	235.225	100%	325.044	20%	2343.156	78%	571.631
PBANKA_030240	-	5'-3' exonuclease, putative	Regular liver dev.	50%	363.449	100%	133.846	20%	503.929	20%	478.920
PBANKA_111060	-	conserved Plasmodium protein, unknown function	Compromised liver dev.	100%	182.090	100%	162.006	20%	939.077	33%	572.336
PBANKA_100240	DPAP3	dipeptidyl aminopeptidase 3, putative	Compromised liver dev.	100%	391.743	100%	147.541	10%	220.555	44%	214.048
PBANKA_140410	S2P	site-2 protease S2P	Compromised liver dev.	50%	140.855	100%	239.931	40%	193.369	40%	158.339
PBANKA_051100	HCS1	biotin--protein ligase 1	Compromised liver dev.	100%	270.216	100%	367.366	0%	0.000	0%	0.000
PBANKA_112810	PL	phospholipase	Compromised liver dev.	100%	98.268	100%	307.873	0%	0.000	0%	0.000
PBANKA_141050	MCAT	malonyl CoA-acyl carrier protein transacylase, putative	Compromised liver dev.	100%	192.378	100%	257.355	0%	0.000	0%	0.000
PBANKA_040120	ABCB4	ABC transporter B family member 4, putative	Regular liver dev.	100%	121.567	100%	167.560	0%	0.000	11%	375.869
PBANKA_071490	aLipDH	dihydrolipoyl dehydrogenase, apicoplast, putative	Compromised liver dev.	100%	80.850	100%	160.486	0%	0.000	0%	0.000
PBANKA_011250	MFR1	major facilitator superfamily-related transporter, putative	Compromised liver dev.	50%	118.933	100%	258.781	40%	305.077	50%	358.662
PBANKA_010740	OAT	ornithine aminotransferase, putative	Regular liver dev.	25%	62.304	100%	548.461	40%	460.631	0%	0.000
PBANKA_071120	-	ubiquitin-like protein, putative	Regular liver dev.	50%	74.486	100%	100.422	0%	0.000	0%	0.000
PBANKA_050500	-	dihydrolipoamide acyltransferase, putative	Compromised liver dev.	50%	60.098	100%	110.465	0%	0.000	0%	0.000
PBANKA_011160	ROP14	rhoptry protein ROP14, putative	Regular liver dev.	100%	7050.217	100%	13895.201	100%	18287.825	100%	18116.545
PBANKA_144490	-	vacuolar transporter chaperone, putative	Compromised liver dev.	100%	6647.809	100%	12892.089	100%	6252.992	100%	7537.559

PBANKA_040430	-	P-loop containing nucleoside triphosphate hydrolase, putative	Regular liver dev.	100%	6244.273	100%	5188.536	100%	6675.774	100%	6635.721
PBANKA_051270	-	conserved Plasmodium protein, unknown function	Regular liver dev.	100%	4468.246	100%	6796.699	100%	5254.658	100%	4342.129
PBANKA_061640	-	conserved protein, unknown function	Regular liver dev.	100%	2001.548	100%	3649.851	100%	4094.196	100%	3999.291
PBANKA_021390	-	dynein light chain, putative	Compromised liver dev.	100%	2974.882	100%	2805.240	100%	3522.532	100%	4655.814
PBANKA_091510	CDC50B	LEM3/CDC50 family protein, putative	Compromised liver dev.	100%	1723.325	100%	1971.484	100%	2425.514	100%	2439.520
PBANKA_051535	OTU	OTU-like cysteine protease, putative	Regular liver dev.	100%	1314.597	100%	2038.793	100%	1481.404	100%	1456.822
PBANKA_020350	SELB	selenocysteine-specific elongation factor, putative	Regular liver dev.	100%	535.989	100%	1595.860	100%	1821.093	100%	1351.112
PBANKA_010430	-	cyclin dependent kinase binding protein, putative	Regular liver dev.	100%	338.995	100%	172.252	100%	283.181	80%	281.599
PBANKA_100520	-	conserved Plasmodium protein, unknown function	Compromised liver dev.	100%	5809.347	100%	7482.811	0%	0.000	0%	0.000
PBANKA_050120	UIS4	early transcribed membrane protein	Compromised liver dev.	100%	11647.934	100%	18876.745	0%	0.000	0%	0.000
PBANKA_061960	PELO	protein pelota homolog, putative	Compromised liver dev.	100%	1175.914	100%	1268.727	100%	719.773	100%	876.460
PBANKA_041780	-	conserved protein, unknown function	Compromised liver dev.	100%	1167.667	100%	1811.536	100%	967.178	100%	1904.752
PBANKA_090520	CAP93	oocyst capsule protein Cap93	Compromised liver dev.	100%	1343.374	100%	1860.751	100%	951.264	100%	853.903
PBANKA_020420	-	tubulin-specific chaperone a, putative	Regular liver dev.	100%	1473.557	100%	396.613	100%	662.159	80%	940.569
PBANKA_010110	PALM	liver merozoite formation protein	Compromised liver dev.	100%	6929.463	100%	9908.808	0%	0.000	0%	0.000
PBANKA_021450	IMP2	IMP1-like protein, putative	Regular liver dev.	100%	804.122	100%	1696.461	100%	1257.012	80%	1018.267
PBANKA_070200	-	conserved protein, unknown function	Regular liver dev.	100%	1094.209	100%	944.489	100%	706.173	100%	923.925
PBANKA_094020	DNA2	DNA replication ATP-dependent helicase/nuclease DNA2, putative	Compromised liver dev.	100%	956.908	100%	835.927	100%	1257.787	60%	674.222
PBANKA_031270	-	DEAD/DEAH box helicase, putative	Compromised liver dev.	100%	2587.409	100%	775.132	100%	399.816	100%	457.768
PBANKA_140440	-	conserved Plasmodium protein, unknown function	Compromised liver dev.	100%	974.366	100%	448.723	100%	393.434	100%	908.962
PBANKA_041490	-	dynein intermediate light chain, putative	Compromised liver dev.	100%	968.195	100%	471.882	60%	395.986	80%	602.180
PBANKA_134810	-	AMMECR1 domain-containing protein, putative	Compromised liver dev.	100%	1047.325	100%	107.114	60%	334.170	80%	256.728

PBANKA_143090	-	SUN domain-containing protein, putative	Compromised liver dev.	100%	299.133	100%	115.799	80%	496.482	80%	330.811
PBANKA_010620	SAS6	spindle assembly abnormal protein 6	Regular liver dev.	100%	573.560	100%	259.101	40%	639.593	60%	231.216
PBANKA_052180	RRF2	ribosome-recycling factor, putative	Regular liver dev.	100%	232.485	100%	189.621	100%	179.605	100%	323.002
PBANKA_010160	JmjC2	JmjC domain-containing protein 2, putative	Regular liver dev.	100%	226.412	100%	107.114	40%	127.366	80%	151.540
PBANKA_031660	Pb235	reticulocyte binding protein, putative	Regular liver dev.	100%	116.450	100%	254.759	80%	552.200	60%	116.292
PBANKA_134650	DEH	3-hydroxyacyl-CoA dehydratase DEH	Compromised liver dev.	100%	1325.617	100%	1437.360	0%	0.000	0%	0.000
PBANKA_100220	P36p	6-cysteine protein P52	Compromised liver dev.	100%	1072.760	100%	1645.075	0%	0.000	0%	0.000
PBANKA_071750	CBP20	nuclear cap-binding protein subunit 2, putative	Compromised liver dev.	100%	1082.063	100%	175.147	20%	421.982	0%	0.000
PBANKA_110480	ALP2b	actin-like protein, putative	Compromised liver dev.	100%	652.946	100%	147.644	40%	178.492	40%	205.225
PBANKA_041010	-	E3 ubiquitin-protein ligase, putative	Regular liver dev.	50%	67.261	100%	74.546	20%	66.180	40%	168.711
PBANKA_142710	AQP2	aquaporin, putative	Compromised liver dev.	100%	269.218	100%	144.025	60%	249.466	40%	165.077
PBANKA_112780	-	DnaJ protein, putative	Compromised liver dev.	100%	888.919	100%	120.142	0%	0.000	0%	0.000
PBANKA_144140	PCNA2	proliferating cell nuclear antigen 2	Compromised liver dev.	100%	261.028	100%	822.899	60%	82.990	20%	86.941
PBANKA_133820	FabZ	beta-hydroxyacyl-ACP dehydratase, putative	Compromised liver dev.	100%	409.541	100%	1141.348	0%	0.000	0%	0.000
PBANKA_090980	-	RNA-binding protein, putative	Compromised liver dev.	100%	392.739	100%	626.764	20%	285.445	0%	0.000
PBANKA_100630	PLP1	perforin-like protein 1	Compromised liver dev.	100%	343.837	100%	1226.750	0%	0.000	0%	0.000
PBANKA_030770	-	conserved Plasmodium protein, unknown function	Regular liver dev.	100%	348.329	100%	958.240	0%	0.000	40%	68.727
PBANKA_090240	-	conserved Plasmodium protein, unknown function	Compromised liver dev.	100%	165.555	100%	170.804	20%	353.570	40%	267.423
PBANKA_061610	-	prefoldin subunit 3, putative	Regular liver dev.	100%	208.122	100%	132.446	60%	177.849	40%	57.271
PBANKA_020830	NPT1	novel putative transporter 1	Regular liver dev.	100%	631.735	100%	77.441	0%	0.000	0%	0.000
PBANKA_082090	ELO-A	elongation of fatty acids protein, putative	Compromised liver dev.	100%	419.880	100%	489.252	0%	0.000	0%	0.000
PBANKA_072070	-	regulator of chromosome condensation, putative	Compromised liver dev.	100%	162.298	100%	114.352	20%	218.863	40%	332.925
PBANKA_093100	Pb115	MFS domain-containing protein P115	Compromised liver dev.	100%	338.376	100%	138.236	0%	0.000	40%	170.798
PBANKA_102460	LISP1	liver specific protein 1	Compromised liver dev.	100%	303.724	100%	278.642	0%	0.000	0%	0.000

PBANKA_030820	-	apicoplast beta-ketoacyl-acyl carrier protein synthase III precursor, putative	Compromised liver dev.	100%	293.116	100%	381.414	0%	0.000	0%	0.000
PBANKA_082100	-	chaperone, putative	Compromised liver dev.	100%	316.064	100%	81.060	20%	77.861	0%	0.000

Abbreviations are as follows: Dev. – development.